

# Inverse Particle and Ensemble Kalman Filters

**Himali Singh**

*Department of Electrical Engineering  
Indian Institute of Technology Delhi, India.*

EEZ208426@EE.IITD.AC.IN

**Arpan Chattopadhyay\***

*Department of Electrical Engineering,  
Bharti School of Telecommunication Technology and Management,  
Indian Institute of Technology Delhi, India.*

ARPANC@EE.IITD.AC.IN

**Kumar Vijay Mishra\***

*United States DEVCOM Army Research Laboratory  
Adelphi, MD 20783 USA.*

KVM@IEEE.ORG

## Abstract

In cognitive systems, recent emphasis has been placed on studying the cognitive processes of the subject whose behavior was the primary focus of the system's cognitive response. This approach, known as *inverse cognition*, arises in counter-adversarial applications and has motivated the development of inverse Bayesian filters. In this context, a cognitive adversary, such as a radar, uses a forward Bayesian filter to track its target of interest. An inverse filter is then employed to infer the adversary's estimate of the target's or defender's state. Previous studies have addressed this inverse filtering problem by introducing methods like the inverse Kalman filter (I-KF), inverse extended KF (I-EKF), and inverse unscented KF (I-UKF). However, these inverse filters typically assume additive Gaussian noise models and/or rely on local approximations of non-linear dynamics at the state estimates, limiting their practical application. In contrast, this paper adopts a global filtering approach and presents the development of an inverse particle filter (I-PF). The particle filter framework employs Monte Carlo (MC) methods to approximate arbitrary posterior distributions. Moreover, under mild system-level conditions, the proposed I-PF demonstrates convergence to the optimal inverse filter. Additionally, we explore MC techniques to approximate Gaussian posteriors and introduce the inverse Gaussian PF (I-GPF) and inverse ensemble KF (I-EnKF) methods. Our I-GPF and I-EnKF can efficiently handle non-Gaussian noises with suitable modifications. Additionally, we propose the differentiable I-PF, differentiable I-EnKF, and reproducing kernel Hilbert space-based EnKF (RKHS-EnKF) methods to address scenarios where system information is unknown to the defender. Using the recursive Cramér-Rao lower bound and non-credibility index (NCI), our numerical experiments for several different applications demonstrate the estimation performance and time complexity of the proposed filters.

**Keywords:** Bayesian filtering, cognitive systems, counter-adversarial systems, ensemble Kalman filter, inverse filtering, particle filter.

---

\*. A. C. and K. V. M. have made equal contributions.

## 1 Introduction

Several applications in engineering such as communications, sensing, robotics, and human-machine interactions frequently employ *cognitive* agents that perceive their surroundings and adapt their actions based on the information learned to attain optimum efficiency. A cognitive surveillance radar (Mishra et al., 2023, 2020), for example, modifies its transmit waveform and receive processing to enhance target detection (Mishra and Eldar, 2017) and tracking (Bell et al., 2015; Sharaga et al., 2015). In this context, *inverse cognition* has recently been introduced as a method for a ‘defender’ agent to identify its adversarial ‘attacker’ agent’s cognitive behavior and infer the information learned about the defender (Krishnamurthy and Rangaswamy, 2019; Krishnamurthy et al., 2020). This facilitates the development of counter-adversarial systems to assist or desist the adversary (Mattila et al., 2020; Krishnamurthy and Rangaswamy, 2019). For instance, an intelligent target can observe its adversarial radar’s waveform adaptations and develop smart interference that forces the latter to change its course of actions (Krishnamurthy et al., 2021; Kang et al., 2023). Interactive learning, fault diagnosis, and cyber-physical security are further examples of counter-adversarial applications (Krishnamurthy and Rangaswamy, 2019; Mattila et al., 2020). A similar formulation can also be found in inverse reinforcement learning (IRL) (Ng and Russell, 2000; Choi and Kim, 2011).

Counter-adversarial applications involves *inference* by both the defender and attacker, wherein they estimate the posterior distributions of an underlying state that cannot be directly observed but is inferred through an observation process conditioned on that state. Posterior distributions provide not only *point estimates*, i.e. single-number estimate such as mean of the posterior distributions, but also quantify their uncertainty. In sequential state estimation, states are inferred from a sequence of observations, with posteriors updated recursively. When state-space models are available, Bayesian filtering is a probabilistic technique for sequential state estimation that has been extensively applied to visual tracking in computer vision (Zhang et al., 2017; Dai et al., 2019), localization in robotics (Ullah et al., 2019; Fox et al., 1999), and other signal processing problems (Yousefi et al., 2019; Liu et al., 2019).

In inverse cognition, the attacker employs a (forward) Bayesian filter to infer the kinematic state of the defender, which the former then uses to cognitively adapt its actions. In order to predict the attacker’s future actions, a defender assesses the attacker’s inference using an *inverse Bayesian filter* (Krishnamurthy and Rangaswamy, 2019) that estimates the posterior distribution of the forward filter given noisy measurements of the attacker’s actions. In this context, Kalman filter (KF) is a well-known Bayesian filter for linear Gaussian systems, providing estimates optimal in the minimum mean-squared error (MMSE) sense. However, posterior computation becomes intractable for general non-linear and non-Gaussian systems. To address this, approximate approaches like the extended KF (EKF) (Anderson and Moore, 2012), unscented KF (UKF) (Julier and Uhlmann, 2004), and grid-based filters (Bucy and Senne, 1971) have been proposed, but these methods often perform poorly in high-dimensional and highly non-linear systems (Doucet et al., 2001).

EKF and UKF, being Gaussian filters, assume Gaussian state posteriors and are only applicable to systems with Gaussian noises (Li et al., 2017). While they provide closed-form analytic solutions for posteriors, their appropriateness varies by application, often failing

with highly non-linear models or multi-modal posteriors (Kotecha and Djuric, 2003b; Cappé et al., 2007). Techniques like Gaussian mixture (GM) (Alspach and Sorenson, 1972) or grid-based (Kramer and Sorenson, 1988) filters, proposed to mitigate these limitations, become computationally expensive in high-dimensional systems. The curse of dimensionality also affects deterministic numerical integration methods like cubature KF (CKF) (Arasaratnam and Haykin, 2009) and quadrature KF (QKF) (Ito and Xiong, 2000; Arasaratnam et al., 2007), making them difficult to implement for high-dimensional states, with the rate of convergence of the approximation error decreasing as the state dimension increases (Crisan and Doucet, 2002).

In practice, counter-adversarial applications are often non-linear and non-Gaussian, limiting the applicability of Gaussian approximations in EKF/UKF. Non-linear filtering methods that do not rely on this assumption use sequential importance sampling (SIS) and resampling Gordon et al. (1993), leading to sequential Monte Carlo (SMC) or particle filtering (PF) methods (Cappé et al., 2007). SMC methods employ random sampling to achieve asymptotically exact integral computation, though with higher computational complexity. PFs (Ristic et al., 2003; Arulampalam et al., 2002) are the most general and widely used SMC-based filters. Whereas EKF and UKF are local techniques for estimating posterior distributions at state estimates (Li et al., 2017), PFs use a global approximation approach. They start with a set of sample points representing the initial state distribution and propagate them through the actual nonlinear dynamics, with the ensemble of these samples providing an approximate posterior. Consequently, PFs are suitable for non-Gaussian dynamics and have been successfully applied to mobile robot localization (Fox et al., 1999), simultaneous localization and mapping (SLAM) (Montemerlo et al., 2003), and planning in partially observable environments (Somani et al., 2013). Additionally, quasi-MC methods (Guo and Wang, 2006; Avron et al., 2016) are deterministic alternatives to MC methods, using regularly distributed points rather than random ones to approximate the posterior. In this paper, we develop inverse filters using SMC-based techniques for estimating the attacker’s inference in highly non-linear, non-Gaussian counter-adversarial systems.

## 1.1 Prior Art

Our work is closely connected to a rich tradition of research in the development of PFs resulting in a vast body of literature. However, as detailed in the sequel, almost all previous studies have concentrated on forward filters. Following Gordon et al. (1993)’s bootstrap PF formulation, several variants of PFs have been developed for enhanced performance. Auxiliary PFs (Pitt and Shephard, 1999; Branchini and Elvira, 2021) direct particles to higher-density regions of the posterior distribution whereas unscented PFs (Van Der Merwe et al., 2000; Rui and Chen, 2001) include the current observation into proposal distribution using UKF. In Murphy and Russell (2001), Rao-Blackwellised PF is proposed for systems wherein the state can be partitioned such that the posterior distribution of one part is tractable conditioned on the other. Kurle et al. (2020) further generalizes Rao-Blackwellised PFs to switching linear Gaussian systems. On the other hand, high-dimensional systems can be efficiently handled by multiple PF (Djuric et al., 2007) and particle flow PFs (Bunch and Godsill, 2016; Li and Coates, 2017). In Vermaak et al. (2003), multiple targets are tracked using mixture PF models. The PF framework has also been used to implement Bernoulli

filters (Ristic et al., 2013) (for randomly switching systems), possibility PFs (Ristic et al., 2019) (for mismatched models), and probability hypothesis density (PHD) filters (Mahler, 2003) (for high-dimensional multi-object Bayesian inference).

Despite the fact that the Gaussianity assumption limits practical applications, it frequently presents a trade-off between accuracy and ease of implementation. Hence, SMC approaches have also been used in Gaussian systems. Gaussian PF (GPF) (Kotecha and Djuric, 2003b) assumes a Gaussian posterior and approximates its mean and covariance using the PF framework. In particular, the posterior mean and covariance estimates are computed from a set of randomly generated particles with associated weights based on SIS. GPF can be further viewed as an extension of the conventional Gaussian filters using the MC integration and Bayesian update rules (Wu et al., 2005). In Kotecha and Djuric (2003a), Gaussian-sum PFs (GSPFs) are developed for non-Gaussian systems. On the other hand, ensemble KF (EnKF) (Evensen, 2003; Katzfuss et al., 2016) is an MC extension of standard KF. EnKF approximates the state distribution by storing, propagating, and updating an ensemble of state vectors (Evensen, 2003). While the standard KF works with the entire state distribution explicitly, EnKF can be viewed as a form of dimension reduction wherein a small ensemble is propagated instead of the joint distribution with full covariance matrix (Katzfuss et al., 2016). In particular, EnKF, when combined with localization or covariance tapering techniques (Furrer and Bengtsson, 2007; Houtekamer and Mitchell, 2001; Furrer et al., 2006), leads to computationally tractable filters for very high-dimensional systems. Mixture KF (Chen and Liu, 2000) and MC-KF (Song, 2000) are two other examples that use latent variable representation to extend the KF framework to conditional linear Gaussian systems and discrete models, respectively. In Stordal et al. (2011), a hybrid PF-EnKF is also proposed that combines local KF-type update with PF’s weighting/resampling.

## 1.2 Connection of PFs with learning literature

Classical Bayesian filters assume known state-space models, but in many real-world applications, the state evolution and observation models contain unknown parameters that need to be estimated. PFs also rely heavily on accurate system dynamics and effective proposal densities. The simplest method for parameter estimation is augmenting the state with the unknown parameters, but this often results in poor parameter space exploration due to the pseudo-dynamic nature of the parameters (Ionides et al., 2006). A widely used PF-based Bayesian approach to parameter estimation is Particle Markov chain Monte Carlo (P-MCMC) (Andrieu et al., 2010; Lindsten et al., 2014), which combines SMC with MCMC sampling. P-MCMC is a likelihood-based batch-processing method using PF to obtain an unbiased estimate of data log-likelihood. Alternatively, SMC<sup>2</sup> estimates both parameters and latent states simultaneously with two layers of PF (Chopin et al., 2013), while Singh et al. (2023a) uses Fisher’s identity to approximate the log-likelihood gradient with PF. Variational inference (Bishop, 2006), another approach, employs parametric distributions to approximate the state posterior and jointly optimizes them with model parameters using a lower bound on the log-likelihood. Variational SMC methods (Maddison et al., 2017; Naesseth et al., 2018) use PF to construct this lower bound.

While the aforementioned methods work well when the system dynamics has a state-space representation, sometimes building probabilistic models itself is infeasible. For in-

stance, in robot localization with an onboard camera, the observation model is a probabilistic distribution over all possible camera images conditioned on a continuous robot state and given environment. Such an enormous observation space can not be represented using state-space models. Hence, machine learning (ML) techniques such as neural networks (NNs) and gradient descent have been suggested for learning both the model and PF’s proposal distribution, resulting in differentiable PFs (DPFs) (Karkus et al., 2018; Wen et al., 2021; Chen et al., 2021; Corenflos et al., 2021). Incorporating NN into Bayesian filters, particularly PFs, provides flexibility in model learning. Haarnoja et al. (2016) further proposed differentiable KF with Gaussian belief and end-to-end learnable measurement model whereas Chen et al. (2022) developed differentiable EnKF. Karl et al. (2016); Watter et al. (2015) learn the latent state space model from raw images for the long-term sequence prediction. In Okuma et al. (2004), mixture PF is integrated with Adaboost to learn proposal distributions for automatic multiple object tracking. In an IRL scenario (Samejima et al., 2003), PF is employed to estimate the internal parameters of an RL agent given a sequence of observable variables. Note that IRL passively learns the associated reward function based on the behavior of an expert. In contrast, the inverse cognition agent actively explores its adversarial agent and can thus be regarded as a generalization of IRL.

### 1.3 Comparisons with related work on inverse stochastic filters

In the context of inverse stochastic filtering, Mattila et al. (2020) examined finite state-space models and proposed an *inverse hidden Markov model* to estimate the adversary’s observations and observation likelihood. Krishnamurthy and Rangaswamy (2019) developed an *inverse KF* (I-KF) to estimate the defender’s state based on a forward KF’s estimation. For non-linear counter-adversarial systems, we recently developed *inverse extended KF* (I-EKF) and *inverse unscented KF* (I-UKF) in Singh et al. (2022, 2023b) and Singh et al. (2023d, 2024b), respectively. In the case of I-EKF, the adversary employs a forward EKF, which utilizes Taylor series expansion of the non-linear dynamics. As a result, EKF necessitates Jacobian computation, is susceptible to initialization/modeling errors, and performs poorly when significant non-linearities are present (Li et al., 2017). We addressed some of these shortcomings in the context of inverse cognition using advanced variants of I-EKF (Singh et al., 2023c). I-UKF, on the other hand, is an alternative derivative-free technique for efficiently dealing with nonlinear systems. Based on the unscented transform, UKF (Julier and Uhlmann, 2004) uses a weighted sum of function evaluations at a finite number of deterministic sigma points and approximates the posterior distribution of a random variable under non-linear transformation. CKF (Arasaratnam and Haykin, 2009) and QKF (Ito and Xiong, 2000; Arasaratnam et al., 2007) are further examples of derivative-free nonlinear filters that use efficient numerical integration techniques to compute the Bayesian recursive integrals. These formulations for inverse CKF and QKF were proposed and studied recently in Singh et al. (2024a). However, the inverses of PFs have remained unexamined in prior works.

### 1.4 Our Contributions

Our main contributions in this paper are as follows:

- 1) **Inverse PF.** Gaussian inverse filters such as I-EKF (Singh et al., 2023b) and I-UKF

(Singh et al., 2024b) are not applicable to general non-Gaussian systems. To address this, we develop inverse PF (I-PF). At the  $k$ -th time instant, our I-PF considers the joint conditional distribution of the attacker’s current state estimate and observation given the defender’s knowledge of its own true states and observations of the attacker’s actions up to the current instant. Initially, we assume perfect system model information, including a general but known forward filter at the defender’s end. Our I-PF seeks to empirically approximate the optimal inverse filter’s (joint) posterior and samples the particles from the optimal importance sampling density. This is in contrast to the typical PF, where the optimal density is often unavailable. The known forward filter assumption allows sampling from the optimal density in I-PF; see also Remark 2.

**2) Convergence of I-PF.** In PFs, the particles interact and are not statistically independent, rendering classical convergence results for Monte Carlo methods, which rely on central limit theorems under i.i.d. assumptions, inapplicable. Despite this, it is essential to study PFs’ convergence to the true posterior as they approximate optimal filters. In this work, we examine the convergence of our proposed inverse particle filter (I-PF) in the  $L^4$ -sense. Specifically, we demonstrate that our I-PF’s estimates converge to the optimal inverse filter’s estimates for bounded observation densities, given that the estimated function grows at a slower rate than the defender’s observation density. Moreover, convergence in the  $L^4$ -sense implies almost sure convergence of our I-PF to the optimal inverse filter’s posterior.

**3) Inverse GPF and EnKF.** We next explore SMC approaches for Gaussian approximations in the inverse filtering context. To this end, we develop inverse GPF (I-GPF) and inverse EnKF (I-EnKF). Note that EnKF implicitly assumes linear Gaussian state-space models. In fact, for linear Gaussian systems, EnKF’s estimates converge in probability to KF’s estimates as the ensemble size grows (Butala et al., 2008). Hence, in our work, we develop I-EnKF considering non-linear systems with additive Gaussian noises. On the other hand, I-GPF and I-PF consider general probabilistic system dynamics. While I-GPF, like I-PF, also considers a general forward filter, I-EnKF follows the inverse filtering framework of I-KF (Krishnamurthy and Rangaswamy, 2019), I-EKF (Singh et al., 2023b) and I-UKF (Singh et al., 2024b). In particular, I-EnKF assumes a forward EnKF employed by the attacker, while I-KF, I-EKF, and I-UKF, respectively, assume forward KF, EKF, and UKF.

**4) Generalization to non-Gaussian systems.** Prior inverse Gaussian filters, I-KF (Krishnamurthy and Rangaswamy, 2019), I-EKF (Singh et al., 2023b) and I-UKF (Singh et al., 2024b), assumed additive Gaussian noises. However, under certain conditions, GPF and, hence, I-GPF can be applied to non-Gaussian systems as well. Similarly, EnKF shows remarkable robustness to deviations from the Gaussianity assumption and has been successfully applied to many extremely high-dimensional, non-linear, and non-Gaussian problems (Katzfuss et al., 2016). To efficiently handle non-Gaussian and highly non-linear systems, maximum correntropy and maximum likelihood EnKFs have also been proposed in Tao et al. (2023) and Zupanski (2005), respectively. In this work, we also generalize our I-GPF and I-EnKF formulations to non-Gaussian systems. To this end, we consider Gaussian mixture (GM) (Kotecha and Djuric, 2003a) and maximum correntropy criterion (MCC) (Izanloo et al., 2016) to modify I-GPF and I-EnKF and obtain inverse GSPF (I-GSPF) and MCC-modified I-EnKF, respectively.

**5) Unknown system dynamics.** The applications of the aforementioned inverse filters,

including prior works (Krishnamurthy and Rangaswamy, 2019; Singh et al., 2023b, 2024b) are limited to cases when perfect system information is available. However, in practical counter-adversarial systems, the forward filter and the strategy adopted by the attacker to adapt its actions may not be known to the defender. Similarly, the attacker may not have complete information about the defender’s state evolution. We address this case of unknown dynamics by proposing differentiable I-PF, differentiable I-EnKF, and reproducing kernel Hilbert space (RKHS)-based EnKF (RKHS-EnKF). Recall that DPF and differentiable EnKF are differentiable implementations of PF and EnKF, respectively, that exploit NNs to learn the system dynamics. On the other hand, RKHS-EnKF considers non-linear state-space dynamics with the state-transition and observation models unknown to the agent employing the stochastic filter. Finally, our numerical experiments show that the proposed filters provide accurate estimates even when assuming a forward filter other than the attacker’s actual forward filter.

The rest of the paper is organized as follows. The next section describes the system model and develops the optimal inverse filter recursions. In Section 3, we develop I-PF and also provide its convergence results. I-GPF and I-EnKF are then developed in Section 4 while Section 5 addresses the unknown system case. We discuss numerical experiments for the proposed filters’ performance in Section 6, before concluding in Section 7.

Throughout the paper, we reserve boldface lowercase and uppercase letters for vectors (column vectors) and matrices, respectively, and  $\{a_i\}_{i_1 \leq i \leq i_2}$  denotes a set of elements indexed by an integer  $i$ . The notation  $[\mathbf{a}]_i$  is used to denote the  $i$ -th component of vector  $\mathbf{a}$ . The transpose operation is  $(\cdot)^T$ , expectation operation is  $\mathbb{E}[\cdot]$  and the  $l_2$  norm of a vector is  $\|\cdot\|$ . The notation  $\|f\|_\infty$  denotes the supremum norm of the real-valued function  $f(\cdot)$ . Also,  $\mathbf{I}_n$  and  $\mathbf{0}$  denote a ‘ $n \times n$ ’ identity matrix and an all-zero matrix, respectively. The function  $\delta(x - x_0)$  is the Dirac-delta function in variable  $x$  centered at  $x_0$ . The Gaussian distribution is represented as  $\mathcal{N}(\mathbf{x}; \boldsymbol{\mu}, \mathbf{Q})$  with mean  $\boldsymbol{\mu}$  and covariance matrix  $\mathbf{Q}$  while  $\mathcal{U}[a, b]$  represents a uniform distribution over interval  $[a, b]$ . We use shorthand  $\mathbb{P}(\mathbf{X} \in d\mathbf{x})$  to refer to the probability of random variable  $\mathbf{X} \in [\mathbf{x}, \mathbf{x} + d\mathbf{x}]$ , where  $d\mathbf{x}$  is an infinitesimal interval length.

## 2 Optimal Inverse Filter

Before considering the approximate approaches in subsequent sections, we first derive the optimal Bayesian recursions for the inverse filtering problem. We consider a general probabilistic framework for the attacker-defender dynamics in Section 2.1. The optimal inverse filter recursions are provided in Section 2.2.

### 2.1 System model

Consider the ‘ $n_x$ ’-dimensional stochastic process  $\mathbf{X} = \{\mathbf{X}_k\}_{k \geq 0}$  as the defender’s state evolution process. The defender perfectly knows its state  $\mathbf{x}_k \in \mathbb{R}^{n_x \times 1}$  for all  $k \geq 0$ . The process  $\mathbf{X}$  is a Markov process with initial state  $\mathbf{X}_0 \sim \pi_0^x(d\mathbf{x}_0)$  and evolves as

$$\mathbb{P}(\mathbf{X}_{k+1} \in d\mathbf{x}_{k+1} | \mathbf{X}_k = \mathbf{x}_k) = \mathcal{K}(\mathbf{x}_{k+1} | \mathbf{x}_k) d\mathbf{x}_{k+1}, \quad (1)$$

where  $\mathcal{K}(\cdot)$  denotes the transition kernel density (with respect to a Lebesgue measure). The attacker observes the defender’s state as a ‘ $n_y$ ’-dimensional observation process  $\mathbf{Y} = \{\mathbf{Y}_k\}_{k \geq 1}$ . The observations  $\mathbf{Y}$  are conditionally independent given  $\mathbf{X}$  with

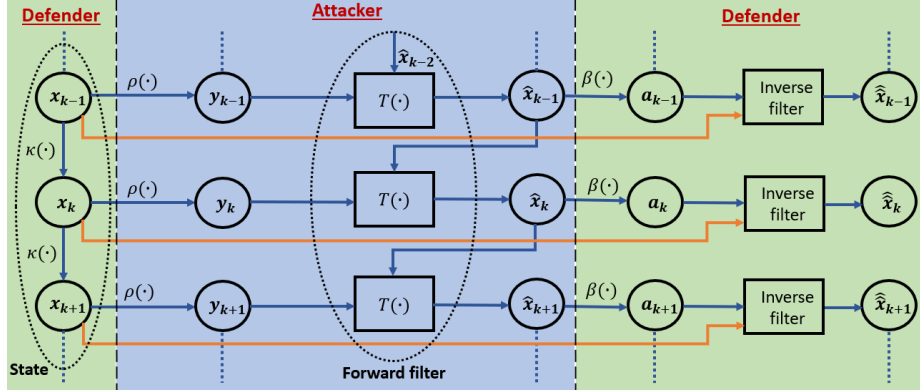


Figure 1: Graphical representation of the forward and inverse filters' recursions.

$$\mathbb{P}(\mathbf{Y}_k \in d\mathbf{y}_k | \mathbf{X}_k = \mathbf{x}_k) = \rho(\mathbf{y}_k | \mathbf{x}_k) d\mathbf{y}_k, \quad (2)$$

where  $\rho(\cdot)$  is the attacker's conditional observation density and  $k$ -th observation  $\mathbf{y}_k \in \mathbb{R}^{n_y \times 1}$ .

The attacker computes an estimate  $\hat{\mathbf{x}}_k$  of the defender's state  $\mathbf{x}_k$  given the available observations  $\{\mathbf{y}_j\}_{1 \leq j \leq k}$  using the forward filter. Consider  $\hat{\mathbf{X}} = \{\hat{\mathbf{X}}_k\}_{k \geq 0}$  as the attacker's state estimation process. The forward filter recursively computes the current estimate  $\hat{\mathbf{x}}_k$  from the previous estimate  $\hat{\mathbf{x}}_{k-1}$  and current observation  $\mathbf{y}_k$  in a deterministic manner as

$$\hat{\mathbf{x}}_k = T(\hat{\mathbf{x}}_{k-1}, \mathbf{y}_k). \quad (3)$$

For instance,  $T(\cdot)$  represents the standard EKF/UKF recursive update if the attacker employs a forward EKF/UKF to compute state estimate  $\hat{\mathbf{x}}_k$ . Note that  $T(\cdot)$  can be a time-dependent function for many forward filters. In the case of EKF/UKF, the mapping  $T(\cdot)$  at the  $k$ -th time instant depends on the covariance matrix estimate computed at the previous  $(k-1)$ -th time instant. For the sake of brevity, we simply denote the forward filter recursion as in (3) but implement the appropriate function for the given time instant. The attacker then uses the estimate  $\hat{\mathbf{x}}_k$  to administer an action which the defender observes as a ' $n_a$ '-dimensional noisy observation process  $\mathbf{A} = \{\mathbf{A}_k\}_{k \geq 1}$ . Given  $\hat{\mathbf{X}}$ , the observations  $\mathbf{A}$  are conditionally independent and

$$\mathbb{P}(\mathbf{A}_k \in d\mathbf{a}_k | \hat{\mathbf{X}}_k = \hat{\mathbf{x}}_k) = \beta(\mathbf{a}_k | \hat{\mathbf{x}}_k) d\mathbf{a}_k, \quad (4)$$

where  $\beta(\cdot)$  is the defender's conditional observation density and the  $k$ -th observation  $\mathbf{a}_k \in \mathbb{R}^{n_a \times 1}$ . Finally, the defender uses  $\{\mathbf{a}_j, \mathbf{x}_j\}_{1 \leq j \leq k}$  to compute the estimate  $\hat{\hat{\mathbf{x}}}_k \in \mathbb{R}^{n_x \times 1}$  of  $\hat{\mathbf{x}}_k$  in the inverse filter. Fig. 1 graphically illustrates the system dynamics for inverse filtering.

In Sections 3-4, we assume that both defender and attacker have perfect knowledge of the system model, i.e., the densities  $\mathcal{K}(\cdot)$ ,  $\rho(\cdot)$  and  $\beta(\cdot)$ . Additionally, the defender assumes a known forward filter  $T(\cdot)$  employed by the attacker. We address the unknown system dynamics case in Section 5 wherein we estimate both the state and the model parameters. Furthermore, our numerical experiments in Section 6 show that the developed inverse filters provide reasonably accurate estimates even when assuming a simple forward EKF, regardless of the attacker's actual forward filter.

*Example:* Consider the special case of additive system noises such that the state evolution and observations are modeled as



$$\mathbf{x}_{k+1} = f(\mathbf{x}_k) + \mathbf{w}_k, \quad (5)$$

$$\mathbf{y}_k = h(\mathbf{x}_k) + \mathbf{v}_k, \quad (6)$$

$$\mathbf{a}_k = g(\hat{\mathbf{x}}_k) + \boldsymbol{\epsilon}_k. \quad (7)$$

Here,  $f(\cdot)$ ,  $h(\cdot)$  and  $g(\cdot)$  represent a general non-linear system dynamics while  $\{\mathbf{w}_k\}$ ,  $\{\mathbf{v}_k\}$  and  $\{\boldsymbol{\epsilon}_k\}$  are mutually independent noise terms. If the probability density functions of  $\mathbf{w}_k$ ,  $\mathbf{v}_k$  and  $\boldsymbol{\epsilon}_k$  are denoted by  $p_w(\cdot)$ ,  $p_v(\cdot)$  and  $p_\epsilon(\cdot)$ , respectively, then  $\mathcal{K}(\mathbf{x}_{k+1}|\mathbf{x}_k) = p_w(\mathbf{x}_{k+1} - f(\mathbf{x}_k))$ ,  $\rho(\mathbf{y}_k|\mathbf{x}_k) = p_v(\mathbf{y}_k - h(\mathbf{x}_k))$ , and  $\beta(\mathbf{a}_k|\hat{\mathbf{x}}_k) = p_\epsilon(\mathbf{a}_k - g(\hat{\mathbf{x}}_k))$ .

## 2.2 Optimal Inverse filter

Consider the (joint) conditional distribution of  $(\hat{\mathbf{x}}_k, \mathbf{y}_k)$  given the defender's knowledge of its own true states and observations of the attacker's actions at the  $k$ -th time instant. As in forward Bayesian filter, the optimal inverse filter computes this conditional distribution recursively using the time and measurement updates. Define the conditional distributions  $\pi_{k|k-1}(d\hat{\mathbf{x}}_k, d\mathbf{y}_k)$  and  $\pi_{k|k}(d\hat{\mathbf{x}}_k, d\mathbf{y}_k)$  as

$$\pi_{k|k-1}(d\hat{\mathbf{x}}_k, d\mathbf{y}_k) \doteq p(\hat{\mathbf{x}}_k, \mathbf{y}_k|\mathbf{x}_{0:k}, \mathbf{a}_{1:k-1})d\hat{\mathbf{x}}_k d\mathbf{y}_k, \quad (8)$$

$$\pi_{k|k}(d\hat{\mathbf{x}}_k, d\mathbf{y}_k) \doteq p(\hat{\mathbf{x}}_k, \mathbf{y}_k|\mathbf{x}_{0:k}, \mathbf{a}_{1:k})d\hat{\mathbf{x}}_k d\mathbf{y}_k. \quad (9)$$

In the time-update step, we obtain  $\pi_{k|k-1}$  from  $\pi_{k-1|k-1}$  considering the true states  $\mathbf{x}_{0:k}$  but observations  $\mathbf{a}_{1:k-1}$  excluding the current observation  $\mathbf{a}_k$ . Finally,  $\pi_{k|k-1}$  is updated using the current observation  $\mathbf{a}_k$  in the measurement update step to obtain  $\pi_{k|k}$ . The defender's MMSE estimate  $\hat{\mathbf{x}}_k$  is then  $\hat{\mathbf{x}}_k = \iint \hat{\mathbf{x}}_k \pi_{k|k}(d\hat{\mathbf{x}}_k, d\mathbf{y}_k)$ .

First, we consider the optimal filter's time update. We have

$$p(\hat{\mathbf{x}}_k, \mathbf{y}_k|\mathbf{x}_{0:k}, \mathbf{a}_{1:k-1}) = \int p(\hat{\mathbf{x}}_k, \mathbf{y}_k|\mathbf{x}_{0:k}, \mathbf{a}_{1:k-1}, \hat{\mathbf{x}}_{k-1})p(\hat{\mathbf{x}}_{k-1}|\mathbf{x}_{0:k}, \mathbf{a}_{1:k-1})d\hat{\mathbf{x}}_{k-1}. \quad (10)$$

However,  $p(\hat{\mathbf{x}}_k, \mathbf{y}_k|\mathbf{x}_{0:k}, \mathbf{a}_{1:k-1}, \hat{\mathbf{x}}_{k-1}) = p(\hat{\mathbf{x}}_k|\mathbf{y}_k, \mathbf{x}_{0:k}, \mathbf{a}_{1:k-1}, \hat{\mathbf{x}}_{k-1})p(\mathbf{y}_k|\mathbf{x}_{0:k}, \mathbf{a}_{1:k-1}, \hat{\mathbf{x}}_{k-1}) = p(\hat{\mathbf{x}}_k|\mathbf{y}_k, \hat{\mathbf{x}}_{k-1})p(\mathbf{y}_k|\mathbf{x}_k)$ , because observation  $\mathbf{y}_k$  is conditionally independent given state  $\mathbf{x}_k$  with  $p(\mathbf{y}_k|\mathbf{x}_k)$  given by (2). Also, the estimate  $\hat{\mathbf{x}}_k$  is independent of  $\{\mathbf{x}_{0:k}, \mathbf{a}_{1:k-1}\}$  given  $\{\mathbf{y}_k, \hat{\mathbf{x}}_{k-1}\}$ . In particular,  $\hat{\mathbf{x}}_k$  is a deterministic function of  $\mathbf{y}_k$  and  $\hat{\mathbf{x}}_{k-1}$  such that  $p(\hat{\mathbf{x}}_k|\mathbf{y}_k, \hat{\mathbf{x}}_{k-1}) = \delta(\hat{\mathbf{x}}_k - T(\hat{\mathbf{x}}_{k-1}, \mathbf{y}_k))$ . Hence, (10) yields

$$p(\hat{\mathbf{x}}_k, \mathbf{y}_k|\mathbf{x}_{0:k}, \mathbf{a}_{1:k-1}) = \int \delta(\hat{\mathbf{x}}_k - T(\hat{\mathbf{x}}_{k-1}, \mathbf{y}_k))\rho(\mathbf{y}_k|\mathbf{x}_k)p(\hat{\mathbf{x}}_{k-1}|\mathbf{x}_{0:k}, \mathbf{a}_{1:k-1})d\hat{\mathbf{x}}_{k-1}. \quad (11)$$

Now,  $p(\hat{\mathbf{x}}_{k-1}, \mathbf{y}_{k-1}|\mathbf{x}_{0:k}, \mathbf{a}_{1:k-1}) = p(\hat{\mathbf{x}}_{k-1}, \mathbf{y}_{k-1}|\mathbf{x}_{0:k-1}, \mathbf{a}_{1:k-1})$  because  $\{\hat{\mathbf{x}}_{k-1}, \mathbf{y}_{k-1}\}$  do not depend on future state  $\mathbf{x}_k$  given  $\mathbf{x}_{0:k-1}$  and  $\mathbf{a}_{1:k-1}$ . Hence, using this and (9), we have the marginal distribution  $\mathbb{P}(\hat{\mathbf{x}}_{k-1} \in d\hat{\mathbf{x}}_{k-1}|\mathbf{x}_{0:k}, \mathbf{a}_{1:k-1}) = \int \pi_{k-1|k-1}(d\hat{\mathbf{x}}_{k-1}, d\mathbf{y}_{k-1})$ . Substituting in (11), the optimal time update becomes

$$p(\hat{\mathbf{x}}_k, \mathbf{y}_k|\mathbf{x}_{0:k}, \mathbf{a}_{1:k-1}) = \iint \delta(\hat{\mathbf{x}}_k - T(\hat{\mathbf{x}}_{k-1}, \mathbf{y}_k))\rho(\mathbf{y}_k|\mathbf{x}_k)\pi_{k-1|k-1}(d\hat{\mathbf{x}}_{k-1}, d\mathbf{y}_{k-1}). \quad (12)$$

Now, consider the measurement update with current observation  $\mathbf{a}_k$ . The joint conditional distribution  $p(\hat{\mathbf{x}}_k, \mathbf{y}_k, \mathbf{a}_k|\mathbf{x}_{0:k}, \mathbf{a}_{1:k-1}) = \beta(\mathbf{a}_k|\hat{\mathbf{x}}_k)\pi_{k|k-1}(d\hat{\mathbf{x}}_k, d\mathbf{y}_k)$  because observation  $\mathbf{a}_k$  is conditionally independent of everything else given  $\hat{\mathbf{x}}_k$  with  $p(\mathbf{a}_k|\hat{\mathbf{x}}_k)$  given by (4). Hence, using Bayes' theorem, we have

Table 1: Summary of different variables and distributions.

Notation	Description
$\mathbf{x}_k$	Defender's state at $k$ -th time instant ( $\in \mathbb{R}^{n_x \times 1}$ )
$\mathbf{y}_k$	Attacker's observation of $\mathbf{x}_k$ at $k$ -th time instant ( $\in \mathbb{R}^{n_y \times 1}$ )
$\mathbf{a}_k$	Defender's observation of attacker's action at $k$ -th time instant ( $\in \mathbb{R}^{n_a \times 1}$ )
$\hat{\mathbf{x}}_k$	Attacker's estimate of $\mathbf{x}_k$ computed via forward filter
$\hat{\hat{\mathbf{x}}}_k$	Defender's estimate of $\hat{\mathbf{x}}_k$ computed via inverse filter
$\pi_0^x(d\mathbf{x}_0)$	Defender's initial state distribution
$\mathcal{K}(\cdot)$	Transitional kernel density for defender's state evolution
$\rho(\cdot)$	Attacker's conditional observation density
$T(\cdot, \cdot)$	Forward filter's recursive update
$\beta(\cdot)$	Defender's conditional observation density
$\pi_{k k-1}(d\hat{\mathbf{x}}_k, d\mathbf{y}_k)$	Optimal inverse filter's prediction distribution, i.e., joint conditional density of $(\hat{\mathbf{x}}_k, \mathbf{y}_k)$ given true states $\mathbf{x}_{0:k}$ (upto time $k$ ) and observations $\mathbf{a}_{1:k-1}$ (upto time $k-1$ )
$\pi_{k k}(d\hat{\hat{\mathbf{x}}}_k, d\mathbf{y}_k)$	Optimal inverse filter's posterior distribution, i.e., joint conditional density of $(\hat{\hat{\mathbf{x}}}_k, \mathbf{y}_k)$ given true states $\mathbf{x}_{0:k}$ (upto time $k$ ) and observations $\mathbf{a}_{1:k}$ (upto time $k$ )

$$\pi_{k|k}(d\hat{\hat{\mathbf{x}}}_k, d\mathbf{y}_k) = \frac{\beta(\mathbf{a}_k|\hat{\mathbf{x}}_k)\pi_{k|k-1}(d\hat{\mathbf{x}}_k, d\mathbf{y}_k)}{\iint \beta(\mathbf{a}_k|\hat{\mathbf{x}}_k)\pi_{k|k-1}(d\hat{\mathbf{x}}_k, d\mathbf{y}_k)}, \quad (13)$$

which is the optimal measurement update. Table 1 summarizes all the variables and distributions defined throughout this section.

In general, the defender estimates a function  $\phi(\hat{\mathbf{x}}, \mathbf{y})$  as  $\mathbb{E}[\phi(\hat{\mathbf{x}}, \mathbf{y})|\mathbf{x}_{0:k}, \mathbf{a}_{1:k}]$  using the inverse filter's posterior distribution. For instance, considering  $\phi(\hat{\mathbf{x}}, \mathbf{y}) = \hat{\mathbf{x}}$  yields the defender's MMSE estimate  $\hat{\hat{\mathbf{x}}}_k$  of  $\hat{\mathbf{x}}_k$ . For the sake of the convergence analysis in Section 3.2, we now introduce some simplified notations for the integrals involved in the optimal filter recursions. Given a measure  $\nu$ , a function  $\phi$  and a Markov transition kernel  $\mathcal{K}$ , we define

$$\langle \nu, \phi \rangle \doteq \int \phi(x)\nu(dx), \quad \mathcal{K}\phi(x) \doteq \int \phi(z)\mathcal{K}(dz|x).$$

With this notation, the optimal filter recursions (12) and (13) can be expressed as

$$\langle \pi_{k|k-1}, \phi \rangle = \langle \pi_{k-1|k-1}, \delta_T \rho \phi \rangle, \quad (14)$$

$$\langle \pi_{k|k}, \phi \rangle = \frac{\langle \pi_{k|k-1}, \beta \phi \rangle}{\langle \pi_{k|k-1}, \beta \rangle}, \quad (15)$$

where  $\delta_T$  denotes function  $\delta(\hat{\mathbf{x}}_k - T(\hat{\mathbf{x}}_{k-1}, \mathbf{y}_k))$ . For brevity, we drop the time parameter  $k$  in our notation  $\delta_T$ , but while implementing, the given time-instant is taken into consideration. Note that the optimal inverse filter exists only if  $\langle \pi_{k|k-1}, \beta \rangle > 0$ .

### 3 Inverse PF

In PF, the posterior distribution is approximated using an empirical distribution from a set of samples/particles with associated weights, evolving randomly in time according to the system dynamics. Such an approximation simplifies the computation of integrals to finite sums. The particles are sampled from a suitable importance density and resampled to avoid particle degeneracy (Ristic et al., 2003; Arulampalam et al., 2002). This SIS algorithm is also known as bootstrap filtering (Gordon et al., 1993), condensation algorithm (MacCormick and Blake, 2000), and interacting particle approximations (Del Moral, 1998). In the following, we first develop the I-PF recursions applying the SIS and resampling methods for the defender-attacker dynamics, analogous to the standard PF. For further details on the SIS-based filtering methods, we refer the readers to Arulampalam et al. (2002) and Chen et al. (2003). Finally, in Section 3.2, we study the convergence of the proposed I-PF to the optimal filter (14)-(15) as the number of particles increases.

#### 3.1 I-PF formulation

Consider  $N$  as the total number of particles. As noted earlier in Section 2.2, in I-PF, we approximate the (joint) posterior distribution of  $(\hat{\mathbf{x}}_k, \mathbf{y}_k)$  at  $k$ -th time instant as

$$p(\hat{\mathbf{x}}_k, \mathbf{y}_k | \mathbf{x}_{0:k}, \mathbf{a}_{1:k}) \approx \sum_{i=1}^N \omega_k^i \delta(\hat{\mathbf{x}}_k - \hat{\mathbf{x}}_k^i, \mathbf{y}_k - \mathbf{y}_k^i),$$

where  $\{\hat{\mathbf{x}}_k^i, \mathbf{y}_k^i\}_{1 \leq i \leq N}$  are the current particles with associated importance weights  $\{\omega_k^i\}_{1 \leq i \leq N}$  and the defender knows  $\mathbf{x}_{0:k}$  and  $\mathbf{a}_{1:k}$ . To this end, we first consider the joint conditional density  $p(\hat{\mathbf{x}}_{0:k}, \mathbf{y}_{1:k} | \mathbf{x}_{0:k}, \mathbf{a}_{1:k})$ , which we approximate using particles  $\{\hat{\mathbf{x}}_{0:k}^i, \mathbf{y}_{1:k}^i\}_{1 \leq i \leq N}$ . The particle  $(\hat{\mathbf{x}}_k^i, \mathbf{y}_k^i)$  for approximating the marginal distribution  $p(\hat{\mathbf{x}}_k, \mathbf{y}_k | \mathbf{x}_{0:k}, \mathbf{a}_{1:k})$  is then simply the sub-vector corresponding to  $(\hat{\mathbf{x}}_k, \mathbf{y}_k)$  in the  $i$ -th particle  $(\hat{\mathbf{x}}_{0:k}^i, \mathbf{y}_{1:k}^i)$ . Furthermore, as we will show eventually, our I-PF algorithm only requires storing particles  $\{\hat{\mathbf{x}}_k^i\}$ , i.e., the previous particles  $\{\hat{\mathbf{x}}_{0:k-1}^i, \mathbf{y}_{1:k-1}^i\}$  and the current observation particles  $\{\mathbf{y}_k^i\}$  are discarded. Denote  $q(\cdot)$  as the chosen importance sampling density. Based on the importance sampling method (Ristic et al., 2003), the weights are computed as

$$\omega_k^i = \frac{p(\hat{\mathbf{x}}_{0:k}^i, \mathbf{y}_{1:k}^i | \mathbf{x}_{0:k}, \mathbf{a}_{1:k})}{q(\hat{\mathbf{x}}_{0:k}^i, \mathbf{y}_{1:k}^i | \mathbf{x}_{0:k}, \mathbf{a}_{1:k})}, \quad (16)$$

for  $i = 1, 2, \dots, N$ . In our inverse filtering problem, the joint density simplifies to

$$p(\hat{\mathbf{x}}_{0:k}, \mathbf{y}_{1:k} | \mathbf{x}_{0:k}, \mathbf{a}_{1:k}) \propto p(\mathbf{a}_k | \hat{\mathbf{x}}_k) p(\hat{\mathbf{x}}_k | \hat{\mathbf{x}}_{k-1}, \mathbf{y}_k) p(\mathbf{y}_k | \mathbf{x}_k) p(\hat{\mathbf{x}}_{0:k-1}, \mathbf{y}_{1:k-1} | \mathbf{x}_{0:k-1}, \mathbf{a}_{1:k-1}). \quad (17)$$

Furthermore, analogous to the standard PF (Ristic et al., 2003), we choose a sampling density  $q(\cdot)$  that factorizes as

$$q(\hat{\mathbf{x}}_{0:k}, \mathbf{y}_{1:k} | \mathbf{x}_{0:k}, \mathbf{a}_{1:k}) = q(\hat{\mathbf{x}}_k, \mathbf{y}_k | \hat{\mathbf{x}}_{k-1}, \mathbf{y}_{k-1}, \mathbf{x}_k, \mathbf{a}_k) q(\hat{\mathbf{x}}_{0:k-1}, \mathbf{y}_{1:k-1} | \mathbf{x}_{0:k-1}, \mathbf{a}_{1:k-1}). \quad (18)$$

We provide the detailed steps to obtain (17) and (18) in Appendix A. Substituting (17) and (18) in (16), the optimal weights simplifies to

$$\omega_k^i \propto \omega_{k-1}^i \frac{p(\mathbf{a}_k | \hat{\mathbf{x}}_k^i) p(\hat{\mathbf{x}}_k^i | \hat{\mathbf{x}}_{k-1}^i, \mathbf{y}_k^i) p(\mathbf{y}_k^i | \mathbf{x}_k)}{q(\hat{\mathbf{x}}_k^i, \mathbf{y}_k^i | \hat{\mathbf{x}}_{k-1}^i, \mathbf{y}_{k-1}^i, \mathbf{x}_k, \mathbf{a}_k)}, \quad (19)$$

However, for this choice of importance density, the variance of weights can only increase over time resulting in particle degeneracy (Doucet et al., 2000), i.e., with time, all but one particle will have negligible weights. To this end, resampling is employed to eliminate particles with small weights and multiply the ones with large weights. The optimal  $q(\cdot)$  that minimizes the variance of weights (19) can be trivially obtained as (Doucet et al., 2000)

$$q^*(\hat{\mathbf{x}}_k, \mathbf{y}_k | \hat{\mathbf{x}}_{k-1}, \mathbf{y}_{k-1}, \mathbf{x}_k, \mathbf{a}_k) = p(\hat{\mathbf{x}}_k, \mathbf{y}_k | \hat{\mathbf{x}}_{k-1}, \mathbf{y}_{k-1}, \mathbf{x}_k, \mathbf{a}_k) \approx p(\hat{\mathbf{x}}_k | \hat{\mathbf{x}}_{k-1}, \mathbf{y}_k) p(\mathbf{y}_k | \mathbf{x}_k), \quad (20)$$

where we have ignored the correlation between attacker's observation  $\mathbf{y}_k$  and defender's observation  $\mathbf{a}_k$  via state estimate  $\hat{\mathbf{x}}_k$  and hence, the approximation. The perfect knowledge of distribution  $p(\mathbf{y}_k | \mathbf{x}_k)$  from (2) can compensate for this approximation to some extent. With  $q^*(\cdot)$  as the sampling density, the weights are computed from (19) as

$$\omega_k^i \propto \omega_{k-1}^i p(\mathbf{a}_k | \hat{\mathbf{x}}_k^i). \quad (21)$$

**I-PF recursions:** Consider the sampling density  $q^*(\cdot)$  from (20). We have  $p(\hat{\mathbf{x}}_k | \hat{\mathbf{x}}_{k-1}, \mathbf{y}_k) = \delta(\hat{\mathbf{x}}_k - T(\hat{\mathbf{x}}_{k-1}, \mathbf{y}_k))$  from (3) and  $p(\mathbf{y}_k | \mathbf{x}_k)$  is given by (2). Here, we consider resampling at each time step and  $p(\mathbf{a}_k | \hat{\mathbf{x}}_k)$  in (21) is given by (4). Note that particles  $\{\mathbf{y}_k^i\}$  are sampled from (2) using the true state  $\mathbf{x}_k$  only. Further, since defender knows  $\mathbf{x}_k$ , density (20) and weights (21) do not require previous particles  $\{\mathbf{y}_{k-1}^i\}$  and hence, they need not be stored for the next recursion.

Initialize  $\hat{\mathbf{x}}_0^i \sim \tilde{\pi}_0^x(d\hat{\mathbf{x}}_0)$  where  $\tilde{\pi}_0^x$  is the initial distribution assumed by the defender for the forward filter's initial estimate  $\hat{\mathbf{x}}_0$ . At time  $(k-1)$ , we have particles  $\{\hat{\mathbf{x}}_{k-1}^i\}_{1 \leq i \leq N}$  with equal weights  $(1/N)$  because of resampling. Finally, the I-PF recursions to compute the updated particles  $\{\hat{\mathbf{x}}_k^i\}_{1 \leq i \leq N}$  are as follows.

1. *SIS:* For  $i = 1, 2, \dots, N$ , draw i.i.d. observation particles  $\bar{\mathbf{y}}_k^i \sim \rho(\mathbf{y}_k | \mathbf{x}_k)$  and then obtain state estimate particles  $\hat{\mathbf{x}}_k^i = T(\hat{\mathbf{x}}_{k-1}^i, \bar{\mathbf{y}}_k^i)$ .
2. *Modification:* For a given threshold  $\gamma_k > 0$ , check if  $\frac{1}{N} \sum_{i=1}^N \beta(\mathbf{a}_k | \hat{\mathbf{x}}_k^i) \geq \gamma_k$ . If the inequality is satisfied, we proceed to step 3 (similar to standard PF), otherwise, we return to the previous step and redraw particles from the sampling density.
3. *Weight computation:* Set  $\hat{\mathbf{x}}_k^i = \hat{\mathbf{x}}_k^i$  and  $\tilde{\mathbf{y}}_k^i = \bar{\mathbf{y}}_k^i$  for  $i = 1, 2, \dots, N$ . These particles estimate the prediction distribution  $\pi_{k|k-1}$  as

$$\pi_{k|k-1} \approx \tilde{\pi}_{k|k-1}^N(d\hat{\mathbf{x}}_k, d\mathbf{y}_k) \doteq \frac{1}{N} \sum_{i=1}^N \delta(\hat{\mathbf{x}}_k - \hat{\mathbf{x}}_k^i, \mathbf{y}_k - \tilde{\mathbf{y}}_k^i) d\hat{\mathbf{x}}_k d\mathbf{y}_k.$$

Since particles  $\{\hat{\mathbf{x}}_k^i, \tilde{\mathbf{y}}_k^i\}$  have equal weights due to resampling, using (21), we compute the weights as

$$\tilde{\omega}_k^i = \beta(\mathbf{a}_k | \hat{\mathbf{x}}_k^i), \quad i = 1, 2, \dots, N,$$

and normalize  $\omega_k^i = \tilde{\omega}_k^i / \sum_{j=1}^N \tilde{\omega}_k^j$ . Using  $\{\hat{\mathbf{x}}_k^i, \tilde{\mathbf{y}}_k^i\}$  with weights  $\{\omega_k^i\}$ , we obtain the approximate posterior distribution

$$\pi_{k|k} \approx \tilde{\pi}_{k|k}^N(d\hat{\mathbf{x}}_k, d\mathbf{y}_k) \doteq \sum_{i=1}^N \omega_k^i \delta(\hat{\mathbf{x}}_k - \hat{\mathbf{x}}_k^i, \mathbf{y}_k - \tilde{\mathbf{y}}_k^i) d\hat{\mathbf{x}}_k d\mathbf{y}_k.$$

4. *Resampling*: Resample the particles by drawing  $N$  independent particles as  $(\hat{\mathbf{x}}_k^i, \mathbf{y}_k^i) \sim \tilde{\pi}_{k|k}^N(d\hat{\mathbf{x}}_k, d\mathbf{y}_k)$ . These uniformly weighted particles  $\{\hat{\mathbf{x}}_k^i, \mathbf{y}_k^i\}$  approximate  $\pi_{k|k}$  as

$$\pi_{k|k} \approx \pi_{k|k}^N(d\hat{\mathbf{x}}_k, d\mathbf{y}_k) \doteq \frac{1}{N} \sum_{i=1}^N \delta(\hat{\mathbf{x}}_k - \hat{\mathbf{x}}_k^i, \mathbf{y}_k - \mathbf{y}_k^i) d\hat{\mathbf{x}}_k d\mathbf{y}_k.$$

Here, similar to Hu et al. (2008), we have introduced an optional modification (step 2) for convenience of the convergence analysis in the following section. As mentioned earlier, the resampled particles  $\{\mathbf{y}_k^i\}$  in step 4 are not needed for the next recursion. In general, the estimate of  $\phi(\hat{\mathbf{x}}, \mathbf{y})$  is computed prior to resampling for better accuracy. For instance, we compute defender's state estimate  $\hat{\mathbf{x}}_k$  as  $\hat{\mathbf{x}}_k = \sum_{i=1}^N \omega_k^i \hat{\mathbf{x}}_k^i$ .

**Remark 1** (Threshold  $\gamma_k$  intuition). *Note that the optimal inverse filter (14)-(15) exists if  $\langle \pi_{k|k-1}, \beta \rangle > 0$ . In I-PF, we approximate  $\pi_{k|k-1}$  by  $\tilde{\pi}_{k|k-1}^N$  such that*

$$\langle \pi_{k|k-1}, \beta \rangle \approx \langle \tilde{\pi}_{k|k-1}^N, \beta \rangle = \frac{1}{N} \sum_{i=1}^N \beta(\mathbf{a}_k | \hat{\mathbf{x}}_k^i).$$

*In step 2, we require  $\langle \tilde{\pi}_{k|k-1}^N, \beta \rangle \geq \gamma_k$ . Hence, this condition is motivated by the existence of the optimal filter and has been previously used as an indicator of divergence in PFs (Crisan and Doucet, 2002; Hu et al., 2008). The threshold  $\gamma_k$  must be chosen so that the inequality is satisfied for sufficiently large  $N$  and in practice, modifies the PF algorithm only for small  $N$ . Theorem 1 further guarantees that the algorithm will not run into an infinite loop (in steps 1 and 2) provided that  $\gamma_k$  is chosen small enough.*

For the proposed I-PF, under the assumption of known forward filter, we need to be able to sample from observation distribution  $\rho(\cdot)$  and compute the density  $\beta(\mathbf{a}_k | \hat{\mathbf{x}}_k)$  at current observation  $\mathbf{a}_k$ . I-PF can handle non-Gaussian systems if these conditions are met. Fig. 2 provides a schematic illustration of posterior distributions and their approximations.

**Remark 2** (I-PF's optimal importance density). *For the considered defender-attacker dynamics, we are able to sample from the optimal density (20) under the assumption of known forward filter. Another popular but suboptimal choice of  $q(\cdot)$  is the transitional prior (Ristic et al., 2003), i.e.,  $q(\hat{\mathbf{x}}_k, \mathbf{y}_k | \hat{\mathbf{x}}_{k-1}, \mathbf{y}_{k-1}, \mathbf{x}_k, \mathbf{a}_k) = p(\hat{\mathbf{x}}_k, \mathbf{y}_k | \hat{\mathbf{x}}_{k-1}, \mathbf{y}_{k-1})$  for I-PF. However,  $p(\hat{\mathbf{x}}_k, \mathbf{y}_k | \hat{\mathbf{x}}_{k-1}, \mathbf{y}_{k-1}) = p(\hat{\mathbf{x}}_k | \hat{\mathbf{x}}_{k-1}, \mathbf{y}_k) p(\mathbf{y}_k | \mathbf{y}_{k-1})$  such that to sample from the transitional prior, we need to sample from  $p(\mathbf{y}_k | \mathbf{y}_{k-1})$ . Hence, contrary to the standard PF, it is easier to sample from the I-PF's optimal density (20) than the transitional prior. This is possible because of the perfect knowledge of actual state  $\mathbf{x}_k$  available to the defender such that we can directly sample from  $p(\mathbf{y}_k | \mathbf{x}_k)$ .*

**I-PF variants**: As in the case of standard PF, resampling in I-PF reduces degeneracy of particles over time, but introduces sample impoverishment (Arulampalam et al., 2002). Since the particles with large weights are statistically selected many times, there is a loss of diversity among particles, which may also lead to collapse to a single point in case of small system noises. Different techniques like MCMC move step (Carlin et al., 1992) and regularization (Musso et al., 2001) have been proposed to address sample impoverishment.

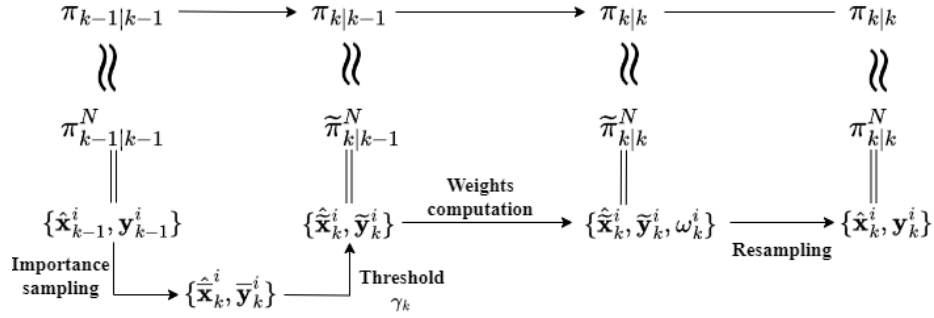


Figure 2: Graphical representation of transformation of posterior distributions in IPF.

The I-PF developed here is a basic inverse filter based on the SIS and resampling techniques. Different choices of sampling density  $q(\cdot)$  and/or modification of the resampling step lead to different variants of PFs. Similar modifications can also be introduced to the basic I-PF to obtain suitable variants for different applications. For instance, in auxiliary PF (Pitt and Shephard, 1999), the previous particles are resampled conditioned on the current measurement before importance sampling such that the particles are most likely close to the current true state. On the other hand, regularized PF (Musso et al., 2001) considers a kernel density  $K_h(\cdot)$  to resample from a continuous distribution instead of a discrete one, i.e.,  $(\hat{\mathbf{x}}_k^i, \mathbf{y}_k^i) \sim \sum_{i=1}^N \omega_k^i K_h(\hat{\mathbf{x}}_k - \tilde{\mathbf{x}}_k^i, \tilde{\mathbf{y}}_k - \mathbf{y}_k^i)$  for  $i = 1, 2, \dots, N$ .

PFs are frequently integrated into ML models for efficient state estimation and flexible parameter learning. For instance, Ma et al. (2020a) suggests PF-based recurrent NNs for robot localization and sequence prediction tasks. In Gu et al. (2015), a neural adaptive SMC method is shown to be effective in training a latent variable RNN. Karkus et al. (2018) encode the system model and PF algorithm in a single NN and learn a model optimized for PF instead of a generic model. Other examples of PF applications include online learning of random forests (Ko et al., 2013) and RL-based wireless indoor positioning system (Villacrés et al., 2019). Ma et al. (2020b) builds a discriminative PF-based RL framework for decision-making in partially observable Markov decision processes (POMDPs). Other applications include variational autoencoders (Burda et al., 2015), sequence generation (Le et al., 2018), and variational RL (Igl et al., 2018). Inverse filtering to infer the information learnt by these systems would then resort to I-PF and, particularly, differentiable I-PF for unknown system dynamics presented in Section 5.1.

### 3.2 Convergence guarantees

Several guarantees for convergence of the standard PF to the optimal filter’s posterior have been provided in the literature (Del Moral, 2004; Crisan and Doucet, 2002). In Le Gland and Oudjane (2004), a Hilbert projective metric is considered to study the optimal filter’s stability, which is then used to derive uniform convergence conditions for PFs. The survey by Crisan and Doucet (2002) showed almost sure convergence assuming a Feller transition kernel and a bounded, continuous, strictly positive observation likelihood. Other approaches include central limit theorems (Del Moral and Guionnet, 1999) and large deviations (Crisan

and Grunwald, 1999; Del Moral and Guionnet, 1998). However, all these prior works assume the (estimated) function  $\phi(\mathbf{x})$  of the underlying state  $\mathbf{x}$  to be bounded and hence, exclude the state estimate itself, i.e.,  $\phi(\mathbf{x}) = \mathbf{x}$ . Recently, Hu et al. (2008) have addressed the general case of the unbounded function  $\phi$  and proved PF's convergence in  $L^4$ -sense under some mild assumptions on the rate of increase of  $\phi$ . An extended result in the  $L^p$ -convergence sense has also been obtained using a Rosenthal-type inequality in Hu et al. (2011).

In the following, we consider the  $L^4$ -approach of Hu et al. (2008) to derive our I-PF's convergence conditions. In particular, we show that for a given time step  $k$  and given observations  $\mathbf{a}_{1:k}$  and known true states  $\mathbf{x}_{0:k}$ , the I-PF's estimate  $\langle \pi_{k|k}^N, \phi \rangle$  converges to the optimal filter's estimate  $\langle \pi_{k|k}, \phi \rangle$  as the number of particles  $N$  increases. Note that for given  $\{\mathbf{a}_{1:k}, \mathbf{x}_{0:k}\}$ , the optimal distribution  $\pi_{k|k}$  is a deterministic function, but  $\pi_{k|k}^N$  is random because of the randomly generated particles. Hence, all the stochastic expectations  $\mathbb{E}$  and almost sure convergence are with respect to these random particles.

We assume that the system model (1)-(4) and estimated function  $\phi$  satisfy the following conditions.

**A1** For given  $\mathbf{x}_{0:s}$  and  $\mathbf{a}_{1:s}$  for  $s = 1, 2, \dots, k$ ,  $\langle \pi_{s|s-1}, \beta \rangle > 0$  and there exists  $\{\gamma_s\}_{1 \leq s \leq k}$  such that  $0 < \gamma_s < \langle \pi_{s|s-1}, \beta \rangle$ .

**A2** The observation densities are bounded, i.e.,  $\beta(\mathbf{a}_s | \hat{\mathbf{x}}_s) < \infty$  and  $\rho(\mathbf{y}_s | \mathbf{x}_s) < \infty$  for  $s = 1, 2, \dots, k$ .

**A3** The function  $\phi$  satisfies  $\sup_{(\hat{\mathbf{x}}_s, \mathbf{y}_s)} |\phi(\hat{\mathbf{x}}_s, \mathbf{y}_s)|^4 \beta(\mathbf{a}_s | \hat{\mathbf{x}}_s) < C(\mathbf{x}_{0:s}, \mathbf{a}_{1:s})$  for given  $\mathbf{x}_{0:s}, \mathbf{a}_{1:s}, s = 1, 2, \dots, k$ . Here,  $C(\mathbf{x}_{0:s}, \mathbf{a}_{1:s})$  is a finite constant which may depend on  $\mathbf{x}_{0:s}$  and  $\mathbf{a}_{1:s}$ .

Recall that  $\{\gamma_s\}$  are the thresholds introduced in the modification step (step 2) of the I-PF algorithm in Section 3.1. As discussed in Remark 1, assumption **A1** is related to the existence of the optimal filter and divergence of PFs. Intuitively, assumption **A3** states that the conditional observation density  $\beta$  must decrease at a rate faster than the function  $\phi$  increases. Furthermore, **A2** and **A3** imply that the conditional fourth moment of  $\phi$  is bounded, i.e.,  $\langle \pi_{s|s}, |\phi|^4 \rangle < \infty$  (Hu et al., 2008). Finally, the I-PF convergence is provided in the following theorem.

**Theorem 1** (I-PF convergence). *Consider the I-PF developed in Section 3.1 (including the modification step). If the assumptions **A1-A3** are satisfied, then the following hold:*

1. For sufficiently large  $N$ , the algorithm will not run into an infinite loop in steps 1 – 2.
2. For any  $\phi$  satisfying **A3**, there exists a constant  $C_{k|k}$ , independent of  $N$  such that

$$\mathbb{E} |\langle \pi_{k|k}^N, \phi \rangle - \langle \pi_{k|k}, \phi \rangle|^4 \leq C_{k|k} \frac{\|\phi\|_{k,4}^4}{N^2}, \quad (22)$$

where  $\|\phi\|_{k,4} \doteq \max\{1, \max_{0 \leq s \leq k} \langle \pi_{s|s}, |\phi|^4 \rangle^{1/4}\}$  and  $\pi_{k|k}^N$  is generated by the I-PF algorithm.

*Proof.* See Appendix B. ■

As a consequence of Theorem 1, the following corollary can be obtained trivially using the Borel-Cantelli lemma as in Athreya and Lahiri (2006, Proposition 7.2.3(a)).

**Corollary 1.** *If **A1-A3** holds, then for any  $\phi$  satisfying **A3**, we have  $\lim_{N \rightarrow \infty} \langle \pi_{k|k}^N, \phi \rangle = \langle \pi_{k|k}, \phi \rangle$  in the almost sure convergence sense.*

**Remark 3** (Dependence on state dimension). *From (22), we observe that the I-PF’s convergence rate does not depend on the state dimension  $n_x$  and hence, I-PF does not suffer from the curse of dimensionality. However, for a given/desired bound on the error, the required number of particles  $N$  depends on constant  $C_{k|k}$ , which can depend on  $n_x$ .*

**Remark 4** (Bound on  $C_{k|k}$ ). *In general, without any additional assumptions, we cannot guarantee that  $C_{k|k}$  will not increase over time. In particular, if the optimal filter does not ‘forget’ its initial condition, the approximation errors accumulate over time such that  $C_{k|k}$  increases (Crisan and Doucet, 2002). Hence, the required number of particles  $N$  also increases proportionally for the error to remain within a given bound. However, prior works Del Moral and Guionnet (2001); Le Gland and Oudjane (2004) provide additional conditions on the system model to ensure the optimal filter mixes quickly (forgets its initial condition) and  $C_{k|k}$  does not increase with time.*

## 4 Inverse GPF and EnKF

The I-PF developed in Section 3 considers a general inverse filtering model without any restrictive assumptions on the system model. However, in many practical applications, the process and observation noises are reasonably assumed to be Gaussian such that the Gaussian posterior assumption can provide a better tradeoff between the computational complexity and the performance of the filter. GPF and EnKF are two popular SMC-based filters that assume Gaussian posteriors. While GPF employs a PF framework to obtain the state estimates, EnKF extends the standard KF to non-linear dynamics using SMC methods. In the following, we consider similar techniques for the inverse filtering problem and develop I-GPF and I-EnKF in Section 4.1 and 4.2, respectively. Section 4.3 discusses the modifications of these filters to handle non-Gaussian noises in the inverse filtering context. Finally, Table 2 highlights the key differences of I-PF, I-GPF, and I-EnKF algorithms.

### 4.1 Inverse GPF

Recall that GPF presents an MC-based extension of Gaussian filters. However, unlike EKF or UKF, GPF’s estimate asymptotically (as number of particles  $N \rightarrow \infty$ ) converges almost surely to the actual MMSE estimate provided that the Gaussian assumption holds true (Kotecha and Djuric, 2003b). Also, contrary to PF, GPF does not suffer from particle degeneracy and hence, resampling is not required. This results in reduced computational complexity and ease of parallel implementation. As mentioned earlier, standard PF does not assume any posterior form and approximates the arbitrary posterior with randomly generated particles. Under the Gaussianity assumption, GPF propagates only the mean and covariance of the posterior, but PF propagates higher-order moments as well.

Consider the optimal filter recursions (12) and (13). In I-GPF, we assume a marginal Gaussian distribution for the attacker’s state estimate as  $p(\hat{\mathbf{x}}_k | \mathbf{x}_{0:k}, \mathbf{a}_{1:k}) \approx \mathcal{N}(\hat{\mathbf{x}}_k; \hat{\mathbf{x}}_k, \bar{\Sigma}_k)$ .



This is in contrast to I-PF developed in Section 3, wherein we aimed to estimate the joint distribution  $p(\hat{\mathbf{x}}_k, \mathbf{y}_k | \mathbf{x}_{0:k}, \mathbf{a}_{1:k})$ . The defender employing the inverse filter has perfect knowledge of its true state  $\mathbf{x}_k$  and hence, using (2), we approximate  $p(\mathbf{y}_k | \mathbf{x}_{0:k}, \mathbf{a}_{1:k}) \approx \rho(\mathbf{y}_k | \mathbf{x}_k)$ . Overall, we assume

$$\pi_{k|k} \approx \mathcal{N}(\hat{\mathbf{x}}_k; \hat{\mathbf{x}}_k, \bar{\Sigma}_k) \rho(\mathbf{y}_k | \mathbf{x}_k). \quad (23)$$

Note that this is an approximation because  $\hat{\mathbf{x}}_k$  and  $\mathbf{y}_k$  are not indeed independent. Furthermore,  $\mathbf{y}_k$  is also correlated with observation  $\mathbf{a}_k$  via estimate  $\hat{\mathbf{x}}_k$ , but we ignore this dependence. The knowledge of true distribution  $\rho(\cdot | \mathbf{x}_k)$  can compensate for this approximation to some extent. Similarly, we assume a Gaussian prediction distribution as  $p(\hat{\mathbf{x}}_k | \mathbf{x}_{0:k}, \mathbf{a}_{1:k-1}) \approx \mathcal{N}(\hat{\mathbf{x}}_k; \hat{\mathbf{x}}_{k|k-1}, \bar{\Sigma}_{k|k-1})$ . Finally, the means ( $\hat{\mathbf{x}}_k$  and  $\hat{\mathbf{x}}_{k|k-1}$ ) and covariances ( $\bar{\Sigma}_k$  and  $\bar{\Sigma}_{k|k-1}$ ) are computed as weighted MC estimates using the PF framework.

Consider  $N$  as the total number of particles. We initialize I-GPF with initial distribution  $\mathcal{N}(\hat{\mathbf{x}}_0; \hat{\mathbf{x}}_0, \bar{\Sigma}_0)$ . Denote  $\{(\hat{\mathbf{x}}_{k|k-1}^i, \mathbf{y}_k^i)\}_{1 \leq i \leq N}$  as the particles generated for the time-update/prediction step, while  $\{\hat{\mathbf{x}}_k^i\}_{1 \leq i \leq N}$  are the particles generated in the measurement update with associated weights  $\{\omega_k^i\}_{1 \leq i \leq N}$ . Similar to I-PF, particle sampling and weight computation do not require previous particles  $\{\mathbf{y}_{k-1}^i\}$ . At the  $k$ -th time instant, I-GPF computes estimate  $\hat{\mathbf{x}}_k$  of  $\hat{\mathbf{x}}_k$  and the corresponding covariance estimate  $\bar{\Sigma}_k$  recursively as

$$\text{Time update: } \{\hat{\mathbf{x}}_{k-1}^i\}_{1 \leq i \leq N} \sim \mathcal{N}(\hat{\mathbf{x}}_{k-1}; \hat{\mathbf{x}}_{k-1}, \bar{\Sigma}_{k-1}), \quad \{\mathbf{y}_k^i\}_{1 \leq i \leq N} \sim \rho(\mathbf{y}_k | \mathbf{x}_k), \quad (24)$$

$$\hat{\mathbf{x}}_{k|k-1}^i = T(\hat{\mathbf{x}}_{k-1}^i, \mathbf{y}_k^i), \quad \text{for } i = 1, 2, \dots, N, \quad (25)$$

$$\hat{\mathbf{x}}_{k|k-1} = \frac{1}{N} \sum_{i=1}^N \hat{\mathbf{x}}_{k|k-1}^i, \quad \bar{\Sigma}_{k|k-1} = \frac{1}{N} \sum_{i=1}^N (\hat{\mathbf{x}}_{k|k-1}^i - \hat{\mathbf{x}}_{k|k-1})(\hat{\mathbf{x}}_{k|k-1}^i - \hat{\mathbf{x}}_{k|k-1})^T, \quad (26)$$

$$\text{Measurement update: } \{\hat{\mathbf{x}}_k^i\}_{1 \leq i \leq N} \sim \mathcal{N}(\hat{\mathbf{x}}_k; \hat{\mathbf{x}}_{k|k-1}, \bar{\Sigma}_{k|k-1}),$$

$$\tilde{\omega}_k^i = \beta(\mathbf{a}_k | \hat{\mathbf{x}}_k^i), \quad \text{for } i = 1, 2, \dots, N, \quad \omega_k^i = \tilde{\omega}_k^i / \sum_{i=1}^N \tilde{\omega}_k^i, \quad \text{for } i = 1, 2, \dots, N,$$

$$\hat{\mathbf{x}}_k = \sum_{i=1}^N \omega_k^i \hat{\mathbf{x}}_k^i, \quad \bar{\Sigma}_k = \sum_{i=1}^N \omega_k^i (\hat{\mathbf{x}}_k^i - \hat{\mathbf{x}}_k)(\hat{\mathbf{x}}_k^i - \hat{\mathbf{x}}_k)^T.$$

Here, similar to I-PF, (24)-(25) represent importance sampling with the optimal sampling density (20) and a Gaussian posterior distribution on  $\hat{\mathbf{x}}_{k-1}$ . The particles are drawn identically with equal weights such that the prediction distribution  $\mathcal{N}(\hat{\mathbf{x}}_k; \hat{\mathbf{x}}_{k|k-1}, \bar{\Sigma}_{k|k-1})$  is obtained in (26). Finally, in the measurement update, we sample from the prediction distribution and compute the associated weights using (21). Overall, we need to sample twice from Gaussian densities and once from the observation distribution  $\rho(\cdot)$  at each recursion. Alternatively, sampling  $\{\hat{\mathbf{x}}_{k-1}^i\}$  can be omitted and weighted samples  $\{\hat{\mathbf{x}}_{k-1}^i, \omega_{k-1}^i\}$  from previous time-step can be considered themselves (Kotecha and Djuric, 2003b). In this case,  $\hat{\mathbf{x}}_{k-1}^i = \hat{\mathbf{x}}_{k-1}^i$  for all  $i = 1, 2, \dots, N$ , and (26) becomes

$$\hat{\mathbf{x}}_{k|k-1} = \sum_{i=1}^N \omega_{k-1}^i \hat{\mathbf{x}}_{k|k-1}^i, \quad \bar{\Sigma}_{k|k-1} = \sum_{i=1}^N \omega_{k-1}^i (\hat{\mathbf{x}}_{k|k-1}^i - \hat{\mathbf{x}}_{k|k-1})(\hat{\mathbf{x}}_{k|k-1}^i - \hat{\mathbf{x}}_{k|k-1})^T.$$

## 4.2 Inverse EnKF

Here, we develop I-EnKF for a non-linear system with additive noises given by (5)-(7). Analogous to standard EnKF, we assume  $\mathbf{w}_k$ ,  $\mathbf{v}_k$  and  $\boldsymbol{\epsilon}_k$  to be Gaussian with distributions  $\mathcal{N}(\mathbf{w}_k; \mathbf{0}, \mathbf{Q}_k)$ ,  $\mathcal{N}(\mathbf{v}_k; \mathbf{0}, \mathbf{R}_k)$  and  $\mathcal{N}(\boldsymbol{\epsilon}_k; \mathbf{0}, \bar{\mathbf{R}}_k)$ , respectively. Unlike I-PF and I-GPF, the attacker is assumed to employ EnKF as its forward filter instead of a general filter  $T(\cdot)$ .

*Forward filter:* Consider  $q$  as the forward EnKF's ensemble size and  $\{\mathbf{x}_k^i\}_{1 \leq i \leq q}$  represents the ensemble at  $k$ -th time step. Denote  $\{\mathbf{w}_{k-1}^i\}_{1 \leq i \leq q}$  and  $\{\mathbf{v}_k^i\}_{1 \leq i \leq q}$  as the i.i.d. noise samples drawn from  $\mathcal{N}(\mathbf{w}_{k-1}; \mathbf{0}, \mathbf{Q}_{k-1})$  and  $\mathcal{N}(\mathbf{v}_k; \mathbf{0}, \mathbf{R}_k)$ , respectively. In the time update step, the previous ensemble  $\{\mathbf{x}_{k-1}^i\}$  is propagated through state evolution (5) to obtain the predicted ensemble  $\{\mathbf{x}_{k|k-1}^i\}$ , which then yields the predicted observation ensemble  $\{\mathbf{y}_k^i\}$  using (6). Finally, in the measurement update, KF-like linear updates are employed to obtain the current ensemble  $\{\mathbf{x}_k^i\}$  with the gain matrix approximated using the ensemble covariances. The overall forward EnKF recursions are summarized as (Gillijns et al., 2006):

$$\begin{aligned}
 &\text{Time update: } \mathbf{x}_{k|k-1}^i = f(\mathbf{x}_{k-1}^i) + \mathbf{w}_{k-1}^i, \text{ for } i = 1, 2, \dots, q, & (27) \\
 &\hat{\mathbf{x}}_{k|k-1} = \frac{1}{q} \sum_{i=1}^q \mathbf{x}_{k|k-1}^i, \quad \mathbf{E}_{k|k-1}^x = \left[ (\mathbf{x}_{k|k-1}^1 - \hat{\mathbf{x}}_{k|k-1}), \dots, (\mathbf{x}_{k|k-1}^q - \hat{\mathbf{x}}_{k|k-1}) \right], \\
 &\mathbf{y}_k^i = h(\mathbf{x}_{k|k-1}^i) + \mathbf{v}_k^i, \text{ for } i = 1, 2, \dots, q, \\
 &\hat{\mathbf{y}}_k = \frac{1}{q} \sum_{i=1}^q \mathbf{y}_k^i, \quad \mathbf{E}_k^y = \left[ (\mathbf{y}_k^1 - \hat{\mathbf{y}}_k), \dots, (\mathbf{y}_k^q - \hat{\mathbf{y}}_k) \right], \\
 &\boldsymbol{\Sigma}_k^{xy} = \frac{1}{q-1} \mathbf{E}_{k|k-1}^x (\mathbf{E}_k^y)^T, \quad \boldsymbol{\Sigma}_k^y = \frac{1}{q-1} \mathbf{E}_k^y (\mathbf{E}_k^y)^T, \\
 &\text{Measurement update: } \mathbf{K}_k = \boldsymbol{\Sigma}_k^{xy} (\boldsymbol{\Sigma}_k^y)^{-1}, \\
 &\mathbf{x}_k^i = \mathbf{x}_{k|k-1}^i + \mathbf{K}_k (\mathbf{y}_k - \mathbf{y}_k^i), \text{ for } i = 1, 2, \dots, q, & (28)
 \end{aligned}$$

and state estimate  $\hat{\mathbf{x}}_k = \frac{1}{q} \sum_{i=1}^q \mathbf{x}_k^i$ . As compared to other SMC algorithms (like PF), which use reweighting and resampling, EnKF employs 'linear-shifting' to update the prior ensemble to a posterior ensemble after each observation (Katzfuss et al., 2016). Consequently, EnKF does not suffer from any weight/particle degeneracy problem.

*Inverse filter:* Unlike I-KF (Krishnamurthy and Rangaswamy, 2019), I-EKF (Singh et al., 2023b) and I-UKF (Singh et al., 2024b), it is impractical to obtain the state-transition for the forward EnKF's state estimate  $\hat{\mathbf{x}}_k$  even under the known forward filter assumption. This is because of the random noise samples involved in computation of the forward EnKF's gain matrix. Hence, in I-EnKF, we consider propagating the updated state ensemble further through the defender's observation model (7). In particular, we start with the previous ensemble  $\{\hat{\mathbf{x}}_{k-1}^j\}_{1 \leq j \leq \bar{q}}$  of size  $\bar{q}$ , where  $\bar{q}$  is chosen independent of the forward EnKF's size  $q$ . This ensemble is propagated through state evolution (5) and attacker's observation (6) similar to the forward filter. An intermediate updated ensemble  $\{\bar{\mathbf{x}}_{k|k-1}^j\}$  is then obtained from the forward EnKF's measurement update (28) with the actual observation  $\mathbf{y}_k$  replaced by simulated observation generated using true state  $\mathbf{x}_k$  according to (6). Finally, the intermediate ensemble is propagated through observation model (7) resulting in observation ensemble  $\{\mathbf{a}_k^j\}$ . Linear KF-like updates then yield the I-EnKF's updated ensemble  $\{\hat{\mathbf{x}}_k^j\}$ . I-EnKF's recursions to infer estimate  $\hat{\mathbf{x}}_k$  of  $\mathbf{x}_k$  are summarized as:

$$\begin{aligned}
&\text{State evolution update: } \tilde{\mathbf{x}}_{k|k-1}^j = f(\hat{\mathbf{x}}_{k-1}^j) + \tilde{\mathbf{w}}_{k-1}^j, \text{ for } j = 1, 2, \dots, \bar{q}, \\
&\hat{\tilde{\mathbf{x}}}_{k|k-1} = \frac{1}{\bar{q}} \sum_{j=1}^{\bar{q}} \tilde{\mathbf{x}}_{k|k-1}^j, \quad \tilde{\mathbf{E}}_{k|k-1}^x = \left[ (\tilde{\mathbf{x}}_{k|k-1}^1 - \hat{\tilde{\mathbf{x}}}_{k|k-1}), \dots, (\tilde{\mathbf{x}}_{k|k-1}^{\bar{q}} - \hat{\tilde{\mathbf{x}}}_{k|k-1}) \right], \\
&\text{Intermediate update: } \tilde{\mathbf{y}}_k^j = h(\tilde{\mathbf{x}}_{k|k-1}^j) + \tilde{\mathbf{v}}_k^j, \text{ for } j = 1, 2, \dots, \bar{q}, \\
&\hat{\tilde{\mathbf{y}}}_k = \frac{1}{\bar{q}} \sum_{j=1}^{\bar{q}} \tilde{\mathbf{y}}_k^j, \quad \tilde{\mathbf{E}}_k^y = \left[ (\tilde{\mathbf{y}}_k^1 - \hat{\tilde{\mathbf{y}}}_k), \dots, (\tilde{\mathbf{y}}_k^{\bar{q}} - \hat{\tilde{\mathbf{y}}}_k) \right], \\
&\tilde{\Sigma}_k^{xy} = \frac{1}{\bar{q}-1} \tilde{\mathbf{E}}_{k|k-1}^x (\tilde{\mathbf{E}}_k^y)^T, \quad \tilde{\Sigma}_k^y = \frac{1}{\bar{q}-1} \tilde{\mathbf{E}}_k^y (\tilde{\mathbf{E}}_k^y)^T, \\
&\tilde{\mathbf{K}}_k = \tilde{\Sigma}_k^{xy} (\tilde{\Sigma}_k^y)^{-1}, \quad \tilde{\mathbf{x}}_{k|k-1}^j = \tilde{\mathbf{x}}_{k|k-1}^j + \tilde{\mathbf{K}}_k (h(\mathbf{x}_k) + \bar{\mathbf{v}}_k^j - \tilde{\mathbf{y}}_k^j), \text{ for } j = 1, 2, \dots, \bar{q}, \\
&\hat{\hat{\tilde{\mathbf{x}}}}_{k|k-1} = \frac{1}{\bar{q}} \sum_{j=1}^{\bar{q}} \tilde{\mathbf{x}}_{k|k-1}^j, \quad \tilde{\mathbf{E}}_{k|k-1}^x = \left[ (\tilde{\mathbf{x}}_{k|k-1}^1 - \hat{\hat{\tilde{\mathbf{x}}}}_{k|k-1}), \dots, (\tilde{\mathbf{x}}_{k|k-1}^{\bar{q}} - \hat{\hat{\tilde{\mathbf{x}}}}_{k|k-1}) \right], \\
&\text{Measurement update: } \mathbf{a}_k^j = g(\tilde{\mathbf{x}}_{k|k-1}^j) + \boldsymbol{\epsilon}_k^j, \text{ for } j = 1, 2, \dots, \bar{q}, \\
&\hat{\mathbf{a}}_k = \frac{1}{\bar{q}} \sum_{j=1}^{\bar{q}} \mathbf{a}_k^j, \quad \mathbf{E}_k^a = \left[ (\mathbf{a}_k^1 - \hat{\mathbf{a}}_k), \dots, (\mathbf{a}_k^{\bar{q}} - \hat{\mathbf{a}}_k) \right], \\
&\bar{\Sigma}_k^{xa} = \frac{1}{\bar{q}-1} \tilde{\mathbf{E}}_{k|k-1}^x (\mathbf{E}_k^a)^T, \quad \bar{\Sigma}_k^a = \frac{1}{\bar{q}-1} \mathbf{E}_k^a (\mathbf{E}_k^a)^T, \\
&\bar{\mathbf{K}}_k = \bar{\Sigma}_k^{xa} (\bar{\Sigma}_k^a)^{-1}, \quad \hat{\mathbf{x}}_k^j = \tilde{\mathbf{x}}_{k|k-1}^j + \bar{\mathbf{K}}_k (\mathbf{a}_k - \mathbf{a}_k^j), \text{ for } j = 1, 2, \dots, \bar{q},
\end{aligned}$$

where  $\{\tilde{\mathbf{w}}_{k-1}^j\}$ ,  $\{\tilde{\mathbf{v}}_k^j, \tilde{\mathbf{v}}_k^j\}$  and  $\{\boldsymbol{\epsilon}_k^j\}$  are noise samples drawn from  $\mathcal{N}(\mathbf{w}_{k-1}; \mathbf{0}, \mathbf{Q}_{k-1})$ ,  $\mathcal{N}(\mathbf{v}_k; \mathbf{0}, \mathbf{R}_k)$  and  $\mathcal{N}(\boldsymbol{\epsilon}_k; \mathbf{0}, \bar{\mathbf{R}}_k)$ , respectively. I-EnKF's estimate  $\hat{\tilde{\mathbf{x}}}_k = \frac{1}{\bar{q}} \sum_{j=1}^{\bar{q}} \hat{\tilde{\mathbf{x}}}_k^j$ . Note that the intermediate gain matrix  $\tilde{\mathbf{K}}_k$  aims to approximate the forward EnKF's gain matrix  $\mathbf{K}_k$ . However, it differs from  $\mathbf{K}_k$  because  $\tilde{\mathbf{K}}_k$  is computed from previous ensemble  $\{\tilde{\mathbf{x}}_{k-1}^j\}$ , which in turn has been propagated through observation (7) at the previous time step. On the other hand, forward EnKF's ensemble propagates only through state evolution (5) and observation (6). But, similar to the standard EnKF, our I-EnKF is observed to be robust to this deviation in different numerical examples considered in Section 6.3 and 6.4.

**Remark 5** (Deterministic I-EnKF). *Unlike UKF which considers deterministic sigma-points, the forward EnKF and I-EnKF considered here work with a randomly generated ensemble. While the number of sigma-points in UKF are of the same order as the state dimension  $n_x$ , the required ensemble size in EnKF is a heuristic (Gillijns et al., 2006). However, deterministic update based EnKFs have also been proposed in the literature (Anderson, 2001; Bishop et al., 2001; Hunt et al., 2007), wherein the prior ensemble is deterministically shifted to the posterior ensemble without relying on simulated observations. In particular, the prior ensemble members are shifted and scaled such that the resulting posterior ensemble members are shifted towards the data with smaller variance than the prior. Analogous approaches can be applied to obtain deterministic variants of the proposed I-EnKF by suitably modifying the intermediate and measurement updates.*

### 4.3 Non-Gaussian systems

In order to employ I-GPF, we only need to be able to sample from observation distribution  $\rho(\cdot)$  and compute density  $\beta(\cdot)$  at the generated particles. As far as these conditions are satisfied, the defender can employ I-GPF to estimate the attacker's estimate in non-Gaussian systems as well. In fact, I-GPF may outperform I-PF if the posterior state distributions are well approximated by Gaussians, as demonstrated in our numerical experiments in Section 6.2. For the case when the posterior distribution cannot be assumed to be a single Gaussian, GSPFs have been proposed in Kotecha and Djuric (2003a) based on GM models using a bank of parallel EKFs or GPFs. In particular, Kotecha and Djuric (2003a) considered two different approaches: (a) the prediction and posterior distributions are approximated by weighted GMs, and (b) the additive process and observation noises are modeled as a finite sum of Gaussians. In the latter case, the non-Gaussian state-space model itself is equivalent to a bank of parallel Gaussian state-space models, each of which can be approximated by (single) Gaussian or GM posteriors. However, in this case, the number of Gaussians increases exponentially with time, but only a few have significant weights. Hence, resampling is introduced to propagate a fixed number of Gaussians at each iteration. Similar approaches can be used to modify I-GPF to address severe non-Gaussianity in the inverse filtering model at a lower computational cost than I-PF.

**Inverse GSPF:** We obtain I-GSPF by approximating the prediction and posterior densities as a mixture of  $G$  Gaussians, i.e.,  $p(\hat{\mathbf{x}}_k | \mathbf{x}_{0:k}, \mathbf{a}_{1:k-1}) \approx \sum_{j=1}^G \gamma_{k|k-1}^j \mathcal{N}(\hat{\mathbf{x}}_k; \boldsymbol{\mu}_{k|k-1}^j, \boldsymbol{\Sigma}_{k|k-1}^j)$  and  $p(\hat{\mathbf{x}}_k | \mathbf{x}_{0:k}, \mathbf{a}_{1:k}) \approx \sum_{j=1}^G \gamma_k^j \mathcal{N}(\hat{\mathbf{x}}_k; \boldsymbol{\mu}_k^j, \boldsymbol{\Sigma}_k^j)$ , respectively. Here,  $\gamma_k^j$  ( $\gamma_{k|k-1}^j$ ),  $\boldsymbol{\mu}_k^j$  ( $\boldsymbol{\mu}_{k|k-1}^j$ ) and  $\boldsymbol{\Sigma}_k^j$  ( $\boldsymbol{\Sigma}_{k|k-1}^j$ ), respectively, denote the weight, mean and covariance of the  $j$ -th Gaussian of the posterior (prediction) distribution at  $k$ -th time step. Hence, (23) becomes  $\pi_{k|k} \approx \sum_{j=1}^G \gamma_k^j \mathcal{N}(\hat{\mathbf{x}}_k; \boldsymbol{\mu}_k^j, \boldsymbol{\Sigma}_k^j) \rho(\mathbf{y}_k | \mathbf{x}_k)$ . I-GSPF generates  $N$  particles per Gaussian to update these GMs using the PF framework and computes  $\hat{\mathbf{x}}_k$  and  $\bar{\boldsymbol{\Sigma}}_k$  as follows:

$$\begin{aligned}
& \text{Time update: } \{\hat{\mathbf{x}}_{k-1}^{j,i}\}_{1 \leq i \leq N} \sim \mathcal{N}(\hat{\mathbf{x}}_k; \boldsymbol{\mu}_k^j, \boldsymbol{\Sigma}_k^j), \quad \{\mathbf{y}_k^{j,i}\}_{1 \leq i \leq N} \sim \rho(\mathbf{y}_k | \mathbf{x}_k) \quad \forall 1 \leq j \leq G, \\
& \hat{\mathbf{x}}_{k|k-1}^{j,i} = T(\hat{\mathbf{x}}_{k-1}^{j,i}, \mathbf{y}_k^{j,i}) \quad \forall 1 \leq i \leq N, 1 \leq j \leq G, \quad \gamma_{k|k-1}^j = \gamma_{k-1}^j \quad \forall 1 \leq j \leq G, \\
& \boldsymbol{\mu}_{k|k-1}^j = \frac{1}{N} \sum_{i=1}^N \hat{\mathbf{x}}_{k|k-1}^{j,i}, \quad \boldsymbol{\Sigma}_{k|k-1}^j = \frac{1}{N} \sum_{i=1}^N (\hat{\mathbf{x}}_{k|k-1}^{j,i} - \boldsymbol{\mu}_{k|k-1}^j)(\hat{\mathbf{x}}_{k|k-1}^{j,i} - \boldsymbol{\mu}_{k|k-1}^j)^T \quad \forall 1 \leq j \leq G, \\
& \text{Measurement update: } \{\hat{\mathbf{x}}_k^{j,i}\}_{1 \leq i \leq N} \sim \mathcal{N}(\hat{\mathbf{x}}_k; \boldsymbol{\mu}_{k|k-1}^j, \boldsymbol{\Sigma}_{k|k-1}^j) \quad \forall 1 \leq j \leq G, \\
& \tilde{\omega}_k^{j,i} = \beta(\mathbf{a}_k | \hat{\mathbf{x}}_k^{j,i}), \quad \omega_k^{j,i} = \tilde{\omega}_k^{j,i} / \sum_{i=1}^N \tilde{\omega}_k^{j,i} \quad \forall 1 \leq i \leq N, 1 \leq j \leq G, \\
& \boldsymbol{\mu}_k^j = \sum_{i=1}^N \omega_k^{j,i} \hat{\mathbf{x}}_k^{j,i}, \quad \boldsymbol{\Sigma}_k^j = \sum_{i=1}^N \omega_k^{j,i} (\hat{\mathbf{x}}_k^{j,i} - \boldsymbol{\mu}_k^j)(\hat{\mathbf{x}}_k^{j,i} - \boldsymbol{\mu}_k^j)^T \quad \forall 1 \leq j \leq G, \\
& \tilde{\gamma}_k^j = \gamma_{k|k-1}^j \sum_{i=1}^N \tilde{\omega}_k^{j,i} / \sum_{j=1}^G \sum_{i=1}^N \tilde{\omega}_k^{j,i}, \quad \gamma_k^j = \tilde{\gamma}_k^j / \sum_{j=1}^G \tilde{\gamma}_k^j \quad \forall 1 \leq j \leq G, \\
& \hat{\mathbf{x}}_k = \sum_{j=1}^G \gamma_k^j \boldsymbol{\mu}_k^j, \quad \bar{\boldsymbol{\Sigma}}_k = \sum_{j=1}^G \gamma_k^j (\boldsymbol{\Sigma}_k^j + (\boldsymbol{\mu}_k^j - \hat{\mathbf{x}}_k)(\boldsymbol{\mu}_k^j - \hat{\mathbf{x}}_k)^T).
\end{aligned}$$

Table 2: Summary of I-PF, I-GPF and I-EnKF.

Feature	I-PF	I-GPF	I-EnKF
System model	General densities (1), (2) and (4)	General densities (1),(2) and (4)	Non-linear system with additive Gaussian noises, i.e., (5)-(7)
Forward filter	$T(\cdot)$ in (3)	$T(\cdot)$ in (3)	EnKF
State posterior distribution	Empirical approximation for the optimal inverse filter's joint posterior $p(\hat{\mathbf{x}}_k, \mathbf{y}_k   \mathbf{x}_{0:k}, \mathbf{a}_{1:k})$ (with no assumptions)	Assumes posterior $p(\hat{\mathbf{x}}_k   \mathbf{x}_{0:k}, \mathbf{a}_{1:k})$ as Gaussian with the mean and covariance computed as weighted MC estimates	Assumes $p(\hat{\mathbf{x}}_k   \mathbf{x}_{0:k}, \mathbf{a}_{1:k})$ as Gaussian with the mean and covariance computed from the ensemble ones
Update	SIS reweighting and resampling	SIS reweighting	KF-like updates
Implementation	Sampling from $\rho(\cdot)$ and $\tilde{\pi}_{k k}^N$ (resampling), and compute $\beta(\cdot)$ at generated particles	Sampling from Gaussian densities and $\rho(\cdot)$ ; and compute $\beta(\cdot)$ at generated particles	Sampling from $\mathcal{N}(\mathbf{w}_{k-1}; \mathbf{0}, \mathbf{Q}_{k-1})$ , $\mathcal{N}(\mathbf{v}_k; \mathbf{0}, \mathbf{R}_k)$ and $\mathcal{N}(\boldsymbol{\epsilon}_k; \mathbf{0}, \bar{\mathbf{R}}_k)$
Convergence	To the optimal Bayesian filter in $L^4$ -sense as $N \rightarrow \infty$ ; cf. Theorem 1	Almost surely to the actual MMSE estimate (Gaussian posterior only).	In probability to KF's estimates as ensemble size increases (linear Gaussian only).
Non-Gaussian noises	Yes, as is	No, except with GM models	No, except with MCC

**MCC-modified I-EnKF:** Although EnKF was designed for linear Gaussian systems, it is also highly efficient for non-linear and non-Gaussian systems, which is a consequence of linear Bayesian estimation. Particularly, linear Bayesian estimation seeks linear estimators given the first and second moments of the prior distributions and likelihoods (Goldstein and Wooff, 2007). In the case of linear Gaussian systems, these estimates coincide with the true Bayesian posterior. However, this linear approach is inefficient in tacking highly non-Gaussian distributions (Katzfuss et al., 2016). Recently, KFs modified using MCC have been suggested to handle non-Gaussian noises (Izanloo et al., 2016; Yang and Huang, 2019; Tao et al., 2023). Our I-EnKF can also be similarly generalized to non-Gaussian systems. For instance, consider the predicted state  $\hat{\mathbf{x}}_{k|k-1} = \frac{1}{q} \sum_{i=1}^q \mathbf{x}_{k|k-1}^i$  and its covariance matrix  $\boldsymbol{\Sigma}_{k|k-1} = \frac{1}{q-1} \mathbf{E}_{k|k-1}^x (\mathbf{E}_{k|k-1}^x)^T$  obtained from the predicted ensemble (27). Forward MCC-EnKF in Tao et al. (2023) considers a scalar  $l_k = G_\sigma(\|\mathbf{y}_k - h(\hat{\mathbf{x}}_{k|k-1})\|_{\mathbf{R}_k^{-1}})$  with  $G_\sigma(\cdot)$  as the Gaussian kernel and computes the modified gain matrix  $\mathbf{K}_k^m = (\boldsymbol{\Sigma}_{k|k-1}^{-1} + \mathbf{H}_k^T \tilde{\mathbf{R}}_k^{-1} \mathbf{H}_k)^{-1} \mathbf{H}_k^T \tilde{\mathbf{R}}_k^{-1}$  (instead of  $\mathbf{K}_k$ ), where  $\tilde{\mathbf{R}}_k^{-1} = \mathbf{R}_k / l_k$  and  $\mathbf{H}_k = \nabla_{\mathbf{x}} h(\mathbf{x})|_{\mathbf{x}=\hat{\mathbf{x}}_{k|k-1}}$ . Here,  $\|\mathbf{x}\|_A \doteq \mathbf{x}^T \mathbf{A} \mathbf{x}$  and  $\nabla_{\mathbf{x}} f(\mathbf{x})$  denotes the Jacobian of function  $f$  with respect to  $\mathbf{x}$ . All other state prediction and update steps remain same as in forward EnKF. While formulating the inverse filter, the modified gain matrix needs to be taken into account in the intermediate update step. Similarly, I-EnKF's gain matrix  $\bar{\mathbf{K}}_k$  is also modified using scalar  $\bar{l}_k$  which is the counterpart of  $l_k$  for the inverse filter's dynamics.

## 5 Unknown system dynamics

So far, we assumed that both the attacker and the defender have perfect system information. Nevertheless, in real-world scenarios, the agents employing the stochastic filters may not have any prior knowledge about the system model. The attacker may not be aware of the defender’s state evolution process (1). On the other hand, the defender may not know the attacker’s action strategy such that (4) is not available. Further, the attacker’s forward filter may be unknown and assuming a simple forward EKF/UKF may be inefficient. To this end, in the following, we present differentiable I-PF, differentiable I-EnKF, and RKHS-EnKF to learn the state estimates and the model parameters.

### 5.1 Differentiable I-PF

DPFs construct the system dynamics and the proposal distributions using NNs and optimize them using gradient descent. However, major challenges in developing DPFs are the non-differentiable importance sampling and resampling steps. Sampling from a proposal distribution is not differentiable because of the absence of explicit dependency between the sampled particles and the distribution parameters. On the other hand, the discrete nature of multinomial resampling makes it inherently non-differentiable, i.e., a small change in input weights can lead to abrupt changes in the resampling output. Additionally, the resampled particles are equally weighted, which is a constant such that the gradients are always zero. Hence, DPFs employ reparameterization-based differentiable sampling, and various differentiable resampling techniques (Chen and Li, 2023; Karkus et al., 2018; Corenflos et al., 2021; Zhu et al., 2020). Another important factor affecting DPFs’ performance is the loss function minimized in gradient descent to optimize NNs’ parameters.

Here, we discuss how this differentiable framework can be integrated into our I-PF to handle unknown dynamics case in inverse filtering. Following I-PF’s formulation in Section 3.1, differentiable I-PF considers the joint density of  $(\hat{\mathbf{x}}_k, \mathbf{y}_k)$  conditioned on the true states  $\mathbf{x}_{0:k}$  and defender’s observations  $\mathbf{a}_{1:k}$ . The formulation then closely follows from standard DPF methods, and hence, we only summarize them here. We refer the readers to Chen and Li (2023) (and the references therein) for further details.

**Proposal distributions:** The simplest choice of proposal distribution in PFs is the system’s state evolution. In DPFs, the sampled particle from this state evolution is computed as a function of the previous particle and an additional noise term. The corresponding function is parameterized by an unknown parameter  $\theta$  and is differentiable with respect to both the previous particle and the noise term. Similarly, in differentiable I-PF, we can consider a differentiable model for the optimal importance sampling density (20). For instance, we can model  $p(\hat{\mathbf{x}}_k | \hat{\mathbf{x}}_{k-1}, \mathbf{y}_k) p(\mathbf{y}_k | \mathbf{x}_k)$  as a jointly Gaussian distribution  $\mathcal{N}(\hat{\mathbf{x}}, \mathbf{y}_k; \mu_\theta(\hat{\mathbf{x}}_{k-1}, \mathbf{x}_k), \Sigma_\theta)$ . In this case, the sampled particles  $(\hat{\mathbf{x}}_k^i, \tilde{\mathbf{y}}_k^i)$  are obtained by adding zero-mean Gaussian noise of covariance  $\Sigma_\theta$  to the mean  $\mu_\theta(\hat{\mathbf{x}}_{k-1}^i, \mathbf{x}_k)$  where  $\hat{\mathbf{x}}_{k-1}^i$  is the (state estimate) particle from previous time instant and  $\mathbf{x}_k$  is the defender’s true state known perfectly. The function  $\mu_\theta(\cdot)$  is a differentiable function of  $\hat{\mathbf{x}}_{k-1}$  while  $\Sigma_\theta$  can be designed manually (Karkus et al., 2018; Wen et al., 2021) or parameterized for learning (Kloss et al., 2021).

Chen et al. (2021) provides an alternative differential sampling technique based on normalizing flows, wherein samples drawn from simple distributions (like Gaussian or uniform) are transformed into arbitrary distributions through a series of invertible mappings under

some mild conditions. Note that even though (20) minimizes the variance of weights, the information from current observation  $\mathbf{a}_k$  is not utilized. In general, constructing proposal distributions with observation  $\mathbf{a}_k$  provides samples that are closer to the true posterior and more uniformly weighted. Both the Gaussian model and normalising flow-based differential samplings can be generalized to include observation  $\mathbf{a}_k$  in the sampling distribution (Chen et al., 2021; Karkus et al., 2021).

**Observation models:** In differentiable I-PF, instead of (4), we consider a parameterized observation model as  $p_\theta(\mathbf{a}_k|\hat{\mathbf{x}}_k) \propto l_\theta(\mathbf{a}_k, \hat{\mathbf{x}}_k)$  where  $l_\theta(\cdot)$  is a differentiable function with respect to  $\mathbf{a}_k$  and  $\hat{\mathbf{x}}_k$ . To this end, we can consider known distribution with learnable parameters (Corenflos et al., 2021) or approximate  $p_\theta(\mathbf{a}_k|\hat{\mathbf{x}}_k)$  using a scalar function learned from NN (Karkus et al., 2018). The observations can also be mapped to an NN-based feature space as  $f_k = F_\theta(\mathbf{a}_k)$  such that  $l_\theta(\mathbf{a}_k, \hat{\mathbf{x}}_k) = h_\theta(f_k, \hat{\mathbf{x}}_k)$ . In Wen et al. (2021) and Chen et al. (2021), NNs are used to extract features from both the observations and states to measure similarity/discrepancy using user-defined metrics. Alternatively, conditional normalizing flows can also be employed to learn the measurement model (Chen and Li, 2022).

**Differentiable resampling:** Soft resampling, optimal transport (OT)-based resampling, and particle transformer-based resampling are popular differentiable techniques employed in DPFs and can be readily applied to differentiable I-PF. Soft resampling (Karkus et al., 2018) aims to generate non-zero gradients by modifying the importance weights by a factor  $\lambda$  as  $\bar{\omega}_k^i = \lambda\omega_k^i + (1 - \lambda)1/N$  where  $N$  is the total number of particles. However, the particles are selected using a multinomial distribution, and hence, the outputs still change abruptly. Soft resampling can be viewed as a linear interpolation between the multinomial distribution of original weights and one with equal weights. Contrarily, resampling using entropy-regularized OT (Corenflos et al., 2021) is fully differentiable. In particular, in differentiable I-PF, OT provides a map between the equally weighted empirical distribution  $\frac{1}{N} \sum_{i=1}^N \delta(\hat{\mathbf{x}}_k - \hat{\mathbf{x}}_k^i, \mathbf{y}_k - \mathbf{y}_k^i)$  and the target empirical distribution  $\sum_{i=1}^N \omega_k^i \delta(\hat{\mathbf{x}}_k - \tilde{\hat{\mathbf{x}}}_k^i, \mathbf{y}_k - \tilde{\mathbf{y}}_k^i)$ . Particle transformers (Zhu et al., 2020) are permutation-invariant and scale-equivalent NNs that take weighted particles  $\{\omega_k^i, (\hat{\mathbf{x}}_k^i, \tilde{\mathbf{y}}_k^i)\}_{1 \leq i \leq N}$  as inputs and output resampled particles  $\{(\hat{\mathbf{x}}_k^i, \mathbf{y}_k^i)\}_{1 \leq i \leq N}$  with equal weights. Particle transformers perform differentiable resampling but require pre-training with available training data.

**Loss functions and training:** Following the standard DPFs, differentiable I-PFs can be trained using supervised losses like root mean squared error (RMSE) or negative state likelihood when the ground truth, i.e., attacker’s state estimate  $\hat{\mathbf{x}}_k$  and observation  $\mathbf{y}_k$  are available (Karkus et al., 2018; Chen et al., 2021; Corenflos et al., 2021). Semi-supervised losses like marginal observation likelihoods are helpful when unlabelled data is abundant but access to labels is limited (Wen et al., 2021). Alternatively, variational inference optimizes evidence lower bound (ELBO) instead of likelihood to learn the model and proposal distribution simultaneously (Maddison et al., 2017; Le et al., 2018). With these objectives, DPFs and hence differentiable I-PFs, can be trained end-to-end (Karkus et al., 2018; Wen et al., 2021) or individually (Karkus et al., 2021; Lee et al., 2020). In end-to-end training, all components of the filter are jointly trained via gradient descent to minimize an overall loss function. Contrarily, in individual training, various components are first pre-trained independently and then fine-tuned jointly for a task-specific objective.

## 5.2 Differentiable I-EnKF and RKHS-EnKF

As in the case of PF, state augmentation-based, and MCMC-based parameter learning approaches have also been considered to generalize EnKF to unknown system dynamics (Anderson, 2001; Drovandi et al., 2022).

**Differentiable I-EnKF:** Recently, following DPF, auto-differentiable EnKF has been proposed in Chen et al. (2022) wherein EnKF’s state estimation procedure is combined with ML framework for learning the unknown dynamical system. Differentiable EnKF leverages EnKF’s ability to efficiently estimate high-dimensional states and automatic differentiation’s ability to train high-dimensional surrogate models. In particular, EnKF algorithm provides approximate data log-likelihoods for learning the unknown dynamics. Chen et al. (2022) consider both cases: (a) parametric system models with unknown parameters, and (b) fully unknown models approximated using NNs. Analogous approaches can be introduced in the I-EnKF framework to develop differentiable I-EnKF for inverse filtering in the unknown system case. Note that differentiable I-EnKF’s (learnt) state transition models the evolution of the attacker’s state estimate  $\hat{\mathbf{x}}_k$  incorporating true state  $\mathbf{x}_k$  information while the observation model corresponds to defender’s observation  $\mathbf{a}_k$ .

**RKHS-EnKF:** In our recent works Singh et al. (2023c) and Singh et al. (2024b), we developed RKHS-EKF and RKHS-UKF, respectively, by coupling EKF/UKF’s recursive state estimation with an approximate online expectation maximization (EM) algorithm to learn the unknown system parameters. To this end, the required expectations under the non-linear transformations were approximated using Taylor series linearization and the unscented transform, respectively, in RKHS-EKF and RKHS-UKF. However, following EnKF, we can approximate these expectations with the randomly generated ensemble that is updated using KF-like updates. Consequently, integrating the approximate online EM and EnKF frameworks, we can obtain RKHS-EnKF. RKHS-EnKF learns the state transition on its own and, therefore, functions as both the attacker’s forward filter and the defender’s inverse filter in the absence of any prior forward filter information. Further, our RKHS-EnKF can be trivially simplified if the agent has perfect prior information about either the state evolution, observation function, or noise covariance matrices. A key difference from standard EnKF is that the latter approximates the statistics of state  $\mathbf{x}_k$  given  $\mathbf{y}_{1:k}$ . However, the EM-based parameter updates also need the statistics of  $\mathbf{x}_{k-1}$  given  $\mathbf{y}_{1:k}$  (Singh et al., 2023c). Hence, RKHS-EnKF is formulated using an augmented state  $\mathbf{z}_k = [\mathbf{x}_k^T \ \mathbf{x}_{k-1}^T]^T$  (dimension  $n_z = 2n_x$ ), but only the ensemble corresponding to current state  $\mathbf{x}_k$  is propagated to the next time step. We refer the readers to Singh et al. (2023c, 2024b) for further details on the EM-based parameter learning procedure for RKHS-based KFs.

## 6 Numerical Experiments

We demonstrate the estimation performance of the proposed filters using different example systems. In Section 6.1, we consider a widely used one-dimensional non-linear system model (Arulampalam et al., 2002; Hu et al., 2008) and compare I-PF, I-GPF and I-EnKF with one another as well as I-EKF (Singh et al., 2023b). Besides the estimation error, we also consider recursive Cramér-Rao lower bound (RCRLB) (Tichavsky et al., 1998) and non-credibility index (NCI) (Li et al., 2001) as performance metrics. RCRLB provides a lower bound on MSE for discrete-time filtering, with simplified closed-form recursions for RCRLB



computation for non-linear systems with additive Gaussian noises provided in (Xiong et al., 2006). On the other hand, NCI is a credibility measure of how statistically close the estimated error covariance of an estimator is to the actual MSE matrix. In Section 6.2, we consider the bearing-only tracking system (Bar-Shalom et al., 2004; Lin et al., 2002) for I-PF and I-GPF, while Van der Pol oscillator and one-dimensional heat conduction systems (Gillijns et al., 2006) are considered for I-EnKF in Section 6.3 and 6.4, respectively. We focus on estimation error and time-complexity of the proposed algorithms in Section 6.2-6.4. The Van der Pol oscillator and heat conduction examples, respectively, represent low-dimensional non-linear and high-dimensional linear systems for which EnKF is known to be an efficient estimator. Note that in practice, a non-linear filter’s performance also depends on the system itself. Choosing a suitable filter for any application usually involves a trade-off between estimation accuracy and computational efforts (Li et al., 2017). The same argument holds for the non-linear inverse filtering problem as well.

Throughout all experiments, for simplicity, we choose EKF as the forward filter  $T(\cdot)$  in I-PF and I-GPF, regardless of the actual forward filter. I-EKF (Singh et al., 2023b) assumes a forward EKF while I-EnKF assumes a forward EnKF (as mentioned in Section 4.2). We choose the defender’s observation function  $g(\cdot)$  in (7) of the same form as the attacker’s observation function  $h(\cdot)$  in (6). Unless mentioned otherwise, all the forward filters are initialized with the same initial distribution. In particular, if  $\mathcal{N}(\mathbf{x}_0; \hat{\mathbf{x}}_0, \Sigma_0)$  is the forward filters’ initial distribution, then we initialize forward EKF/GPF with initial state  $\hat{\mathbf{x}}_0$  and initial covariance matrix  $\Sigma_0$  while forward PF/EnKF consider independent samples drawn from the initial distribution. All the inverse filters are also initialized in a similar manner.

### 6.1 One-dimensional non-linear system

Consider the non-linear system (Arulampalam et al., 2002)

$$x_{k+1} = \frac{x_k}{2} + \frac{25x_k}{1+x_k^2} + 8 \cos(1.2k) + w_k, \quad y_k = \frac{x_k^2}{20} + v_k, \quad a_k = \frac{\hat{x}_k^2}{10} + \epsilon_k,$$

where  $w_k \sim \mathcal{N}(0, 10)$ ,  $v_k \sim \mathcal{N}(0, 1)$  and  $\epsilon_k \sim \mathcal{N}(0, 5)$ . We set the number of particles (or ensemble size) for forward PF, GPF and EnKF as 25 while that for I-PF, I-GPF and I-EnKF as 50. The initial distribution for forward and inverse filters were  $\mathcal{N}(0, 5)$  and  $\mathcal{N}(0, 10)$ , respectively. Also, the function  $T(\cdot)$  is initialized with distribution  $\mathcal{N}(0, 10)$  in I-PF and I-GPF.

Fig. 3a-e show the time-averaged RMSE for the forward and inverse filters, averaged over 250 runs. The I-PF’s error in estimating state estimate  $\hat{\mathbf{x}}_k$  when the attacker’s actual forward filter is EKF is denoted by I-PF-E. The other notations in Fig. 3 and also, in further experiments are similarly defined. In Fig. 3a & b, we also include the corresponding RCRLBs. Note that RCRLB for forward PF/GPF/EnKF cannot be derived in closed-form because of lack of an explicit state-transition function and hence, omitted here. From Fig. 3a, we observe that forward PF, GPF and EnKF outperform forward EKF. While forward EnKF has the highest accuracy, forward PF and GPF have similar errors. This suggests that EKF’s linearization does not work well for the considered non-linear system. Hence, I-EKF also has the largest error in all but I-EKF-E cases (I-EKF-P/GP/En). Similarly, I-EnKF outperforms the other inverse filters in all cases, except for I-EnKF-E in Fig. 3b. For inferring forward EKF’s estimate, I-GPF turns out to be the most suitable

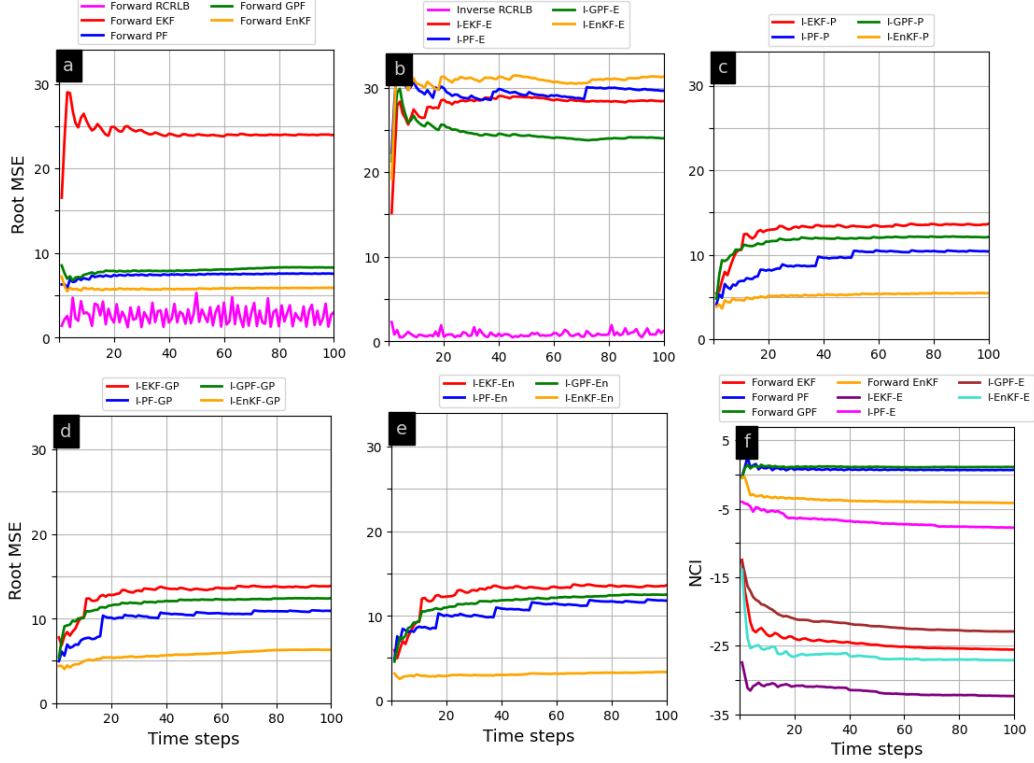


Figure 3: Time-averaged RMSE for (a) forward filters ( $\mathbf{x}_k$  estimation), (b) forward EKF's  $\hat{\mathbf{x}}_k$  estimation, (c) forward PF's  $\hat{\mathbf{x}}_k$  estimation, (d) forward GPF's  $\hat{\mathbf{x}}_k$  estimation, and (e) forward EnKF's  $\hat{\mathbf{x}}_k$  estimation; and (f) NCI (for forward and inverse filters) for non-linear system example, compared with inverse EKF.

estimator as shown in Fig. 3b. In Fig. 3c-e, I-PF and I-GPF are observed to have similar error, but slightly higher than I-EnKF. Fig. 3f shows NCI for different forward filters and inverse filters estimating forward EKF's  $\hat{x}_k$ . We observe that while forward EnKF has lowest estimation error (in Fig. 3a), both forward PF and GPF have almost perfect NCI (i.e., close to 0) and hence, are more credible. On the other hand, in the inverse filtering case, I-PF has the smallest (in magnitude) NCI while I-GPF and I-EnKF are highly pessimistic, i.e., their estimated covariance is larger than the actual MSE matrix.

## 6.2 Bearing only tracking

Consider a moving sensor tracking a target moving along x-axis using bearing measurements only. Denote  $p_k$  and  $v_k$  as the target's position (in m) and velocity (in m/sec), respectively, at the  $k$ -th time instant. The sensor's position is  $(s_k^x, s_k^y)$  with  $s_k^x = 4k + \Delta s_k^x$  and  $s_k^y = 20 + \Delta s_k^y$  where  $\Delta s_k^x$  and  $\Delta s_k^y$  denote perturbations distributed as  $\mathcal{N}(0, 1)$ . Then, the system model is (Lin et al., 2002)

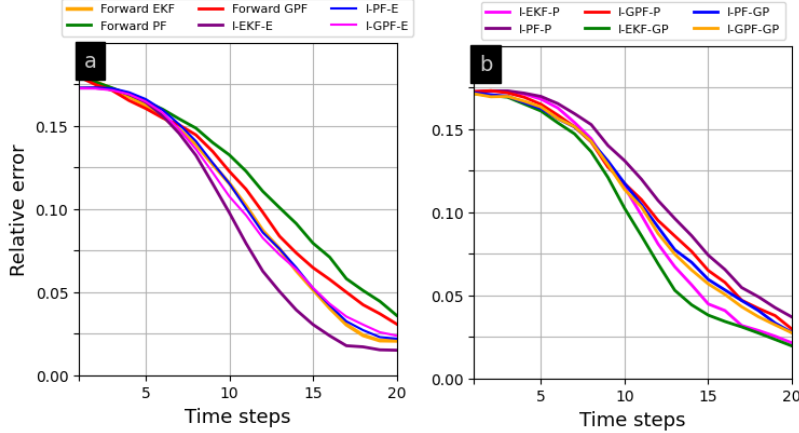


Figure 4: Relative error for (a) forward filters and forward EKF's  $\hat{\mathbf{x}}_k$  estimation, and (b) forward PF's and forward GPF's  $\hat{\mathbf{x}}_k$  estimation for bearing-only tracking system.

Table 3: Run time (in seconds) of different filters for bearing only tracking system.

Filter	$N = 100$	$N = 250$	$N = 500$
Forward EKF	0.0089	0.0098	0.0100
Forward PF	0.0191	0.0236	0.0361
Forward GPF	0.0377	0.0364	0.0486
I-EKF-E	0.0126	0.0103	0.0107
I-PF-E	0.0467	0.0935	0.1741
I-GPF-E	0.0492	0.0837	0.1429

$$\mathbf{x}_{k+1} \doteq \begin{bmatrix} p_{k+1} \\ v_{k+1} \end{bmatrix} = \begin{bmatrix} 1 & T \\ 0 & 1 \end{bmatrix} \begin{bmatrix} p_k \\ v_k \end{bmatrix} + \begin{bmatrix} T^2/2 \\ T \end{bmatrix} w_k, \quad y_k = \tan^{-1} \left( \frac{s_k^y}{p_k - s_k^x} \right) + v_k, \quad a_k = \tan^{-1} \left( \frac{s_k^y}{\hat{p}_k - s_k^x} \right) + \epsilon_k,$$

where  $w_k \sim \mathcal{N}(0, 0.01)$ ,  $v_k \sim \mathcal{N}(0, (3^\circ)^2)$  and  $\epsilon_k \sim \mathcal{N}(0, (5^\circ)^2)$  with  $T = 1$  sec. The initial state  $\mathbf{x}_0$  was  $[80, 1]^T$ . The forward filters were initialized with  $\mathcal{N}(\hat{\mathbf{x}}_0, \Sigma_0)$  where  $\hat{\mathbf{x}}_0 = [20/\tan^{-1}(y_1), 0]^T$  and  $\Sigma_0 = \text{diag}(16, 1)$ . The inverse filters were initialized with  $\mathcal{N}(\mathbf{x}_0, \mathbf{I}_2)$ . For both forward and inverse PFs and GPFs, the number of particles were set to 100. The recursion function  $T(\cdot)$  was also initialized with  $\mathcal{N}(\mathbf{x}_0, \mathbf{I}_2)$ . EKF's implementation for the considered system is provided in Bar-Shalom et al. (2004). Fig. 4 shows the relative error in position for the forward and inverse filters, averaged over 100 runs. For the bearing tracking example, forward PF and GPF have slightly higher error than forward EKF, but EKF requires Jacobian computations. The same is observed for inverse filters, i.e., I-PF and I-GPF have higher errors than I-EKF in all cases. Interestingly, GPF and I-GPF assuming a Gaussian posterior outperform forward PF and I-PF, respectively, with same number of particles. Note that EKF and I-EKF also consider a Gaussian posterior. This suggests that for the considered system, the Gaussian posterior assumption actually leads to better accuracy than the arbitrary distribution case of PF.

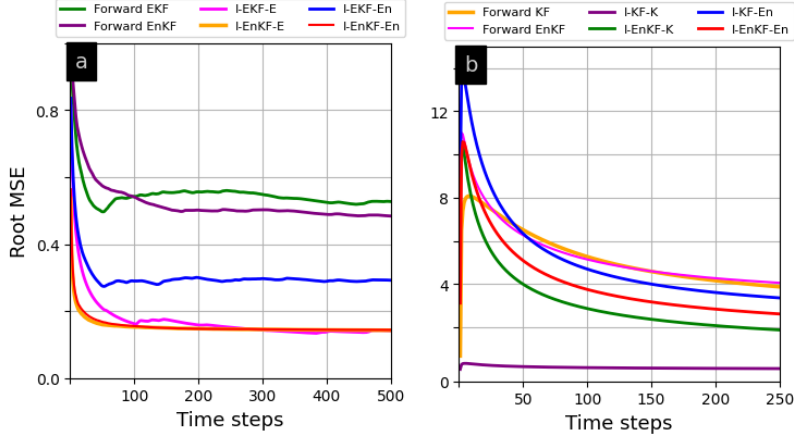


Figure 5: Time-averaged RMSE for forward and inverse EnKF for (a) Van der Pol oscillator, compared with forward and inverse EKF; and (b) One-dimensional heat conduction system, compared with forward and inverse KF.

Table 3 lists the total run time for 20 time steps (in one MC run) of forward and inverse filters estimating forward EKF’s state estimate. As expected, forward PF and GPF have longer run times than forward EKF. While forward PF’s complexity increases rapidly with the increase in number of particles, forward GPF has similar run times. The run times for the inverse filters are longer than the corresponding forward filters because an inverse filter also needs to compute function  $T(\cdot)$  for each sampled particle at each recursion. Interestingly, I-PF and I-GPF have similar run times for all  $N$ .

### 6.3 Van der Pol Oscillator

Consider the Van der Pol oscillator system (Gillijns et al., 2006)

$$\mathbf{x}_{k+1} = \begin{bmatrix} [\mathbf{x}_k]_1 + c_1[\mathbf{x}_k]_2 \\ [\mathbf{x}_k]_2 + c_1(c_2(1 - [\mathbf{x}_k]_1^2)[\mathbf{x}_k]_2 - [\mathbf{x}_k]_1) \end{bmatrix} + \mathbf{w}_k, \quad y_k = [0 \quad 1]\mathbf{x}_k + v_k, \quad a_k = [1 \quad 0]\hat{\mathbf{x}}_k + \epsilon_k,$$

where  $\mathbf{w}_k \sim \mathcal{N}(\mathbf{0}, \text{diag}(0.0262, 0.08))$ ,  $v_k \sim \mathcal{N}(0, 0.003)$  and  $\epsilon_k \sim \mathcal{N}(0, 0.03)$ . We set parameters  $c_1 = 0.1$  and  $c_2 = 1$ . The initial state  $\mathbf{x}_0 = [0, 0]^T$ . Considering forward EnKF’s ensemble size  $q = 30$ , the forward filters were initialized with  $\mathcal{N}(\hat{\mathbf{x}}_0, \Sigma_0)$  where  $\hat{\mathbf{x}}_0 = [1, -1]^T$  and  $\Sigma_0 = \text{diag}(6.3 \times 10^{-4}, 2.2 \times 10^{-4})$ . Similarly, I-EnKF’s ensemble size  $\bar{q} = 50$  and inverse filters were initialized with  $\mathcal{N}(\mathbf{x}_0, \bar{\Sigma}_0)$  where  $\bar{\Sigma}_0 = \text{diag}(6 \times 10^{-3}, 2 \times 10^{-3})$ . I-EKF also assumes the forward EKF’s  $\Sigma_0$  to be  $\bar{\Sigma}_0$ .

Fig. 5a shows the time-averaged RMSE for the forward and inverse filters, averaged over 100 runs. We observe that EnKF as the forward filter provides only mild improvement in estimation performance over EKF. Contrarily, I-EnKF outperforms I-EKF in estimating forward EnKF’s estimate (I-EnKF-En and I-EKF-En cases) and has same error when estimating forward EKF’s estimate (I-EnKF-E and I-EKF-E cases). Furthermore, incorrect assumption about the forward filter degrades I-EKF’s accuracy but not I-EnKF’s. Hence, we conclude that as standard EnKF is robust to system model deviations, our I-EnKF is also

Table 4: Run time (in seconds) of different filters for Van der Pol oscillator system.

Filter	$q = \bar{q} = 30$	$q = \bar{q} = 50$	$q = \bar{q} = 100$
Forward EKF	0.0102	0.0101	0.0102
Forward EnKF	0.1060	0.1513	0.2679
I-EKF-E	0.0193	0.0186	0.0177
I-EnKF-E	0.1053	0.1591	0.2857

Table 5: Run time (in seconds) of different filters for heat conduction example.

Filter	$q = \bar{q} = 100$	$q = \bar{q} = 250$	$q = \bar{q} = 500$
Forward KF	0.0654	0.0517	0.0552
Forward EnKF	0.2176	0.4301	0.6881
I-KF-K	0.1128	0.1149	0.1164
I-EnKF-K	0.2705	0.5692	1.0258

robust to incorrect forward filter assumptions. Table 4 lists the total run time for 500 time steps of forward and inverse EKF and EnKF. As expected, forward EnKF and I-EnKF have longer run times than forward EKF and EnKF, respectively. However, I-EnKF’s complexity is of the same order as forward EnKF increasing with the ensemble size.

#### 6.4 One-dimensional heat conduction

Denote  $\mathcal{T}(p, k)$  as the temperature of a one-dimensional bar of length  $L$  at position  $p$  and time  $k$ . We discretized the spatial grid with 100 cells and time with time-step 0.1 sec. Also,  $\mathcal{T}(0, k) = \mathcal{T}(L, k) = 300$  K for all  $k$ . Two external sinusoidal heat sources  $u_k^1 = 0.1 \sin(0.1\pi k)$  and  $u_k^2 = 0.1 \cos(0.1\pi k)$  act on the bar at  $p = 0.33L$  and  $0.67L$ , respectively. Defining the temperatures  $\mathcal{T}(p, k)$  except  $p = 0$  and  $p = L$  as state  $\mathbf{x}_k$ , the state evolution becomes  $\mathbf{x}_{k+1} = \mathbf{F}\mathbf{x}_k + \mathbf{B} \begin{bmatrix} u_k^1 \\ u_k^2 \end{bmatrix} + \mathbf{w}_k$  (Gillijns et al., 2006), where  $\mathbf{F}$  is a tridiagonal matrix with all diagonal elements 0.8 and off-diagonal elements 0.1, and  $\mathbf{w}_k \sim \mathcal{N}(0, 0.5\mathbf{I}_{100})$ . The observations  $\mathbf{y}_k$  are the noisy measurements of temperatures at  $p = 0.1L, 0.2L, \dots, 0.9L$  with  $\mathbf{v}_k \sim \mathcal{N}(\mathbf{0}, 0.01\mathbf{I}_9)$ . Similarly, observations  $\mathbf{a}_k$  are noisy measurements of the forward filter’s estimates at  $p = 0.05L, 0.15L, \dots, 0.95L$  with  $\boldsymbol{\epsilon}_k \sim \mathcal{N}(\mathbf{0}, 0.1\mathbf{I}_{10})$ . We set initial state and its estimates for forward and inverse KF (linear system) such that  $[\mathbf{x}_0]_i = [\hat{\mathbf{x}}_0]_i = [\hat{\hat{\mathbf{x}}}_0]_i = 10$  for all  $i$  and  $\boldsymbol{\Sigma}_0 = \mathbf{I}_{100}$  and  $\bar{\boldsymbol{\Sigma}}_0 = 0.1\mathbf{I}_{100}$ . I-KF also assumed forward KF’s  $\boldsymbol{\Sigma}_0$  to be  $\bar{\boldsymbol{\Sigma}}_0$ . On the other hand, both forward and inverse EnKF were initialized with samples drawn from  $\mathcal{U}[-10, 10]$  with ensemble sizes  $q = 100$  and  $\bar{q} = 500$ , respectively.

Fig. 5b shows the time-averaged RMSE (per cell) for forward and inverse KF and EnKF, averaged over 50 runs. While forward KF and EnKF have same accuracy, I-EnKF has higher error than I-KF when estimating forward KF’s estimate (I-KF-K and I-EnKF-K cases) because of the incorrect forward filter assumption. Note that I-KF is the optimal inverse filter for the considered linear system provided that the attacker’s true forward filter is also

KF. On the contrary, when the forward KF assumption does not hold, I-KF’s performance degrades such that I-EnKF outperforms I-KF (I-KF-En and I-EnKF-En cases). Table 5 lists the total run time for 250 time-steps of forward and inverse KF and EnKF. Forward EnKF and I-EnKF have longer run times than forward KF and I-KF, respectively, which increases with the ensemble size. Because of the high-dimensionality of the system, unlike Table 4, I-EnKF’s complexity is similar to forward EnKF only for ensemble size upto 250.

## 7 Summary

We studied the inverse filtering problem in counter-adversarial systems and developed I-PF based on the SIS and resampling techniques. Unlike prior inverse filters, the proposed I-PF considers general attacker-defender dynamics, including non-Gaussian systems. Furthermore, we proved that under mild assumptions on the system model, I-PF converges to the optimal inverse filter in the  $L^4$  sense. For practical systems wherein Gaussian posterior assumption works well, we developed I-GPF and I-EnKF, which can be suitably generalized to non-Gaussian systems. Additionally, I-EnKF is an efficient filter for very high-dimensional systems. Differentiable I-PF, differentiable I-EnKF, and RKHS-EnKF provide the attacker’s state estimate and learn the system parameters for unknown system dynamics in the inverse filtering context. Our numerical experiments demonstrated that even under the incorrect forward filter assumption, the proposed inverse filters provide reasonable estimates.

## Acknowledgments and Disclosure of Funding

A. C. acknowledges support via the professional development fund and professional development allowance from IIT Delhi, grant no. GP/2021/ISSC/022 from I-Hub Foundation for Cobotics and grant no. CRG/2022/003707 from Science and Engineering Research Board (SERB), India. H. S. acknowledges support via Prime Minister Research Fellowship. K. V. M. acknowledges support from the National Academies of Sciences, Engineering, and Medicine via Army Research Laboratory Harry Diamond Distinguished Fellowship.

## Appendix A. Proof of (17) and (18)

The densities (17) and (18) follow from the conditional independence of observations and the estimation process assumed in the system model (1)-(4) using the standard PF’s SIS-based non-linear filtering technique (Ristic et al., 2003, Chapter 3.2). Recall from Section 3.1 that we consider the joint density  $p(\hat{\mathbf{x}}_{0:k}, \mathbf{y}_{1:k} | \mathbf{x}_{0:k}, \mathbf{a}_{1:k}) = p(\hat{\mathbf{x}}_{0:k}, \mathbf{y}_{1:k} | \mathbf{a}_k, \mathbf{x}_{0:k}, \mathbf{a}_{1:k-1})$  to obtain I-PF’s optimal sampling density and weights. Using Bayes’ theorem, we have

$$p(\hat{\mathbf{x}}_{0:k}, \mathbf{y}_{1:k} | \mathbf{x}_{0:k}, \mathbf{a}_{1:k}) = \frac{p(\mathbf{a}_k | \hat{\mathbf{x}}_{0:k}, \mathbf{y}_{1:k}, \mathbf{x}_{0:k}, \mathbf{a}_{1:k-1}) p(\hat{\mathbf{x}}_{0:k}, \mathbf{y}_{1:k} | \mathbf{x}_{0:k}, \mathbf{a}_{1:k-1})}{p(\mathbf{a}_k | \mathbf{x}_{0:k}, \mathbf{a}_{1:k-1})}. \quad (29)$$

First, consider  $p(\mathbf{a}_k | \hat{\mathbf{x}}_{0:k}, \mathbf{y}_{1:k}, \mathbf{x}_{0:k}, \mathbf{a}_{1:k-1}) = p(\mathbf{a}_k | \hat{\mathbf{x}}_k, \hat{\mathbf{x}}_{0:k-1}, \mathbf{y}_{1:k}, \mathbf{x}_{0:k}, \mathbf{a}_{1:k-1})$ . From (4), the defender’s observation  $\mathbf{a}_k$  depends only on the state estimate  $\hat{\mathbf{x}}_k$  such that  $p(\mathbf{a}_k | \hat{\mathbf{x}}_{0:k}, \mathbf{y}_{1:k}, \mathbf{x}_{0:k}, \mathbf{a}_{1:k-1}) = p(\mathbf{a}_k | \hat{\mathbf{x}}_k)$ .

Next, we simplify  $p(\hat{\mathbf{x}}_{0:k}, \mathbf{y}_{1:k} | \mathbf{x}_{0:k}, \mathbf{a}_{1:k-1})$  in the numerator of (29). To this end, we have  $p(\hat{\mathbf{x}}_k, \hat{\mathbf{x}}_{0:k-1}, \mathbf{y}_{1:k} | \mathbf{x}_{0:k}, \mathbf{a}_{1:k-1}) = p(\hat{\mathbf{x}}_k | \hat{\mathbf{x}}_{0:k-1}, \mathbf{y}_{1:k}, \mathbf{x}_{0:k}, \mathbf{a}_{1:k-1}) p(\hat{\mathbf{x}}_{0:k-1}, \mathbf{y}_{1:k} | \mathbf{x}_{0:k}, \mathbf{a}_{1:k-1})$ . But,

from (3), given  $T(\cdot)$ , state estimate  $\hat{\mathbf{x}}_k$  is a function of previous estimate  $\hat{\mathbf{x}}_{k-1}$  and observation  $\mathbf{y}_k$  such that  $p(\hat{\mathbf{x}}_k|\hat{\mathbf{x}}_{0:k-1}, \mathbf{y}_{1:k}, \mathbf{x}_{0:k}, \mathbf{a}_{1:k-1})$  simplifies to  $p(\hat{\mathbf{x}}_k|\hat{\mathbf{x}}_{k-1}, \mathbf{y}_k)$ . Also,  $p(\mathbf{y}_k, \hat{\mathbf{x}}_{0:k-1}, \mathbf{y}_{1:k-1}|\mathbf{x}_{0:k}, \mathbf{a}_{1:k-1}) = p(\mathbf{y}_k|\hat{\mathbf{x}}_{0:k-1}, \mathbf{y}_{1:k-1}, \mathbf{x}_{0:k}, \mathbf{a}_{1:k-1})p(\hat{\mathbf{x}}_{0:k-1}, \mathbf{y}_{1:k-1}|\mathbf{x}_{0:k}, \mathbf{a}_{1:k-1})$ . From (2), observation  $\mathbf{y}_k$  depends only on the true state  $\mathbf{x}_k$  such that  $p(\mathbf{y}_k|\hat{\mathbf{x}}_{0:k-1}, \mathbf{y}_{1:k-1}, \mathbf{x}_{0:k}, \mathbf{a}_{1:k-1}) = p(\mathbf{y}_k|\mathbf{x}_k)$ . Lastly, the attacker's estimation process and the observations upto  $(k-1)$ -th time instant are independent of future state  $\mathbf{x}_k$  given the past states, i.e.,  $p(\hat{\mathbf{x}}_{0:k-1}, \mathbf{y}_{1:k-1}|\mathbf{x}_{0:k}, \mathbf{a}_{1:k-1}) = p(\hat{\mathbf{x}}_{0:k-1}, \mathbf{y}_{1:k-1}|\mathbf{x}_{0:k-1}, \mathbf{a}_{1:k-1})$ . Now, substituting  $p(\mathbf{a}_k|\hat{\mathbf{x}}_{0:k}, \mathbf{y}_{1:k}, \mathbf{x}_{0:k}, \mathbf{a}_{1:k-1}) = p(\mathbf{a}_k|\hat{\mathbf{x}}_k)$  and  $p(\hat{\mathbf{x}}_{0:k}, \mathbf{y}_{1:k}|\mathbf{x}_{0:k}, \mathbf{a}_{1:k-1}) = p(\hat{\mathbf{x}}_k|\hat{\mathbf{x}}_{k-1}, \mathbf{y}_k)p(\mathbf{y}_k|\mathbf{x}_k)p(\hat{\mathbf{x}}_{0:k-1}, \mathbf{y}_{1:k-1}|\mathbf{x}_{0:k-1}, \mathbf{a}_{1:k-1})$  in (29) yields

$$p(\hat{\mathbf{x}}_{0:k}, \mathbf{y}_{1:k}|\mathbf{x}_{0:k}, \mathbf{a}_{1:k}) \propto p(\mathbf{a}_k|\hat{\mathbf{x}}_k)p(\hat{\mathbf{x}}_k|\hat{\mathbf{x}}_{k-1}, \mathbf{y}_k)p(\mathbf{y}_k|\mathbf{x}_k)p(\hat{\mathbf{x}}_{0:k-1}, \mathbf{y}_{1:k-1}|\mathbf{x}_{0:k-1}, \mathbf{a}_{1:k-1}),$$

which is (17) provided in Section 3.1.

Now, we consider the sampling density (18) of our I-PF. The standard PF estimating states  $\mathbf{x}_{0:k}$  given observations  $\mathbf{y}_{1:k}$  uses a sampling density  $\tilde{q}(\mathbf{x}_{0:k}|\mathbf{y}_{1:k})$  that factorizes as  $\tilde{q}(\mathbf{x}_{0:k}|\mathbf{y}_{1:k}) \doteq \tilde{q}(\mathbf{x}_k|\mathbf{x}_{0:k-1}, \mathbf{y}_{1:k})\tilde{q}(\mathbf{x}_{0:k-1}|\mathbf{y}_{1:k-1})$  (Ristic et al., 2003, eq. 3.12). In the case of I-PF, we are estimating the joint density of  $(\hat{\mathbf{x}}_{0:k}, \mathbf{y}_{1:k})$  given true states  $\mathbf{x}_{0:k}$  and observations  $\mathbf{a}_{1:k}$ . Hence, we choose a sampling density  $q(\cdot)$  such that

$$q(\hat{\mathbf{x}}_{0:k}, \mathbf{y}_{1:k}|\mathbf{x}_{0:k}, \mathbf{a}_{1:k}) \doteq q(\hat{\mathbf{x}}_k, \mathbf{y}_k|\hat{\mathbf{x}}_{0:k-1}, \mathbf{y}_{1:k-1}, \mathbf{x}_{0:k}, \mathbf{a}_{1:k})q(\hat{\mathbf{x}}_{0:k-1}, \mathbf{y}_{1:k-1}|\mathbf{x}_{0:k-1}, \mathbf{a}_{1:k-1}).$$

Furthermore, when the standard PF requires only the filtered posterior  $p(\mathbf{x}_k|\mathbf{y}_{1:k})$  at each time step, the sampling density  $\tilde{q}(\mathbf{x}_k|\mathbf{x}_{0:k-1}, \mathbf{y}_{1:k})$  is commonly assumed to depend only on  $\mathbf{x}_{k-1}$  and  $\mathbf{y}_k$  (Ristic et al., 2003, Sec. 3.2), i.e.,  $\tilde{q}(\mathbf{x}_k|\mathbf{x}_{0:k-1}, \mathbf{y}_{1:k}) = \tilde{q}(\mathbf{x}_k|\mathbf{x}_{k-1}, \mathbf{y}_k)$ . Similarly, in our I-PF, we assume  $q(\hat{\mathbf{x}}_k, \mathbf{y}_k|\hat{\mathbf{x}}_{0:k-1}, \mathbf{y}_{1:k-1}, \mathbf{x}_{0:k}, \mathbf{a}_{1:k}) = q(\hat{\mathbf{x}}_k, \mathbf{y}_k|\hat{\mathbf{x}}_{k-1}, \mathbf{y}_{k-1}, \mathbf{x}_k, \mathbf{a}_k)$ . Overall, we choose I-PF's sampling density such that  $q(\hat{\mathbf{x}}_{0:k}, \mathbf{y}_{1:k}|\mathbf{x}_{0:k}, \mathbf{a}_{1:k}) = q(\hat{\mathbf{x}}_k, \mathbf{y}_k|\hat{\mathbf{x}}_{k-1}, \mathbf{y}_{k-1}, \mathbf{x}_k, \mathbf{a}_k)q(\hat{\mathbf{x}}_{0:k-1}, \mathbf{y}_{1:k-1}|\mathbf{x}_{0:k-1}, \mathbf{a}_{1:k-1})$ , which is (18) of Section 3.1.

## Appendix B. Proof of Theorem 1

In the following, we first restate some useful Lemma 1-4 from Hu et al. (2008). In Section B.1, some preliminary results are derived, from which the proof of Theorem 1 follows using a standard mathematical induction approach.

**Lemma 1.** *Let  $\{\xi_i\}_{1 \leq i \leq n}$  be conditionally independent random variables given  $\sigma$ -algebra  $\mathcal{G}$  such that  $\mathbb{E}[\xi_i|\mathcal{G}] = 0$  and  $\mathbb{E}[|\xi_i|^4|\mathcal{G}] < \infty$ . Then  $\mathbb{E}\left[\left|\sum_{i=1}^n \xi_i\right|^4|\mathcal{G}\right] \leq \sum_{i=1}^n \mathbb{E}[|\xi_i|^4|\mathcal{G}] + \left(\sum_{i=1}^n \mathbb{E}[|\xi_i|^2|\mathcal{G}]\right)^2$ .*

**Lemma 2.** *If  $\mathbb{E}|\xi|^p < \infty$ , then  $\mathbb{E}|\xi - \mathbb{E}[\xi]|^p \leq 2^p \mathbb{E}|\xi|^p$ , for any  $p \geq 1$ .*

**Lemma 3.** *Let  $\{\xi_i\}_{1 \leq i \leq n}$  be conditionally independent random variables given  $\sigma$ -algebra  $\mathcal{G}$  such that  $\mathbb{E}[\xi_i|\mathcal{G}] = 0$  and  $\mathbb{E}[|\xi_i|^4|\mathcal{G}] < \infty$ . Then  $\mathbb{E}\left[\left|\frac{1}{n} \sum_{i=1}^n \xi_i\right|^4|\mathcal{G}\right] \leq 2 \max_{1 \leq i \leq n} \mathbb{E}[|\xi_i|^4|\mathcal{G}]/n^2$ .*

**Lemma 4.** *Denote  $A^c$  as the complementary set of a given set  $A$ . Also,  $I_A$  denotes the indicator function for a set  $A$ . Consider a random variable  $\eta$  with probability density function  $p(x)$  such that  $\mathbb{P}(\eta \in A^c) \leq \epsilon < 1$ . Define a random variable  $\xi$  with probability density function as  $\frac{p(x)I_A}{\mathbb{P}(A)}$  where  $\mathbb{P}(A) = \int p(y)I_A dy$ . If  $\psi$  be a measurable function satisfying  $\mathbb{E}[\psi^2(\eta)] < \infty$ , then  $|\mathbb{E}[\psi(\xi)] - \mathbb{E}[\psi(\eta)]| \leq \frac{2\sqrt{\mathbb{E}[\psi^2(\eta)]}}{1-\epsilon} \sqrt{\epsilon}$ . In the case when  $\mathbb{E}|\psi(\eta)| < \infty$ , we have  $\mathbb{E}|\psi(\xi)| \leq \frac{\mathbb{E}|\psi(\eta)|}{1-\epsilon}$ .*

## B.1 Preliminaries to the proof

Denote  $\mathcal{F}_{k-1} = \sigma\{(\hat{\mathbf{x}}_{k-1}^i, \mathbf{y}_{k-1}^i) \text{ for } 1 \leq i \leq N\}$  as the  $\sigma$ -algebra generated by particles at the previous  $(k-1)$ -th time step. For Lemma 5-7, we assume (22) holds for the previous time instant  $(k-1)$ . In (43) of Appendix B.2, it is shown that (22) also holds for  $k=0$ . Further, we assume

$$\mathbb{E}|\langle \pi_{k-1|k-1}^N, |\phi|^4 \rangle| \leq M_{k-1|k-1} \|\phi\|_{k-1,4}^4. \quad (30)$$

where  $M_{k-1|k-1} > 0$  is a constant independent of the number of particles  $N$ . This inequality is necessary for the proof of the theorem and also proved to hold for all  $k \geq 0$  in Section B.2.

**Lemma 5.** *Consider the particles  $\{(\hat{\mathbf{x}}_k^i, \bar{\mathbf{y}}_k^i)\}$  drawn in the I-PF's importance sampling step. Assume that (22) holds for  $(k-1)$ -th time instant. Then, for sufficiently large  $N$ , we have*

$$\mathbb{P}\left(\frac{1}{N} \sum_{i=1}^N \beta(\mathbf{a}_k | \hat{\mathbf{x}}_k^i) < \gamma_k | \mathcal{F}_{k-1}\right) < \epsilon_k \quad (31)$$

for some  $0 < \epsilon_k < 1$ , which implies that the I-PF algorithm will not run into an infinite loop in steps 1 and 2.

*Proof.* Note that  $(\hat{\mathbf{x}}_k^i, \bar{\mathbf{y}}_k^i)$  are drawn from the distribution  $\langle \pi_{k-1|k-1}^N, \delta_T \rho \rangle$  in the importance sampling step such that

$$\mathbb{E}[\phi(\hat{\mathbf{x}}_k^i, \bar{\mathbf{y}}_k^i) | \mathcal{F}_{k-1}] = \langle \pi_{k-1|k-1}^N, \delta_T \rho \phi \rangle, \quad (32)$$

Further, since  $(\hat{\mathbf{x}}_k^i, \bar{\mathbf{y}}_k^i)$  have equal weights (because of resampling at each step), we have  $\frac{1}{N} \sum_{i=1}^N \beta(\mathbf{a}_k | \hat{\mathbf{x}}_k^i) = \langle \pi_{k-1|k-1}^N, \delta_T \rho \beta \rangle$ . Because of the modification, the distribution of  $\{(\hat{\mathbf{x}}_k^i, \tilde{\mathbf{y}}_k^i)\}$  is obtained from the distribution of  $\{(\hat{\mathbf{x}}_k^i, \bar{\mathbf{y}}_k^i)\}$  conditioned on the event  $\Gamma_k \doteq \{\langle \pi_{k-1|k-1}^N, \delta_T \rho \beta \rangle \geq \gamma_k\}$ . In order to use Lemma 4 to handle the difference in the empirical distributions of  $\{(\hat{\mathbf{x}}_k^i, \bar{\mathbf{y}}_k^i)\}$  and  $\{(\hat{\mathbf{x}}_k^i, \tilde{\mathbf{y}}_k^i)\}$ , we require the probability of  $\Gamma_k^c = \{\langle \pi_{k-1|k-1}^N, \delta_T \rho \beta \rangle < \gamma_k\}$ . Consider

$$\begin{aligned} \mathbb{P}(\langle \pi_{k-1|k-1}^N, \delta_T \rho \beta \rangle < \gamma_k) &= \mathbb{P}(\langle \pi_{k-1|k-1}^N, \delta_T \rho \beta \rangle - \langle \pi_{k-1|k-1}, \delta_T \rho \beta \rangle < \gamma_k - \langle \pi_{k-1|k-1}, \delta_T \rho \beta \rangle) \\ &\leq \mathbb{P}(|\langle \pi_{k-1|k-1}^N, \delta_T \rho \beta \rangle - \langle \pi_{k-1|k-1}, \delta_T \rho \beta \rangle| > |\gamma_k - \langle \pi_{k-1|k-1}, \delta_T \rho \beta \rangle|), \end{aligned}$$

because  $\gamma_k - \langle \pi_{k-1|k-1}, \delta_T \rho \beta \rangle < 0$  from assumption **A1**. Using Markov's inequality and then, (22) replacing  $k$  by  $k-1$  with the indicator function being bounded by 1 yields

$$\begin{aligned} \mathbb{P}(\langle \pi_{k-1|k-1}^N, \delta_T \rho \beta \rangle < \gamma_k) &\leq \frac{\mathbb{E}|\langle \pi_{k-1|k-1}^N, \delta_T \rho \beta \rangle - \langle \pi_{k-1|k-1}, \delta_T \rho \beta \rangle|^4}{|\gamma_k - \langle \pi_{k-1|k-1}, \delta_T \rho \beta \rangle|^4} \\ &\leq \frac{C_{k-1|k-1} \|\rho\|_\infty^4}{|\gamma_k - \langle \pi_{k-1|k-1}, \delta_T \rho \beta \rangle|^4} \times \frac{\|\beta\|_{k-1,4}^4}{N^2}. \end{aligned}$$

Hence, (31) will hold for some  $0 < \epsilon_k < 1$  for sufficiently large  $N$ . In the following, we denote  $C_{\gamma_k} = \frac{C_{k-1|k-1} \|\rho\|_\infty^4}{|\gamma_k - \langle \pi_{k-1|k-1}, \delta_T \rho \beta \rangle|^4}$ . ■



**Lemma 6.** Consider the optimal filter's prediction distribution  $\pi_{k|k-1}$  and its approximation  $\tilde{\pi}_{k|k-1}^N$  obtained in I-PF. Define

$$\Pi_1 \doteq \langle \tilde{\pi}_{k|k-1}^N, \phi \rangle - \frac{1}{N} \sum_{i=1}^N \mathbb{E}[\phi(\hat{\mathbf{x}}_k^i, \tilde{\mathbf{y}}_k^i) | \mathcal{F}_{k-1}], \quad (33)$$

$$\Pi_2 \doteq \frac{1}{N} \sum_{i=1}^N \mathbb{E}[\phi(\hat{\mathbf{x}}_k^i, \tilde{\mathbf{y}}_k^i) | \mathcal{F}_{k-1}] - \langle \pi_{k-1|k-1}^N, \delta_T \rho \phi \rangle, \quad (34)$$

$$\Pi_3 \doteq \langle \pi_{k-1|k-1}^N, \delta_T \rho \phi \rangle - \langle \pi_{k|k-1}, \phi \rangle. \quad (35)$$

Then,  $\Pi_1$ ,  $\Pi_2$  and  $\Pi_3$  satisfy

$$\mathbb{E}[|\Pi_1|^4] \leq C_{\Pi_1} \frac{\|\phi\|_{k-1,4}^4}{N^2}, \quad (36)$$

$$\mathbb{E}[|\Pi_2|^4] \leq C_{\Pi_2} \frac{\|\phi\|_{k-1,4}^4}{N^2}, \quad (37)$$

$$\mathbb{E}[|\Pi_3|^4] \leq C_{\Pi_3} \frac{\|\phi\|_{k-1,4}^4}{N^2}, \quad (38)$$

for suitable constants  $C_{\Pi_1}, C_{\Pi_2}$  and  $C_{\Pi_3} > 0$ . Note that  $\Pi_1, \Pi_2$  and  $\Pi_3$  are defined for given  $\pi_{k|k-1}$  and  $\tilde{\pi}_{k|k-1}^N$  distributions while constants  $C_{\Pi_1}, C_{\Pi_2}$  and  $C_{\Pi_3}$  do not dependent on  $N$ .

*Proof.* **(a)  $\Pi_1$  term:** Recall that  $\tilde{\pi}_{k|k-1}^N$  is the empirical distribution obtained from particles  $\{(\hat{\mathbf{x}}_k^i, \tilde{\mathbf{y}}_k^i)\}$ . Hence,

$$\begin{aligned} \mathbb{E}[|\Pi_1|^4 | \mathcal{F}_{k-1}] &= \mathbb{E} \left[ \left| \frac{1}{N} \sum_{i=1}^N (\phi(\hat{\mathbf{x}}_k^i, \tilde{\mathbf{y}}_k^i) - \mathbb{E}[\phi(\hat{\mathbf{x}}_k^i, \tilde{\mathbf{y}}_k^i) | \mathcal{F}_{k-1}]) \right|^4 \middle| \mathcal{F}_{k-1} \right] \\ &\leq \frac{1}{N^4} \sum_{i=1}^N \mathbb{E}[|\phi(\hat{\mathbf{x}}_k^i, \tilde{\mathbf{y}}_k^i) - \mathbb{E}[\phi(\hat{\mathbf{x}}_k^i, \tilde{\mathbf{y}}_k^i) | \mathcal{F}_{k-1}]|^4 | \mathcal{F}_{k-1}] + \frac{1}{N^4} \left( \sum_{i=1}^N \mathbb{E}[|\phi(\hat{\mathbf{x}}_k^i, \tilde{\mathbf{y}}_k^i) - \mathbb{E}[\phi(\hat{\mathbf{x}}_k^i, \tilde{\mathbf{y}}_k^i) | \mathcal{F}_{k-1}]|^2 | \mathcal{F}_{k-1}] \right)^2 \\ &\leq \frac{1}{N^4} \left( \sum_{i=1}^N 2^4 \mathbb{E}[|\phi(\hat{\mathbf{x}}_k^i, \tilde{\mathbf{y}}_k^i)|^4 | \mathcal{F}_{k-1}] + \left( \sum_{i=1}^N 2^2 \mathbb{E}[|\phi(\hat{\mathbf{x}}_k^i, \tilde{\mathbf{y}}_k^i)|^2 | \mathcal{F}_{k-1}] \right)^2 \right), \end{aligned}$$

where the first and second inequalities are obtained using Lemma 1 and 2, respectively. Since  $(\hat{\mathbf{x}}_k^i, \bar{\mathbf{y}}_k^i)$  are obtained from  $(\hat{\mathbf{x}}_k^i, \tilde{\mathbf{y}}_k^i)$  such that  $\Gamma_k$  (defined in Lemma 5) occurs and  $\mathbb{P}(\Gamma_k^c) < \epsilon_k$ , using Lemma 4 yields

$$\begin{aligned} \mathbb{E}[|\Pi_1|^4 | \mathcal{F}_{k-1}] &\leq \frac{2^4}{N^4} \left( \sum_{i=1}^N \frac{\mathbb{E}[|\phi(\hat{\mathbf{x}}_k^i, \bar{\mathbf{y}}_k^i)|^4 | \mathcal{F}_{k-1}]}{1 - \epsilon_k} + \left( \sum_{i=1}^N \frac{\mathbb{E}[|\phi(\hat{\mathbf{x}}_k^i, \bar{\mathbf{y}}_k^i)|^2 | \mathcal{F}_{k-1}]}{1 - \epsilon_k} \right)^2 \right) \\ &= \frac{2^4}{N^4 (1 - \epsilon_k)^2} \sum_{i=1}^N (1 - \epsilon_k) \mathbb{E}[|\phi(\hat{\mathbf{x}}_k^i, \bar{\mathbf{y}}_k^i)|^4 | \mathcal{F}_{k-1}] + \frac{2^4}{N^4 (1 - \epsilon_k)^2} \left( \sum_{i=1}^N \mathbb{E}[|\phi(\hat{\mathbf{x}}_k^i, \bar{\mathbf{y}}_k^i)|^2 | \mathcal{F}_{k-1}] \right)^2 \\ &\leq \frac{2^4}{N^4 (1 - \epsilon_k)^2} \left( \sum_{i=1}^N \mathbb{E}[|\phi(\hat{\mathbf{x}}_k^i, \bar{\mathbf{y}}_k^i)|^4 | \mathcal{F}_{k-1}] + \left( \sum_{i=1}^N \mathbb{E}[|\phi(\hat{\mathbf{x}}_k^i, \bar{\mathbf{y}}_k^i)|^2 | \mathcal{F}_{k-1}] \right)^2 \right), \end{aligned}$$

where the last inequality is obtained using  $1 - \epsilon_k < 1$ . Expressing the expectations as in (32), we have

$$\begin{aligned} \mathbb{E}[|\Pi_1|^4 | \mathcal{F}_{k-1}] &\leq \frac{2^4}{N^4(1 - \epsilon_k)^2} \left( \sum_{i=1}^N \langle \pi_{k-1|k-1}^N, \delta_T \rho |\phi|^4 \rangle + \left( \sum_{i=1}^N \langle \pi_{k-1|k-1}^N, \delta_T \rho |\phi|^2 \rangle \right)^2 \right) \\ &= \frac{2^4}{(1 - \epsilon_k)^2} \left( \frac{\langle \pi_{k-1|k-1}^N, \delta_T \rho |\phi|^4 \rangle}{N^3} + \frac{\langle \pi_{k-1|k-1}^N, \delta_T \rho |\phi|^2 \rangle^2}{N^2} \right) \\ &\leq \frac{2^4}{(1 - \epsilon_k)^2} \left( \frac{\langle \pi_{k-1|k-1}^N, \delta_T \rho |\phi|^4 \rangle}{N^3} + \frac{\langle \pi_{k-1|k-1}^N, \delta_T \rho |\phi|^4 \rangle}{N^2} \right) \leq \frac{2^5}{(1 - \epsilon_k)^2} \frac{\langle \pi_{k-1|k-1}^N, \delta_T \rho |\phi|^4 \rangle}{N^2}, \end{aligned}$$

where the second last and last inequalities result from Jensen's inequality and  $N > 1$ , respectively. Finally, using (30) with the indicator function being bounded by 1, we have

$$\mathbb{E}[|\Pi_1|^4] \leq \frac{2^5}{(1 - \epsilon_k)^2} \|\rho\|_\infty M_{k-1|k-1} \frac{\|\phi\|_{k-1,4}^4}{N^2},$$

which gives (36) with  $C_{\Pi_1} \doteq \frac{2^5}{(1 - \epsilon_k)^2} \|\rho\|_\infty M_{k-1|k-1}$ .

**(b)  $\Pi_2$  term:** Using (32), we have

$$|\Pi_2|^4 = \left| \frac{1}{N} \sum_{i=1}^N (\mathbb{E}[\phi(\hat{\mathbf{x}}_k^i, \tilde{\mathbf{y}}_k^i) | \mathcal{F}_{k-1}] - \mathbb{E}[\phi(\hat{\mathbf{x}}_k^i, \bar{\mathbf{y}}_k^i) | \mathcal{F}_{k-1}]) \right|^4 \leq \frac{1}{N} \sum_{i=1}^N |\mathbb{E}[\phi(\hat{\mathbf{x}}_k^i, \tilde{\mathbf{y}}_k^i) | \mathcal{F}_{k-1}] - \mathbb{E}[\phi(\hat{\mathbf{x}}_k^i, \bar{\mathbf{y}}_k^i) | \mathcal{F}_{k-1}]|^4,$$

from the Jensen's inequality. As mentioned earlier  $\{(\hat{\mathbf{x}}_k^i, \bar{\mathbf{y}}_k^i)\}$  are obtained from  $\{(\hat{\mathbf{x}}_k^i, \tilde{\mathbf{y}}_k^i)\}$  such that  $\Gamma_k$  occurs such that using Lemma 4 and then Jensen's inequality, we obtain

$$|\Pi_2|^4 \leq \frac{1}{N} \sum_{i=1}^N \left( \frac{2\sqrt{\mathbb{E}[\phi(\hat{\mathbf{x}}_k^i, \bar{\mathbf{y}}_k^i)^2 | \mathcal{F}_{k-1}]} \sqrt{\epsilon_k}}{1 - \epsilon_k} \right)^4 \leq \frac{2^4 \epsilon_k^2}{N(1 - \epsilon_k)^4} \sum_{i=1}^N \mathbb{E}[\phi(\hat{\mathbf{x}}_k^i, \bar{\mathbf{y}}_k^i)^4 | \mathcal{F}_{k-1}].$$

Substituting  $\epsilon_k = C_{\gamma_k} \|\beta\|_{k-1,4}^4 / N^2$  (from Lemma 5) and (32), we have

$$|\Pi_2|^4 \leq \frac{2^4}{(1 - \epsilon_k)^4} C_{\gamma_k}^2 \frac{\|\beta\|_{k-1,4}^8}{N^4} \langle \pi_{k-1|k-1}^N, \delta_T \rho \phi^4 \rangle.$$

Denote  $C'_{\Pi_2} = 2^4 C_{\gamma_k}^2 \|\beta\|_{k-1,4}^8 / (1 - \epsilon_k)^4$ . Finally, using (30) with the indicator function being bounded by 1, we have

$$\mathbb{E}[|\Pi_2|^4] \leq C'_{\Pi_2} \frac{\mathbb{E}[|\langle \pi_{k-1|k-1}^N, \delta_T \rho \phi^4 \rangle|]}{N^4} \leq C'_{\Pi_2} M_{k-1|k-1} \|\rho\|_\infty \frac{\|\phi\|_{k-1,4}^4}{N^4},$$

which yields (37) using  $N > 1$  and  $C_{\Pi_2} = C'_{\Pi_2} M_{k-1|k-1} \|\rho\|_\infty$ .

**(c)  $\Pi_3$  term:** Using (14) and (22) replacing  $k$  by  $k - 1$ , we have

$$\begin{aligned} \mathbb{E}[|\Pi_3|^4] &= \mathbb{E}[\langle \pi_{k-1|k-1}^N, \delta_T \rho \phi \rangle - \langle \pi_{k-1|k-1}, \phi \rangle]^4 = \mathbb{E}[\langle \pi_{k-1|k-1}^N, \delta_T \rho \phi \rangle - \langle \pi_{k-1|k-1}, \delta_T \rho \phi \rangle]^4 \\ &\leq C_{k-1|k-1} \|\rho\|_\infty^4 \frac{\|\phi\|_{k-1,4}^4}{N^2}, \end{aligned}$$

which yields (38) defining  $C_{\Pi_3} \doteq C_{k-1|k-1} \|\rho\|_\infty^4$ . ■

**Lemma 7.** *If (30) holds, then*

$$\mathbb{E} \left| \langle \tilde{\pi}_{k|k-1}^N, |\phi|^4 \rangle - \frac{1}{N} \sum_{i=1}^N \mathbb{E}[|\phi(\hat{\mathbf{x}}_k^i, \tilde{\mathbf{y}}_k^i)|^4 | \mathcal{F}_{k-1}] \right| \leq \frac{2}{(1 - \epsilon_k)} M_{k-1|k-1} \|\rho\|_\infty \|\phi\|_{k-1,4}^4, \quad (39)$$

$$\mathbb{E} \left| \frac{1}{N} \sum_{i=1}^N \mathbb{E}[|\phi(\hat{\mathbf{x}}_k^i, \tilde{\mathbf{y}}_k^i)|^4 | \mathcal{F}_{k-1}] - \langle \pi_{k-1|k-1}^N, \delta_T \rho |\phi|^4 \rangle \right| \leq \frac{2 - \epsilon_k}{1 - \epsilon_k} M_{k-1|k-1} \|\rho\|_\infty \|\phi\|_{k-1,4}^4 \quad (40)$$

$$\mathbb{E} |\langle \pi_{k-1|k-1}^N, \delta_T \rho |\phi|^4 \rangle - \langle \pi_{k|k-1}, |\phi|^4 \rangle| \leq \|\rho\|_\infty (M_{k-1|k-1} + 1) \|\phi\|_{k-1,4}^4, \quad (41)$$

where  $\epsilon_k$  is the same as defined in Lemma 5.

*Proof.* Consider the first inequality (39). Since  $\tilde{\pi}_{k|k-1}^N$  is the empirical distribution obtained from particles  $\{(\hat{\mathbf{x}}_k^i, \tilde{\mathbf{y}}_k^i)\}$ , we have

$$\begin{aligned} \mathbb{E} \left[ \mathbb{E} \left| \langle \tilde{\pi}_{k|k-1}^N, |\phi|^4 \rangle - \frac{1}{N} \sum_{i=1}^N \mathbb{E}[|\phi(\hat{\mathbf{x}}_k^i, \tilde{\mathbf{y}}_k^i)|^4 | \mathcal{F}_{k-1}] \right| \middle| \mathcal{F}_{k-1} \right] &= \frac{1}{N} \mathbb{E} \left[ \mathbb{E} \left| \sum_{i=1}^N (|\phi(\hat{\mathbf{x}}_k^i, \tilde{\mathbf{y}}_k^i)|^4 - \mathbb{E}[|\phi(\hat{\mathbf{x}}_k^i, \tilde{\mathbf{y}}_k^i)|^4 | \mathcal{F}_{k-1}]) \right| \middle| \mathcal{F}_{k-1} \right] \\ &\leq \frac{2}{N} \mathbb{E} \left[ \sum_{i=1}^N \mathbb{E}[|\phi(\hat{\mathbf{x}}_k^i, \tilde{\mathbf{y}}_k^i)|^4 | \mathcal{F}_{k-1}] \right] \leq \frac{2}{N(1 - \epsilon_k)} \mathbb{E} \left[ \sum_{i=1}^N \mathbb{E}[|\phi(\hat{\mathbf{x}}_k^i, \tilde{\mathbf{y}}_k^i)|^4 | \mathcal{F}_{k-1}] \right] = \frac{2}{(1 - \epsilon_k)} \mathbb{E}[\langle \pi_{k-1|k-1}^N, \delta_T \rho |\phi|^4 \rangle], \end{aligned}$$

where the first and second inequalities are obtained using Lemma 2 and 4, respectively. The last equality follows because particles  $\{(\hat{\mathbf{x}}_k^i, \tilde{\mathbf{y}}_k^i)\}$  are drawn from distribution  $\langle \pi_{k-1|k-1}^N, \delta_T \rho \rangle$ . Finally, using (30), we obtain (39).

Next, we consider the inequality (40). Using (32) replacing  $\phi$  by  $|\phi|^4$ , we have

$$\begin{aligned} \mathbb{E} \left| \frac{1}{N} \sum_{i=1}^N \mathbb{E}[|\phi(\hat{\mathbf{x}}_k^i, \tilde{\mathbf{y}}_k^i)|^4 | \mathcal{F}_{k-1}] - \langle \pi_{k-1|k-1}^N, \delta_T \rho |\phi|^4 \rangle \right| &= \mathbb{E} \left| \frac{1}{N} \sum_{i=1}^N (\mathbb{E}[|\phi(\hat{\mathbf{x}}_k^i, \tilde{\mathbf{y}}_k^i)|^4 | \mathcal{F}_{k-1}] - \mathbb{E}[|\phi(\hat{\mathbf{x}}_k^i, \bar{\mathbf{y}}_k^i)|^4 | \mathcal{F}_{k-1}]) \right| \\ &\leq \frac{1}{N} \sum_{i=1}^N \left( \mathbb{E}[\mathbb{E}[|\phi(\hat{\mathbf{x}}_k^i, \tilde{\mathbf{y}}_k^i)|^4 | \mathcal{F}_{k-1}]] + \mathbb{E}[\mathbb{E}[|\phi(\hat{\mathbf{x}}_k^i, \bar{\mathbf{y}}_k^i)|^4 | \mathcal{F}_{k-1}]] \right). \end{aligned}$$

Now, using Lemma 4, we have

$$\begin{aligned} \mathbb{E} \left| \frac{1}{N} \sum_{i=1}^N \mathbb{E}[|\phi(\hat{\mathbf{x}}_k^i, \tilde{\mathbf{y}}_k^i)|^4 | \mathcal{F}_{k-1}] - \langle \pi_{k-1|k-1}^N, \delta_T \rho |\phi|^4 \rangle \right| &\leq \frac{1}{N} \sum_{i=1}^N \left( \frac{\mathbb{E}[\mathbb{E}[|\phi(\hat{\mathbf{x}}_k^i, \bar{\mathbf{y}}_k^i)|^4 | \mathcal{F}_{k-1}]]}{1 - \epsilon_k} + \mathbb{E}[\mathbb{E}[|\phi(\hat{\mathbf{x}}_k^i, \bar{\mathbf{y}}_k^i)|^4 | \mathcal{F}_{k-1}]] \right) \\ &= \frac{2 - \epsilon_k}{1 - \epsilon_k} \mathbb{E}[\langle \pi_{k-1|k-1}^N, \delta_T \rho |\phi|^4 \rangle], \end{aligned}$$

which yields (40) using assumption (30).

Finally, consider the last inequality (41). From (14) and triangle inequality, we have

$$\begin{aligned} \mathbb{E} |\langle \pi_{k-1|k-1}^N, \delta_T \rho |\phi|^4 \rangle - \langle \pi_{k|k-1}, |\phi|^4 \rangle| &\leq \mathbb{E} |\langle \pi_{k-1|k-1}^N, \delta_T \rho |\phi|^4 \rangle| + |\langle \pi_{k-1|k-1}, \delta_T \rho |\phi|^4 \rangle| \\ &\leq \|\rho\|_\infty M_{k-1|k-1} \|\phi\|_{k-1,4}^4 + \|\rho\|_\infty \|\phi\|_{k-1,4}^4, \end{aligned}$$

where the last inequality results from the assumption (30) and the definition of  $\|\phi\|_{k-1,4}$  (from Theorem 1). Hence, (41) is proved.  $\blacksquare$

## B.2 Proof of the theorem

As mentioned earlier, the proof employs an induction framework. To this end, we prove that (22) holds for the  $k$ -th time step provided that the inequality holds for  $(k-1)$ -th time step. Additionally, we also show that

$$\mathbb{E}|\langle \pi_{k|k}^N, |\phi|^4 \rangle| \leq M_{k|k} \|\phi\|_{k,4}^4, \quad (42)$$

which is (30) with  $k-1$  replaced by  $k$ . The first part of Theorem 1, i.e., the algorithm does not run into an infinite loop, follows from Lemma 5. For the second part of the theorem, we analyze the empirical distributions obtained in different steps of the I-PF algorithm and obtain the corresponding inequalities of (22) and (42).

**Initialization:** Following the induction framework, we first show that (22) and (42) hold for  $k=0$ . Consider  $\{\hat{\mathbf{x}}_0^i\}_{1 \leq i \leq N}$  and  $\{\mathbf{y}_0^i\}_{1 \leq i \leq N}$  as the i.i.d. and mutually independent (initial) samples drawn from distributions  $\tilde{\pi}_0^x(d\hat{\mathbf{x}}_0)$  and  $\rho(\mathbf{y}_0|\mathbf{x}_0)$ , respectively. Recall that  $\tilde{\pi}_0^x$  is the initial distribution assumed in I-PF. Denote  $\pi_0$  as the joint distribution for particles  $\{(\hat{\mathbf{x}}_0^i, \mathbf{y}_0^i)\}_{1 \leq i \leq N}$  such that  $\langle \pi_0, \phi \rangle = \mathbb{E}[\phi(\hat{\mathbf{x}}_0^i, \mathbf{y}_0^i)]$  irrespective of  $i$ . Also,  $\phi_0^N$  is the empirical distribution obtained from particles  $\{(\hat{\mathbf{x}}_0^i, \mathbf{y}_0^i)\}_{1 \leq i \leq N}$ . We have

$$\mathbb{E}|\langle \pi_0^N, \phi \rangle - \langle \pi_0, \phi \rangle|^4 = \mathbb{E} \left| \frac{1}{N} \sum_{i=1}^N (\phi(\hat{\mathbf{x}}_0^i, \mathbf{y}_0^i) - \mathbb{E}[\phi(\hat{\mathbf{x}}_0^i, \mathbf{y}_0^i)]) \right|^4.$$

Using Lemma 3, we obtain

$$\mathbb{E}|\langle \pi_0^N, \phi \rangle - \langle \pi_0, \phi \rangle|^4 \leq \frac{2}{N^2} \mathbb{E} |\phi(\hat{\mathbf{x}}_0^i, \mathbf{y}_0^i) - \mathbb{E}[\phi(\hat{\mathbf{x}}_0^i, \mathbf{y}_0^i)]|^4,$$

because  $(\hat{\mathbf{x}}_0^i, \mathbf{y}_0^i)$  are identically distributed for all  $i = 1, 2, \dots, N$ . Finally, using Lemma 2 with  $\mathbb{E}|\phi(\hat{\mathbf{x}}_0^i, \mathbf{y}_0^i)|^4 = \langle \pi_0, |\phi|^4 \rangle$ , we have

$$\mathbb{E}|\langle \pi_0^N, \phi \rangle - \langle \pi_0, \phi \rangle|^4 \leq \frac{32}{N^2} \|\phi\|_{0,4}^4 \doteq C_{0|0} \frac{\|\phi\|_{0,4}^4}{N^2}, \quad (43)$$

because  $\|\phi\|_{0,4} = \max\{1, \langle \pi_0, |\phi|^4 \rangle\}^{1/4}$  from Theorem 1.

Similarly, using Lemma 2, we obtain

$$\mathbb{E}|\langle \pi_0^N, |\phi|^4 \rangle - \langle \pi_0, |\phi|^4 \rangle| = \mathbb{E} \left| \frac{1}{N} \sum_{i=1}^N (|\phi(\hat{\mathbf{x}}_0^i, \mathbf{y}_0^i)|^4 - \mathbb{E}|\phi(\hat{\mathbf{x}}_0^i, \mathbf{y}_0^i)|^4) \right| \leq \frac{1}{N} \sum_{i=1}^N 2\mathbb{E}|\phi(\hat{\mathbf{x}}_0^i, \mathbf{y}_0^i)|^4 = 2\mathbb{E}|\phi(\hat{\mathbf{x}}_0^i, \mathbf{y}_0^i)|^4. \quad (44)$$

From triangle inequality, we have

$$\mathbb{E}|\langle \pi_0^N, |\phi|^4 \rangle| \leq \mathbb{E}|\langle \pi_0^N, |\phi|^4 \rangle - \langle \pi_0, |\phi|^4 \rangle| + |\langle \pi_0, |\phi|^4 \rangle|.$$

Note that  $\pi_0^N$  is a random function obtained from the randomly generated particles, but  $\pi_0$  is a given initial distribution. Hence, using (44) and  $\langle \pi_0, |\phi|^4 \rangle = \mathbb{E}|\phi(\hat{\mathbf{x}}_0^i, \mathbf{y}_0^i)|^4$ , we have

$$\mathbb{E}|\langle \pi_0^N, |\phi|^4 \rangle| \leq 3\mathbb{E}|\phi(\hat{\mathbf{x}}_0^i, \mathbf{y}_0^i)|^4 \leq \|\phi\|_{0,4}^4 \doteq M_{0|0} \|\phi\|_{0,4}^4. \quad (45)$$

Inequalities (43) and (45) show that (22) and (42) hold for  $k=0$ . Next, we assume that these inequalities hold at  $(k-1)$ -th time instant, i.e.,

$$\mathbb{E}|\langle \pi_{k-1|k-1}^N, \phi \rangle - \langle \pi_{k-1|k-1}, \phi \rangle|^4 \leq C_{k-1|k-1} \frac{\|\phi\|_{k-1,4}^4}{N^2}, \quad (46)$$

$$\mathbb{E}|\langle \pi_{k-1|k-1}^N, |\phi|^4 \rangle| \leq M_{k-1|k-1} \|\phi\|_{k-1,4}^4, \quad (47)$$

where (47) is same as (30), repeated here as a ready reference.

**Importance sampling with modification:** Recall that in the sampling step, we draw particles  $\{(\hat{\mathbf{x}}_k^i, \hat{\mathbf{y}}_k^i)\}$  until the inequality  $\frac{1}{N} \sum_{i=1}^N \beta(\mathbf{a}_k | \hat{\mathbf{x}}_k^i) \geq \gamma_k$  is satisfied. Finally,  $\{(\tilde{\mathbf{x}}_k^i, \tilde{\mathbf{y}}_k^i)\}$  are the particles for which the condition holds, resulting in empirical distribution  $\tilde{\pi}_{k|k-1}^N$  as an approximation of  $\pi_{k|k-1}$ . Now, we consider bounds on  $\mathbb{E}|\langle \tilde{\pi}_{k|k-1}^N, \phi \rangle - \langle \pi_{k|k-1}, \phi \rangle|^4$  and  $\mathbb{E}|\langle \tilde{\pi}_{k|k-1}^N, |\phi|^4 \rangle - \langle \pi_{k|k-1}, |\phi|^4 \rangle|$ .

Consider  $\langle \tilde{\pi}_{k|k-1}^N, \phi \rangle - \langle \pi_{k|k-1}, \phi \rangle = \Pi_1 + \Pi_2 + \Pi_3$  with  $\Pi_1$ ,  $\Pi_2$  and  $\Pi_3$  as defined in (33)-(35) with appropriate bounds derived in Lemma 6. From Minkowski's inequality, we have

$$\mathbb{E}^{1/4}|\langle \tilde{\pi}_{k|k-1}^N, \phi \rangle - \langle \pi_{k|k-1}, \phi \rangle|^4 \leq \mathbb{E}^{1/4}|\Pi_1|^4 + \mathbb{E}^{1/4}|\Pi_2|^4 + \mathbb{E}^{1/4}|\Pi_3|^4,$$

such that using (36)-(38) yields

$$\mathbb{E}|\langle \tilde{\pi}_{k|k-1}^N, \phi \rangle - \langle \pi_{k|k-1}, \phi \rangle|^4 \leq \tilde{C}_{k|k-1} \frac{\|\phi\|_{k-1,4}^4}{N^2}, \quad (48)$$

where constant  $\tilde{C}_{k|k-1} \doteq (C_{\Pi_1}^{1/4} + C_{\Pi_2}^{1/4} + C_{\Pi_3}^{1/4})^4$ .

Next, we consider  $\mathbb{E}|\langle \tilde{\pi}_{k|k-1}^N, |\phi|^4 \rangle - \langle \pi_{k|k-1}, |\phi|^4 \rangle|$  and employ a similar separation method. In particular, we have

$$\begin{aligned} \langle \tilde{\pi}_{k|k-1}^N, |\phi|^4 \rangle - \langle \pi_{k|k-1}, |\phi|^4 \rangle &= \langle \tilde{\pi}_{k|k-1}^N, |\phi|^4 \rangle - \frac{1}{N} \sum_{i=1}^N \mathbb{E}[\phi(\hat{\mathbf{x}}_k^i, \tilde{\mathbf{y}}_k^i)^4 | \mathcal{F}_{k-1}] \\ &+ \frac{1}{N} \sum_{i=1}^N \mathbb{E}[\phi(\hat{\mathbf{x}}_k^i, \tilde{\mathbf{y}}_k^i)^4 | \mathcal{F}_{k-1}] - \langle \pi_{k-1|k-1}^N, \delta_T \rho |\phi|^4 \rangle + \langle \pi_{k-1|k-1}^N, \delta_T \rho |\phi|^4 \rangle - \langle \pi_{k|k-1}, |\phi|^4 \rangle. \end{aligned}$$

Using bounds (39)-(41) from Lemma 7, we obtain

$$\mathbb{E}|\langle \tilde{\pi}_{k|k-1}^N, |\phi|^4 \rangle - \langle \pi_{k|k-1}, |\phi|^4 \rangle| \leq \tilde{M}_{k|k-1} \|\phi\|_{k-1,4}^4, \quad (49)$$

where constant

$$\tilde{M}_{k|k-1} \doteq \|\rho\|_\infty \left( \frac{2}{1 - \epsilon_k} M_{k-1|k-1} + \frac{2 - \epsilon_k}{1 - \epsilon_k} M_{k-1|k-1} + M_{k-1|k-1} + 1 \right).$$

The inequalities (48) and (49) are the counterparts of inequalities (22) and (42), respectively, for the (approximate) prediction distribution  $\tilde{\pi}_{k|k-1}^N$  obtained from the modified importance sampling in I-PF.

**Weight computation:** The posterior distribution  $\tilde{\pi}_{k|k}^N$  is obtained from the prediction distribution  $\tilde{\pi}_{k|k-1}^N$  by associating weight  $\omega_k^i$  with each particle  $(\hat{\mathbf{x}}_k^i, \mathbf{y}_k^i)$ . Hence, we now analyze  $\mathbb{E}|\langle \tilde{\pi}_{k|k}^N, \phi \rangle - \langle \pi_{k|k}, \phi \rangle|^4$  and  $\mathbb{E}|\langle \tilde{\pi}_{k|k}^N, |\phi|^4 \rangle|$  based on (48) and (49). In particular, we obtain the counterparts of inequalities (22) and (42) for  $\tilde{\pi}_{k|k}^N$  in following Claims 1 and 2, respectively.

**Claim 1.** *The optimal filter's posterior distribution  $\pi_{k|k}$  and its approximation  $\tilde{\pi}_{k|k}^N$  in I-PF satisfy*

$$\mathbb{E}|\langle \tilde{\pi}_{k|k}^N, \phi \rangle - \langle \pi_{k|k}, \phi \rangle|^4 \leq \tilde{C}_{k|k} \frac{\|\phi\|_{k-1,4}^4}{N^2}, \quad (50)$$

for suitable  $\tilde{C}_{k|k} > 0$ .

*Proof.* Using (15), we again employ a separation method as

$$\langle \tilde{\pi}_{k|k}^N, \phi \rangle - \langle \pi_{k|k}, \phi \rangle = \frac{\langle \tilde{\pi}_{k|k-1}^N, \beta \phi \rangle}{\langle \tilde{\pi}_{k|k-1}^N, \beta \rangle} - \frac{\langle \pi_{k|k-1}, \beta \phi \rangle}{\langle \pi_{k|k-1}, \beta \rangle} \doteq \tilde{\Pi}_1 + \tilde{\Pi}_2,$$

where  $\tilde{\Pi}_1 = \frac{\langle \tilde{\pi}_{k|k-1}^N, \beta \phi \rangle}{\langle \tilde{\pi}_{k|k-1}^N, \beta \rangle} - \frac{\langle \tilde{\pi}_{k|k-1}^N, \beta \phi \rangle}{\langle \pi_{k|k-1}, \beta \rangle}$  and  $\tilde{\Pi}_2 = \frac{\langle \tilde{\pi}_{k|k-1}^N, \beta \phi \rangle}{\langle \pi_{k|k-1}, \beta \rangle} - \frac{\langle \pi_{k|k-1}, \beta \phi \rangle}{\langle \pi_{k|k-1}, \beta \rangle}$ . As noted in Remark 1, the modification step implies that  $\langle \tilde{\pi}_{k|k}^N, \beta \rangle \geq \gamma_k$ . Hence, under assumptions **A2** and **A3**, we have

$$|\tilde{\Pi}_1| = \left| \frac{\langle \tilde{\pi}_{k|k-1}^N, \beta \phi \rangle}{\langle \tilde{\pi}_{k|k-1}^N, \beta \rangle} \times \frac{\langle \pi_{k|k-1}, \beta \rangle - \langle \tilde{\pi}_{k|k-1}^N, \beta \rangle}{\langle \pi_{k|k-1}, \beta \rangle} \right| \leq \frac{\|\beta \phi\|_\infty}{\gamma_k \langle \pi_{k|k-1}, \beta \rangle} |\langle \pi_{k|k-1}, \beta \rangle - \langle \tilde{\pi}_{k|k-1}^N, \beta \rangle|.$$

Now, using Minkowski's inequality, we have

$$\begin{aligned} \mathbb{E}^{1/4} |\langle \tilde{\pi}_{k|k}^N, \phi \rangle - \langle \pi_{k|k}, \phi \rangle|^4 &\leq \mathbb{E}^{1/4} |\tilde{\Pi}_1|^4 + \mathbb{E}^{1/4} |\tilde{\Pi}_2|^4 \\ &\leq \frac{\|\beta \phi\|_\infty}{\gamma_k \langle \pi_{k|k-1}, \beta \rangle} \mathbb{E}^{1/4} |\langle \pi_{k|k-1}, \beta \rangle - \langle \tilde{\pi}_{k|k-1}^N, \beta \rangle|^4 + \frac{1}{\langle \pi_{k|k-1}, \beta \rangle} \mathbb{E}^{1/4} |\langle \tilde{\pi}_{k|k-1}^N, \beta \phi \rangle - \langle \pi_{k|k-1}, \beta \phi \rangle|^4. \end{aligned}$$

Finally, using (48), we obtain

$$\begin{aligned} \mathbb{E}^{1/4} |\langle \tilde{\pi}_{k|k}^N, \phi \rangle - \langle \pi_{k|k}, \phi \rangle|^4 &\leq \frac{\|\beta \phi\|_\infty}{\gamma_k \langle \pi_{k|k-1}, \beta \rangle} \tilde{C}_{k|k-1}^{1/4} \frac{\|\beta\|_\infty}{N^{1/2}} + \frac{1}{\langle \pi_{k|k-1}, \beta \rangle} \tilde{C}_{k|k-1}^{1/4} \|\beta\|_\infty \frac{\|\phi\|_{k-1,4}}{N^{1/2}} \\ &\leq \frac{\tilde{C}_{k|k-1}^{1/4} \|\beta\|_\infty}{\gamma_k \langle \pi_{k|k-1}, \beta \rangle} (\|\beta \phi\|_\infty + \gamma_k) \frac{\|\phi\|_{k-1,4}}{N^{1/2}}, \end{aligned}$$

where the last inequality follows because by definition  $\|\phi\|_{k-1,4} > 1$ . Defining  $\tilde{C}_{k|k}^{1/4} \doteq \frac{\tilde{C}_{k|k-1}^{1/4} \|\beta\|_\infty}{\gamma_k \langle \pi_{k|k-1}, \beta \rangle} (\|\beta \phi\|_\infty + \gamma_k)$  proves the claim.  $\blacksquare$

**Claim 2.** *The distributions  $\pi_{k|k}$  and  $\tilde{\pi}_{k|k}^N$  satisfy*

$$\mathbb{E}|\langle \tilde{\pi}_{k|k}^N, |\phi|^4 \rangle| \leq \tilde{M}_{k|k} \|\phi\|_{k,4}^4, \quad (51)$$

for suitable  $\tilde{M}_{k|k} > 0$ .

*Proof.* Using a similar separation method as in proof of Claim 1, we have

$$\begin{aligned} \mathbb{E}|\langle \tilde{\pi}_{k|k}^N, |\phi|^4 \rangle - \langle \pi_{k|k}, |\phi|^4 \rangle| &\leq \mathbb{E} \left| \frac{\langle \tilde{\pi}_{k|k-1}^N, \beta |\phi|^4 \rangle - \langle \pi_{k|k-1}, \beta |\phi|^4 \rangle}{\langle \pi_{k|k-1}, \beta \rangle} \right| \\ &\quad + \mathbb{E} \left| \frac{\langle \tilde{\pi}_{k|k-1}^N, \beta |\phi|^4 \rangle}{\langle \tilde{\pi}_{k|k-1}^N, \beta \rangle} \times \frac{\langle \pi_{k|k-1}, \beta \rangle - \langle \tilde{\pi}_{k|k-1}^N, \beta \rangle}{\langle \pi_{k|k-1}, \beta \rangle} \right|. \end{aligned}$$

Again using assumption **A2** and (49), we obtain

$$\begin{aligned} \mathbb{E}|\langle \tilde{\pi}_{k|k}^N, |\phi|^4 \rangle - \langle \pi_{k|k}, |\phi|^4 \rangle| &\leq \frac{\|\beta\phi^4\|_\infty}{\gamma_k \langle \pi_{k|k-1}, \beta \rangle} \mathbb{E}|\langle \pi_{k|k-1}, \beta \rangle - \langle \tilde{\pi}_{k|k-1}^N, \beta \rangle| + \frac{1}{\langle \pi_{k|k-1}, \beta \rangle} \widetilde{M}_{k|k-1} \|\beta\|_\infty \|\phi\|_{k-1,4}^4 \\ &\leq \frac{\|\beta\phi^4\|_\infty 2\|\beta\|_\infty}{\gamma_k \langle \pi_{k|k-1}, \beta \rangle} \|\phi\|_{k-1,4}^4 + \frac{\widetilde{M}_{k|k-1} \|\beta\|_\infty}{\langle \pi_{k|k-1}, \beta \rangle} \|\phi\|_{k-1,4}^4, \end{aligned}$$

because by definition  $\|\phi\|_{k-1,4} > 1$ . Hence,

$$\mathbb{E}|\langle \tilde{\pi}_{k|k}^N, |\phi|^4 \rangle| \leq \frac{\|\beta\phi^4\|_\infty 2\|\beta\|_\infty}{\gamma_k \langle \pi_{k|k-1}, \beta \rangle} \|\phi\|_{k-1,4}^4 + \frac{\widetilde{M}_{k|k-1} \|\beta\|_\infty}{\langle \pi_{k|k-1}, \beta \rangle} \|\phi\|_{k-1,4}^4 + \langle \pi_{k|k}, |\phi|^4 \rangle.$$

But,  $\langle \pi_{k|k}, |\phi|^4 \rangle \leq \|\phi\|_{k,4}^4$  and  $\|\phi\|_{k,4}$  is increasing in  $k$  such that

$$\mathbb{E}|\langle \tilde{\pi}_{k|k}^N, |\phi|^4 \rangle| \leq 3 \max \left\{ \frac{\|\beta\phi^4\|_\infty 2\|\beta\|_\infty}{\gamma_k \langle \pi_{k|k-1}, \beta \rangle}, \frac{\widetilde{M}_{k|k-1} \|\beta\|_\infty}{\langle \pi_{k|k-1}, \beta \rangle}, 1 \right\} \|\phi\|_{k,4}^4,$$

which proves the claim with  $\widetilde{M}_{k|k} \doteq 3 \max \left\{ \frac{\|\beta\phi^4\|_\infty 2\|\beta\|_\infty}{\gamma_k \langle \pi_{k|k-1}, \beta \rangle}, \frac{\widetilde{M}_{k|k-1} \|\beta\|_\infty}{\langle \pi_{k|k-1}, \beta \rangle}, 1 \right\}$ .  $\blacksquare$

**Resampling:** In this step, we draw  $N$  independent particles  $(\hat{\mathbf{x}}_k^i, \mathbf{y}_k^i)$  from the posterior distribution  $\tilde{\pi}_{k|k}^N$  and obtain the empirical distribution  $\pi_{k|k}^N$  with equally weighted particles. Note that  $\pi_{k|k}^N$  also approximates  $\pi_{k|k}$  and is the I-PF's output posterior distribution. Now, we finally show that (22) and (42) hold true if we assume (46) and (47) hold at  $(k-1)$ -th time, which completes the induction proof. To this end, we analyze  $\mathbb{E}|\langle \pi_{k|k}^N, \phi \rangle - \langle \pi_{k|k}, \phi \rangle|^4$  and  $\mathbb{E}|\langle \pi_{k|k}^N, |\phi|^4 \rangle|$  based on (50) and (51), and prove the following claims.

**Claim 3.** *The distribution  $\pi_{k|k}$  and its approximation  $\pi_{k|k}^N$  satisfy*

$$\mathbb{E}|\langle \pi_{k|k}^N, \phi \rangle - \langle \pi_{k|k}, \phi \rangle|^4 \leq C_{k|k} \frac{\|\phi\|_{k,4}^4}{N^2}. \quad (52)$$

*Proof.* Consider the separation  $\langle \pi_{k|k}^N, \phi \rangle - \langle \pi_{k|k}, \phi \rangle = \bar{\Pi}_1 + \bar{\Pi}_2$  where  $\bar{\Pi}_1 = \langle \pi_{k|k}^N, \phi \rangle - \langle \tilde{\pi}_{k|k}^N, \phi \rangle$  and  $\bar{\Pi}_2 = \langle \tilde{\pi}_{k|k}^N, \phi \rangle - \langle \pi_{k|k}, \phi \rangle$ . Denote  $\mathcal{G}_k$  as the  $\sigma$ -algebra generated by  $\{(\hat{\mathbf{x}}_k^i, \tilde{\mathbf{y}}_k^i)\}_{i=1}^N$ . Since  $(\hat{\mathbf{x}}_k^i, \mathbf{y}_k^i)$  are drawn independently from  $\tilde{\pi}_{k|k}^N$ , we have  $\mathbb{E}[\phi(\hat{\mathbf{x}}_k^i, \mathbf{y}_k^i) | \mathcal{G}_k] = \langle \tilde{\pi}_{k|k}^N, \phi \rangle$  such that  $\bar{\Pi}_1 = \frac{1}{N} \sum_{i=1}^N (\phi(\hat{\mathbf{x}}_k^i, \mathbf{y}_k^i) - \mathbb{E}[\phi(\hat{\mathbf{x}}_k^i, \mathbf{y}_k^i) | \mathcal{G}_k])$ . Using Lemma 3 and 2, and finally (51), we obtain

$$\mathbb{E}[|\bar{\Pi}_1|^4 | \mathcal{G}_k] \leq 2^5 \widetilde{M}_{k|k} \frac{\|\phi\|_{k,4}^4}{N^2}. \quad (53)$$

Again, using the Minkowski's inequality, and (50) and (53), we have

$$\begin{aligned} \mathbb{E}^{1/4} |\langle \pi_{k|k}^N, \phi \rangle - \langle \pi_{k|k}, \phi \rangle|^4 &\leq \mathbb{E}^{1/4} |\bar{\Pi}_1|^4 + \mathbb{E}^{1/4} |\bar{\Pi}_2|^4 \\ &\leq (2^5 \widetilde{M}_{k|k})^{1/4} \frac{\|\phi\|_{k,4}}{N^{1/2}} + \widetilde{C}_{k|k}^{1/4} \frac{\|\phi\|_{k-1,4}}{N^{1/2}} \leq ((2^5 \widetilde{M}_{k|k})^{1/4} + \widetilde{C}_{k|k}^{1/4}) \frac{\|\phi\|_{k,4}}{N^{1/2}}, \end{aligned}$$

because  $\|\phi\|_{k,4}$  is increasing in  $k$ . Hence, defining  $C_{k|k}^{1/4} \doteq ((2^5 \widetilde{M}_{k|k})^{1/4} + \widetilde{C}_{k|k}^{1/4})$  yields (52).  $\blacksquare$

**Claim 4.** *The distributions  $\pi_{k|k}$  and  $\pi_{k|k}^N$  satisfy*

$$\mathbb{E}|\langle \pi_{k|k}^N, |\phi|^4 \rangle| \leq M_{k|k} \|\phi\|_{k,4}^4. \quad (54)$$

*Proof.* Since,  $(\hat{\mathbf{x}}_k^i, \mathbf{y}_k^i) \sim \tilde{\pi}_{k,k}^N$ , we have  $\langle \tilde{\pi}_{k|k}^N, |\phi|^4 \rangle = \mathbb{E}[|\phi(\hat{\mathbf{x}}_k^i, \mathbf{y}_k^i)|^4 | \mathcal{G}_k]$ . Then, using Lemma 2 and (51), we obtain

$$\begin{aligned} \mathbb{E}|\langle \pi_{k|k}^N, |\phi|^4 \rangle - \langle \pi_{k|k}, |\phi|^4 \rangle| &\leq \mathbb{E}|\langle \pi_{k|k}^N, |\phi|^4 \rangle - \langle \tilde{\pi}_{k|k}^N, |\phi|^4 \rangle| + \mathbb{E}|\langle \tilde{\pi}_{k|k}^N, |\phi|^4 \rangle - \langle \pi_{k|k}, |\phi|^4 \rangle| \\ &\leq \mathbb{E} \left| \frac{1}{N} \sum_{i=1}^N (|\phi(\hat{\mathbf{x}}_k^i, \mathbf{y}_k^i)|^4 - \mathbb{E}[|\phi(\hat{\mathbf{x}}_k^i, \mathbf{y}_k^i)|^4 | \mathcal{G}_k]) \right| + \mathbb{E}|\langle \tilde{\pi}_{k|k}^N, |\phi|^4 \rangle| + \langle \pi_{k|k}, |\phi|^4 \rangle \\ &\leq \frac{1}{N} \sum_{i=1}^N 2\mathbb{E}[\mathbb{E}[|\phi(\hat{\mathbf{x}}_k^i, \mathbf{y}_k^i)|^4 | \mathcal{G}_k]] + \widetilde{M}_{k|k} \|\phi\|_{k,4}^4 + \|\phi\|_{k,4}^4 \\ &= 2\mathbb{E}[\langle \tilde{\pi}_{k|k}^N, |\phi|^4 \rangle] + (\widetilde{M}_{k|k} + 1) \|\phi\|_{k,4}^4 \leq (3\widetilde{M}_{k|k} + 1) \|\phi\|_{k,4}^4, \end{aligned}$$

Hence,

$$\mathbb{E}|\langle \pi_{k|k}^N, |\phi|^4 \rangle| \leq (3\widetilde{M}_{k|k} + 2) \|\phi\|_{k,4}^4, \quad (55)$$

which proves the claim with  $M_{k|k} \leq (3\widetilde{M}_{k|k} + 2)$ . ■

Claims 3 and 4 show that inequalities (22) and (42) hold for  $k$ -th time instant, completing the induction proof.

## References

- Daniel Alspach and Harold Sorenson. Nonlinear Bayesian estimation using Gaussian sum approximations. *IEEE Transactions on Automatic Control*, 17(4):439–448, 1972.
- Brian DO Anderson and John B Moore. *Optimal filtering*. Courier Corporation, 2012.
- Jeffrey L Anderson. An ensemble adjustment Kalman filter for data assimilation. *Monthly weather review*, 129(12):2884–2903, 2001.
- Christophe Andrieu, Arnaud Doucet, and Roman Holenstein. Particle Markov chain Monte Carlo methods. *Journal of the Royal Statistical Society Series B: Statistical Methodology*, 72(3):269–342, 2010.
- Ienkaran Arasaratnam and Simon Haykin. Cubature Kalman Filters. *IEEE Transactions on Automatic Control*, 54(6):1254–1269, 2009.
- Ienkaran Arasaratnam, Simon Haykin, and Robert J Elliott. Discrete-time nonlinear filtering algorithms using Gauss-Hermite quadrature. *Proceedings of the IEEE*, 95(5):953–977, 2007.
- M Sanjeev Arulampalam, Simon Maskell, Neil Gordon, and Tim Clapp. A tutorial on particle filters for online nonlinear/non-Gaussian Bayesian tracking. *IEEE Transactions on Signal Processing*, 50(2):174–188, 2002.



- Krishna B Athreya and Soumendra N Lahiri. *Measure theory and probability theory*, volume 19. Springer, 2006.
- Haim Avron, Vikas Sindhwani, Jiyan Yang, and Michael W. Mahoney. Quasi-Monte Carlo Feature Maps for Shift-Invariant Kernels. *Journal of Machine Learning Research*, 17(120):1–38, 2016.
- Yaakov Bar-Shalom, X Rong Li, and Thiagalingam Kirubarajan. *Estimation with applications to tracking and navigation: Theory algorithms and software*. John Wiley & Sons, 2004.
- Kristine L Bell, Christopher J Baker, Graeme E Smith, Joel T Johnson, and Muralidhar Rangaswamy. Cognitive radar framework for target detection and tracking. *IEEE Journal of Selected Topics in Signal Processing*, 9(8):1427–1439, 2015.
- Christopher M Bishop. *Pattern Recognition and Machine learning*. Springer, 2006.
- Craig H Bishop, Brian J Etherton, and Sharanya J Majumdar. Adaptive sampling with the ensemble transform Kalman filter. Part I: Theoretical aspects. *Monthly weather review*, 129(3):420–436, 2001.
- Nicola Branchini and Víctor Elvira. Optimized auxiliary particle filters: adapting mixture proposals via convex optimization. In *Uncertainty in Artificial Intelligence*, pages 1289–1299. PMLR, 2021.
- Richard S Bucy and Kenneth D Senne. Digital synthesis of non-linear filters. *Automatica*, 7(3):287–298, 1971.
- Pete Bunch and Simon Godsill. Approximations of the optimal importance density using Gaussian particle flow importance sampling. *Journal of the American Statistical Association*, 111(514):748–762, 2016.
- Yuri Burda, Roger Grosse, and Ruslan Salakhutdinov. Importance weighted autoencoders. *arXiv preprint arXiv:1509.00519*, 2015.
- Mark D Butala, Jonghyun Yun, Yuguo Chen, Richard A Frazin, and Farzad Kamalabadi. Asymptotic convergence of the ensemble Kalman filter. In *IEEE International Conference on Image Processing*, pages 825–828, 2008.
- Olivier Cappé, Simon J Godsill, and Eric Moulines. An overview of existing methods and recent advances in sequential Monte Carlo. *Proceedings of the IEEE*, 95(5):899–924, 2007.
- Bradley P Carlin, Nicholas G Polson, and David S Stoffer. A Monte Carlo approach to nonnormal and nonlinear state-space modeling. *Journal of the American Statistical Association*, 87(418):493–500, 1992.
- Rong Chen and Jun S Liu. Mixture Kalman filters. *Journal of the Royal Statistical Society: Series B (Statistical Methodology)*, 62(3):493–508, 2000.

- Xiongjie Chen and Yunpeng Li. Conditional measurement density estimation in sequential Monte Carlo via normalizing flow. In *30th European Signal Processing Conference (EUSIPCO)*, pages 782–786. IEEE, 2022.
- Xiongjie Chen and Yunpeng Li. An overview of differentiable particle filters for data-adaptive sequential Bayesian inference. *arXiv preprint arXiv:2302.09639*, 2023.
- Xiongjie Chen, Hao Wen, and Yunpeng Li. Differentiable particle filters through conditional normalizing flow. In *2021 IEEE 24th International Conference on Information Fusion (FUSION)*, pages 1–6, 2021.
- Yuming Chen, Daniel Sanz-Alonso, and Rebecca Willett. Autodifferentiable ensemble Kalman filters. *SIAM Journal on Mathematics of Data Science*, 4(2):801–833, 2022.
- Zhe Chen et al. Bayesian filtering: From Kalman filters to particle filters, and beyond. *Statistics*, 182(1):1–69, 2003.
- Jaedeug Choi and Kee-Eung Kim. Inverse Reinforcement learning in Partially Observable Environments. *Journal of Machine Learning Research*, 12(21):691–730, 2011.
- Nicolas Chopin, Pierre E Jacob, and Omiros Papaspiliopoulos. Smc2: an efficient algorithm for sequential analysis of state space models. *Journal of the Royal Statistical Society Series B: Statistical Methodology*, 75(3):397–426, 2013.
- Adrien Corenflos, James Thornton, George Deligiannidis, and Arnaud Doucet. Differentiable particle filtering via entropy-regularized optimal transport. In *International Conference on Machine Learning*, pages 2100–2111. PMLR, 2021.
- Dan Crisan and Arnaud Doucet. A survey of convergence results on particle filtering methods for practitioners. *IEEE Transactions on Signal Processing*, 50(3):736–746, 2002.
- Dan Crisan and Malte Grunwald. Large deviation comparison of branching algorithms versus resampling algorithms: application to discrete time stochastic filtering. *Statist. Lab., Cambridge Univ., Cambridge, UK, Tech. Rep., TR1999-9*, 1999.
- Kenan Dai, Dong Wang, Huchuan Lu, Chong Sun, and Jianhua Li. Visual tracking via adaptive spatially-regularized correlation filters. In *Proceedings of the IEEE Conference on Computer Vision and Pattern Recognition*, pages 4670–4679, 2019.
- Pierre Del Moral. Measure-valued processes and interacting particle systems. Application to nonlinear filtering problems. *The Annals of Applied Probability*, 8(2):438–495, 1998.
- Pierre Del Moral. Applications. In *Feynman-Kac formulae: Genealogical and interacting particle systems with applications*, pages 427–522. Springer, 2004.
- Pierre Del Moral and Alice Guionnet. Large deviations for interacting particle systems: applications to non-linear filtering. *Stochastic processes and their applications*, 78(1):69–95, 1998.
- Pierre Del Moral and Alice Guionnet. Central limit theorem for nonlinear filtering and interacting particle systems. *Annals of Applied Probability*, pages 275–297, 1999.

- Pierre Del Moral and Alice Guionnet. On the stability of interacting processes with applications to filtering and genetic algorithms. In *Annales de l'Institut Henri Poincaré (B) Probability and Statistics*, volume 37, pages 155–194. Elsevier, 2001.
- Petar M Djuric, Ting Lu, and Mónica F Bugallo. Multiple particle filtering. In *IEEE International Conference on Acoustics, Speech and Signal Processing (ICASSP)*, volume 3, pages 1181–1184, 2007.
- Arnaud Doucet, Simon Godsill, and Christophe Andrieu. On sequential Monte Carlo sampling methods for Bayesian filtering. *Statistics and computing*, 10:197–208, 2000.
- Arnaud Doucet, Nando De Freitas, and Neil Gordon. An introduction to Sequential Monte Carlo methods. *Sequential Monte Carlo methods in practice*, pages 3–14, 2001.
- Christopher Drovandi, Richard G Everitt, Andrew Golightly, and Dennis Prangle. Ensemble MCMC: accelerating pseudo-marginal MCMC for state space models using the ensemble Kalman filter. *Bayesian Analysis*, 17(1):223–60, 2022.
- Geir Evensen. The ensemble Kalman filter: Theoretical formulation and practical implementation. *Ocean Dynamics*, 53(4):343–367, 2003.
- Dieter Fox, Wolfram Burgard, Frank Dellaert, and Sebastian Thrun. Monte carlo localization: Efficient position estimation for mobile robots. *Proceedings of AAAI/IAAI*, pages 343–349, 1999.
- Reinhard Furrer and Thomas Bengtsson. Estimation of high-dimensional prior and posterior covariance matrices in Kalman filter variants. *Journal of Multivariate Analysis*, 98(2): 227–255, 2007.
- Reinhard Furrer, Marc G Genton, and Douglas Nychka. Covariance tapering for interpolation of large spatial datasets. *Journal of Computational and Graphical Statistics*, 15(3): 502–523, 2006.
- Steven Gillijns, O Barrero Mendoza, Jaganath Chandrasekar, BLR De Moor, DS Bernstein, and A Ridley. What is the ensemble Kalman filter and how well does it work? In *2006 American Control Conference*. IEEE, 2006.
- Michael Goldstein and David Wooff. *Bayes linear statistics: Theory and methods*. John Wiley & Sons, 2007.
- Neil J Gordon, David J Salmond, and Adrian FM Smith. Novel approach to nonlinear/non-Gaussian Bayesian state estimation. In *IEE proceedings F (radar and signal processing)*, volume 140, pages 107–113. IET, 1993.
- Shixiang Shane Gu, Zoubin Ghahramani, and Richard E Turner. Neural adaptive sequential monte carlo. *Advances in Neural Information Processing Systems*, 28, 2015.
- Dong Guo and Xiaodong Wang. Quasi-Monte Carlo filtering in nonlinear dynamic systems. *IEEE Transactions on Signal Processing*, 54(6):2087–2098, 2006.

- Tuomas Haarnoja, Anurag Ajay, Sergey Levine, and Pieter Abbeel. Backprop KF: Learning discriminative deterministic state estimators. *Advances in Neural Information Processing Systems*, 29, 2016.
- Peter L Houtekamer and Herschel L Mitchell. A sequential ensemble Kalman filter for atmospheric data assimilation. *Monthly Weather Review*, 129(1):123–137, 2001.
- Xiao-Li Hu, Thomas B Schon, and Lennart Ljung. A basic convergence result for particle filtering. *IEEE Transactions on Signal Processing*, 56(4):1337–1348, 2008.
- Xiao-Li Hu, Thomas B Schon, and Lennart Ljung. A general convergence result for particle filtering. *IEEE Transactions on Signal Processing*, 59(7):3424–3429, 2011.
- Brian R Hunt, Eric J Kostelich, and Istvan Szunyogh. Efficient data assimilation for spatiotemporal chaos: A local ensemble transform Kalman filter. *Physica D: Nonlinear Phenomena*, 230(1-2):112–126, 2007.
- Maximilian Igl, Luisa Zintgraf, Tuan Anh Le, Frank Wood, and Shimon Whiteson. Deep variational reinforcement learning for POMDPs. In *International Conference on Machine Learning*, pages 2117–2126. PMLR, 2018.
- Edward L Ionides, Carles Bretó, and Aaron A King. Inference for nonlinear dynamical systems. *Proceedings of the National Academy of Sciences*, 103(49):18438–18443, 2006.
- Kazufumi Ito and Kaiqi Xiong. Gaussian filters for nonlinear filtering problems. *IEEE Transactions on Automatic Control*, 45(5):910–927, 2000.
- Reza Izanloo, Seyed Abolfazl Fakoorian, Hadi Sadoghi Yazdi, and Dan Simon. Kalman filtering based on the maximum correntropy criterion in the presence of non-gaussian noise. In *Annual Conference on Information Science and Systems (CISS)*, pages 500–505. IEEE, 2016.
- Simon J Julier and Jeffrey K Uhlmann. Unscented filtering and nonlinear estimation. *Proceedings of the IEEE*, 92(3):401–422, 2004.
- Bosung Kang, Vikram Krishnamurthy, Kunal Pattanayak, Sandeep Gogineni, and Muralidhar Rangaswamy. Smart Interference Signal Design to a Cognitive Radar. In *IEEE Radar Conference (RadarConf23)*, pages 1–6, 2023.
- Peter Karkus, David Hsu, and Wee Sun Lee. Particle filter networks with application to visual localization. In *Conference on robot learning*, pages 169–178. PMLR, 2018.
- Peter Karkus, Shaojun Cai, and David Hsu. Differentiable slam-net: Learning particle slam for visual navigation. In *Proceedings of the IEEE Conference on Computer Vision and Pattern Recognition*, pages 2815–2825, 2021.
- Maximilian Karl, Maximilian Soelch, Justin Bayer, and Patrick Van der Smagt. Deep variational Bayes filters: Unsupervised learning of state space models from raw data. *arXiv preprint arXiv:1605.06432*, 2016.

- Matthias Katzfuss, Jonathan R Stroud, and Christopher K Wikle. Understanding the ensemble Kalman filter. *The American Statistician*, 70(4):350–357, 2016.
- Alina Kloss, Georg Martius, and Jeannette Bohg. How to train your differentiable filter. *Autonomous Robots*, 45(4):561–578, 2021.
- Byoung Chul Ko, Joon-Young Kwak, and Jae-Yeal Nam. Human tracking in thermal images using adaptive particle filters with online random forest learning. *Optical Engineering*, 52(11):113105:1–14, 2013.
- Jayesh H Kotecha and Petar M Djuric. Gaussian sum particle filtering. *IEEE Transactions on Signal Processing*, 51(10):2602–2612, 2003a.
- J.H. Kotecha and P.M. Djuric. Gaussian particle filtering. *IEEE Transactions on Signal Processing*, 51(10):2592–2601, 2003b.
- Stuart C Kramer and Harold W Sorenson. Recursive Bayesian estimation using piece-wise constant approximations. *Automatica*, 24(6):789–801, 1988.
- V. Krishnamurthy, D. Angley, R. Evans, and B. Moran. Identifying cognitive radars - Inverse reinforcement learning using revealed preferences. *IEEE Transactions on Signal Processing*, 68:4529–4542, 2020.
- Vikram Krishnamurthy and Muralidhar Rangaswamy. How to calibrate your adversary’s capabilities? Inverse filtering for counter-autonomous systems. *IEEE Transactions on Signal Processing*, 67(24):6511–6525, 2019.
- Vikram Krishnamurthy, Kunal Pattanayak, Sandeep Gogineni, Bosung Kang, and Muralidhar Rangaswamy. Adversarial radar inference: Inverse tracking, identifying cognition, and designing smart interference. *IEEE Transactions on Aerospace and Electronic Systems*, 57(4):2067–2081, 2021.
- Richard Kurle, Syama Sundar Rangapuram, Emmanuel de Bézenac, Stephan Günnemann, and Jan Gasthaus. Deep rao-blackwellised particle filters for time series forecasting. *Advances in Neural Information Processing Systems*, 33:15371–15382, 2020.
- Tuan Anh Le, Maximilian Igl, Tom Rainforth, Tom Jin, and Frank Wood. Auto-Encoding Sequential Monte Carlo. In *International Conference on Learning Representations*, 2018.
- François Le Gland and Nadia Oudjane. Stability and uniform approximation of nonlinear filters using the Hilbert metric and application to particle filters. *The Annals of Applied Probability*, 14(1):144–187, 2004.
- Michelle A Lee, Brent Yi, Roberto Martín-Martín, Silvio Savarese, and Jeannette Bohg. Multimodal sensor fusion with differentiable filters. In *2020 IEEE/RSJ International Conference on Intelligent Robots and Systems (IROS)*, pages 10444–10451, 2020.
- Tian Cheng Li, Jin Ya Su, Wei Liu, and Juan M Corchado. Approximate Gaussian conjugacy: parametric recursive filtering under nonlinearity, multimodality, uncertainty, and constraint, and beyond. *Frontiers of Information Technology & Electronic Engineering*, 18(12):1913–1939, 2017.

- X Rong Li, Zhanlue Zhao, and Vesselin P Jilkov. Practical measures and test for credibility of an estimator. In *Proc. Workshop on Estimation, Tracking, and Fusion—A Tribute to Yaakov Bar-Shalom*, pages 481–495. Citeseer, 2001.
- Yunpeng Li and Mark Coates. Particle filtering with invertible particle flow. *IEEE Transactions on Signal Processing*, 65(15):4102–4116, 2017.
- Xiangdong Lin, Thiagalingam Kirubarajan, Yaakov Bar-Shalom, and Simon Maskell. Comparison of EKF, pseudomeasurement, and particle filters for a bearing-only target tracking problem. In *Signal and Data Processing of Small Targets*, volume 4728, pages 240–250. SPIE, 2002.
- Fredrik Lindsten, Michael I Jordan, and Thomas B Schon. Particle Gibbs with ancestor sampling. *Journal of Machine Learning Research*, 15:2145–2184, 2014.
- Yang Liu, Volkan Kılıç, Jian Guan, and Wenwu Wang. Audio–visual particle flow SMC-PHD filtering for multi-speaker tracking. *IEEE Transactions on Multimedia*, 22(4):934–948, 2019.
- Xiao Ma, Peter Karkus, David Hsu, and Wee Sun Lee. Particle filter recurrent neural networks. In *Proceedings of the AAAI Conference on Artificial Intelligence*, volume 34, pages 5101–5108, 2020a.
- Xiao Ma, Peter Karkus, David Hsu, Wee Sun Lee, and Nan Ye. Discriminative particle filter reinforcement learning for complex partial observations. *arXiv preprint arXiv:2002.09884*, 2020b.
- John MacCormick and Andrew Blake. A probabilistic exclusion principle for tracking multiple objects. *International Journal of Computer Vision*, 39:57–71, 2000.
- Chris J Maddison, John Lawson, George Tucker, Nicolas Heess, Mohammad Norouzi, Andriy Mnih, Arnaud Doucet, and Yee Teh. Filtering variational objectives. *Advances in Neural Information Processing Systems*, 30, 2017.
- Ronald PS Mahler. Multitarget Bayes filtering via first-order multitarget moments. *IEEE Transactions on Aerospace and Electronic Systems*, 39(4):1152–1178, 2003.
- Robert Mattila, Cristian R. Rojas, Vikram Krishnamurthy, and Bo Wahlberg. Inverse filtering for hidden Markov models with applications to counter-adversarial autonomous systems. *IEEE Transactions on Signal Processing*, 68:4987–5002, 2020.
- K. V. Mishra, M. R. B. Shankar, and M. Rangaswamy. *Next-Generation Cognitive Radar Systems*. IET Press, 2023.
- Kumar Vijay Mishra and Yonina C Eldar. Performance of time delay estimation in a cognitive radar. In *IEEE International Conference on Acoustics, Speech and Signal Processing*, pages 3141–3145, 2017.
- Kumar Vijay Mishra, MR Bhavani Shankar, and Björn Ottersten. Toward metacognitive radars: Concept and applications. In *IEEE International Radar Conference*, pages 77–82, 2020.

- Michael Montemerlo, Sebastian Thrun, Daphne Koller, Ben Wegbreit, et al. FastSLAM 2.0: An improved particle filtering algorithm for simultaneous localization and mapping that provably converges. In *16th International Joint Conference on Artificial Intelligence (IJCAI)*, volume 3, pages 1151–1156, 2003.
- Kevin Murphy and Stuart Russell. Rao-blackwellised particle filtering for dynamic bayesian networks. In *Sequential Monte Carlo methods in practice*, pages 499–515. Springer, 2001.
- Christian Musso, Nadia Oudjane, and Francois Le Gland. Improving regularised particle filters. In *Sequential Monte Carlo methods in practice*, pages 247–271. Springer, 2001.
- Christian Naesseth, Scott Linderman, Rajesh Ranganath, and David Blei. Variational sequential monte carlo. In *International Conference on Artificial intelligence and Statistics*, pages 968–977. PMLR, 2018.
- Andrew Y Ng and Stuart J Russell. Algorithms for inverse reinforcement learning. In *International Conference on Machine Learning*, pages 663–670, 2000.
- Kenji Okuma, Ali Taleghani, Nando De Freitas, James J Little, and David G Lowe. A boosted particle filter: Multitarget detection and tracking. In *Computer Vision-ECCV 2004: 8th European Conference on Computer Vision, Prague, Czech Republic, May 11-14, 2004. Proceedings, Part I 8*, pages 28–39. Springer, 2004.
- Michael K Pitt and Neil Shephard. Filtering via simulation: Auxiliary particle filters. *Journal of the American Statistical Association*, 94(446):590–599, 1999.
- Branko Ristic, Sanjeev Arulampalam, and Neil Gordon. *Beyond the Kalman filter: Particle filters for tracking applications*. Artech house, 2003.
- Branko Ristic, Ba-Tuong Vo, Ba-Ngu Vo, and Alfonso Farina. A tutorial on Bernoulli filters: theory, implementation and applications. *IEEE Transactions on Signal Processing*, 61(13):3406–3430, 2013.
- Branko Ristic, Jeremie Houssineau, and Sanjeev Arulampalam. Robust target motion analysis using the possibility particle filter. *IET Radar, Sonar & Navigation*, 13(1):18–22, 2019.
- Yong Rui and Yunqiang Chen. Better proposal distributions: Object tracking using unscented particle filter. In *IEEE Conference on Computer Vision and Pattern Recognition (CVPR)*, volume 2, pages 786–793, 2001.
- Kazuyuki Samejima, Kenji Doya, Yasumasa Ueda, and Minoru Kimura. Estimating internal variables and paramters of a learning agent by a particle filter. *Advances in Neural Information Processing Systems*, 16, 2003.
- Nathan Sharaga, Joseph Tabrikian, and Hagit Messer. Optimal cognitive beamforming for target tracking in MIMO radar/sonar. *IEEE Journal of Selected Topics in Signal Processing*, 9(8):1440–1450, 2015.

- Angad Singh, Omar Makhlouf, Maximilian Igl, Joao Messias, Arnaud Doucet, and Shimon Whiteson. Particle-Based Score Estimation for State Space Model Learning in Autonomous Driving. In *Conference on Robot Learning*, pages 1168–1177. PMLR, 2023a.
- Himali Singh, Arpan Chattopadhyay, and Kumar Vijay Mishra. Inverse cognition in nonlinear sensing systems. In *Asilomar Conference on Signals, Systems, and Computers*, pages 1116–1120, 2022.
- Himali Singh, Arpan Chattopadhyay, and Kumar Vijay Mishra. Inverse Extended Kalman filter - Part I: Fundamentals. *IEEE Transactions on Signal Processing*, 71:2936–2951, 2023b.
- Himali Singh, Arpan Chattopadhyay, and Kumar Vijay Mishra. Inverse Extended Kalman filter – Part II: Highly non-linear and uncertain systems. *IEEE Transactions on Signal Processing*, 71:2952–2967, 2023c.
- Himali Singh, Kumar Vijay Mishra, and Arpan Chattopadhyay. Counter-adversarial learning with Inverse Unscented Kalman filter. In *62nd IEEE Conference on Decision and Control (CDC)*, pages 7661–7666, 2023d.
- Himali Singh, Kumar Vijay Mishra, and Arpan Chattopadhyay. Inverse Cubature and Quadrature Kalman filters. *IEEE Transactions on Aerospace and Electronic Systems*, 2024a. in press.
- Himali Singh, Kumar Vijay Mishra, and Arpan Chattopadhyay. Inverse Unscented Kalman filter. *IEEE Transactions on Signal Processing*, 72:2692–2709, 2024b.
- Adhiraj Somani, Nan Ye, David Hsu, and Wee Sun Lee. DESPOT: Online POMDP planning with regularization. *Advances in Neural Information Processing Systems*, 26, 2013.
- Peter Xue-Kun Song. Monte Carlo Kalman filter and smoothing for multivariate discrete state space models. *Canadian Journal of Statistics*, 28(3):641–652, 2000.
- Andreas S Stordal, Hans A Karlsen, Geir Nævdal, Hans J Skaug, and Brice Vallès. Bridging the ensemble Kalman filter and particle filters: the adaptive Gaussian mixture filter. *Computational Geosciences*, 15:293–305, 2011.
- Yangtianze Tao, Jiayi Kang, and Stephen Shing-Toung Yau. Maximum Correntropy Ensemble Kalman Filter. In *2023 62nd IEEE Conference on Decision and Control (CDC)*, pages 8659–8664, 2023.
- Petr Tichavsky, Carlos H Muravchik, and Arye Nehorai. Posterior Cramér-Rao bounds for discrete-time nonlinear filtering. *IEEE Transactions on Signal Processing*, 46(5):1386–1396, 1998.
- Inam Ullah, Yu Shen, Xin Su, Christian Esposito, and Chang Choi. A localization based on unscented Kalman filter and particle filter localization algorithms. *IEEE Access*, 8: 2233–2246, 2019.



- Rudolph Van Der Merwe, Arnaud Doucet, Nando De Freitas, and Eric Wan. The unscented particle filter. *Advances in neural information processing systems*, 13, 2000.
- Vermaak, Doucet, and Perez. Maintaining multimodality through mixture tracking. In *IEEE International Conference on Computer Vision*, pages 1110–1116, 2003.
- José Luis Carrera Villacrés, Zhongliang Zhao, Torsten Braun, and Zan Li. A particle filter-based reinforcement learning approach for reliable wireless indoor positioning. *IEEE Journal on Selected Areas in Communications*, 37(11):2457–2473, 2019.
- Manuel Watter, Jost Springenberg, Joschka Boedecker, and Martin Riedmiller. Embed to control: A locally linear latent dynamics model for control from raw images. *Advances in Neural Information Processing Systems*, 28, 2015.
- Hao Wen, Xiongjie Chen, Georgios Papagiannis, Conghui Hu, and Yunpeng Li. End-to-end semi-supervised learning for differentiable particle filters. In *2021 IEEE International Conference on Robotics and Automation (ICRA)*, pages 5825–5831, 2021.
- Yuanxin Wu, Xiaoping Hu, Dewen Hu, and Meiping Wu. Comments on “Gaussian particle filtering”. *IEEE Transactions on Signal Processing*, 53(8):3350–3351, 2005.
- Kai Xiong, HY Zhang, and CW Chan. Performance evaluation of UKF-based nonlinear filtering. *Automatica*, 42(2):261–270, 2006.
- Yulin Yang and Guoquan Huang. Map-based localization under adversarial attacks. In *Robotics Research: The 18th International Symposium ISRR*, pages 775–790. Springer, 2019.
- Ali Yousefi, Anna K Gillespie, Jennifer A Guidera, Mattias Karlsson, Loren M Frank, and Uri T Eden. Efficient decoding of multi-dimensional signals from population spiking activity using a Gaussian mixture particle filter. *IEEE Transactions on Biomedical Engineering*, 66(12):3486–3498, 2019.
- Tianzhu Zhang, Changsheng Xu, and Ming-Hsuan Yang. Multi-task correlation particle filter for robust object tracking. In *Proceedings of the IEEE Conference on Computer Vision and Pattern Recognition*, pages 4335–4343, 2017.
- Michael Zhu, Kevin Murphy, and Rico Jonschkowski. Towards differentiable resampling. *arXiv preprint arXiv:2004.11938*, 2020.
- Milija Zupanski. Maximum likelihood ensemble filter: Theoretical aspects. *Monthly Weather Review*, 133(6):1710–1726, 2005.